2009

Spatial-temporal responses of Louisiana forests to climate change and hurricane disturbance

Fugui Wang
Louisiana State University and Agricultural and Mechanical College

SPATIAL-TEMPORAL RESPONSES OF LOUISIANA FORESTS TO CLIMATE CHANGE AND HURRICANE DISTURBANCE

A Dissertation

Submitted to the Graduate Faculty of the
Louisiana State University and
Agricultural and Mechanical College
In partial fulfillment of the
requirements for the degree of
Doctor of Philosophy

In

The School of Renewable Natural Resources

By

Fugui Wang

B.S. Northwest A&F University, China, 1992
M.S. Northwest A&F University, China, 1995
M.S. The University of Memphis, TN, 2004

August 2009

DEDICATION

This dissertation is dedicated to:

my grandparents

Mr. Zhengguan Wang and Mrs. Suihua Liang

and parents

Mr. Lichuan Wang and Mrs. Gailin Cui

for supporting and educating me to pursue my academic career and work on my interests

my wife

Dr. Shuwen Li

for her complete support

and

my children

Kaitlynn Li Wang and Nolan Li Wang

for their lovely smiles.

ACKNOWLEDGMENTS

Studying and performing research for a PhD is a long tough journey. As I moved along this path, there have been many people who encouraged, guided, supported, and believed in me. Without them, I would not have been able to reach my goal.

My deepest gratitude firstly goes to my advisor, Dr. Y. Jun Xu. I have been amazingly fortunate to have him as my advisor, who inspires me to develop novel ideas and thoughts in research projects, as well as supplies the necessary facilities to support me. I am grateful to him for teaching me how to write high quality, scientific documents. Any documents after incorporation of his constructive comments and word-by-word revision are definitely improved. Dr. Xu is truly a master teacher, who willingly guided me, not only to be an outstanding student right now, but also to have a successful career in the future. I express my appreciation for his guidance, assistance, sound advice, inspiration, and dedication.

I am profoundly grateful to Drs. Thomas J. Dean, Nina S. Lam, Eurico D'Sa, and Elijah W. Ramsey III for serving on my dissertation committee, reviewing my writings, giving me constructive comments on my research activities, and supporting me through all the steps of my graduate career. The shared experiences will always be remembered and treasured.

In addition, Dr. John D. Aber, graduate student Julian Jenkins, and Dr. Scott V. Ollinger at the University of New Hampshire instructed me on how to apply the PnET model. Graduate student Philip Saksa at Louisiana State University traveled to fields to help me identify the hurricane disturbance to forests and also reviewed my manuscripts. Dr. Quang V. Cao aided in interpretation of the vegetation indices derived from satellite images. I would like to express my deep and sincere gratitude to them for their support and assistance, which allowed me to overcome setbacks in my research activities.

Finally, I would like to express my heart-felt gratitude to my family for all of their support along the way. They have been a constant source of love, concern, support, and strength all these years. My special appreciation goes to my grandparents, Mr. Zhengguan Wang and Mrs. Suihua Liang, and my parents, Mr. Lichuan Wang and Mrs. Gailin Cui, for the earliest and the most important education, guidance, and inspiration during those poor and tough years; my dearest lovely and supportive wife, Shuwen Li for her positive expectations, patience, and love; as well as my two beautiful children, Kaitlynn and Nolan, for their lovely smiles. This dissertation is dedicated to them.

This research was supported in part by USDA McIntire-Stennis funds and by the Louisiana Board of Regents under award LEQSF (2004-07)-RD-A-04. I gratefully acknowledge the financial support.

TABLE OF CONTENTS

LIST OF TABLES

LIST OF FIGURES

ABSTRACT

This dissertation research focused on three questions: (1) what is the current carbon stock in Louisiana's forest ecosystems? (2) how will the biomass carbon stock respond to future climate change? and (3) how vulnerable are the coastal forest resources to natural disturbances, such as hurricanes? The research utilized a geographic information system, remote sensing techniques, ecosystem modeling, and statistical approaches with existing data and *in-situ* measurements. Future climate changes were adapted from predictions by the Community Climate System Model on the basis of low (B1), moderate (A1B), and high (A2) greenhouse gas emission scenarios. The study on forest carbon assessment found that Louisiana's forests currently store 219.2 Tg of biomass carbon, 90% of which is stored in wetland and evergreen forests. Spatial variation of the carbon storage was mainly affected by forest biomass distribution. No correlation was identified between carbon storage in watersheds with the average watershed slope and drainage density. The modeling study on growth response to future climate found that forest net primary productivity (NPP) would decline from 2000 to 2050 under scenario B1, but may increase under scenarios A1B and A2 due primarily to minimum temperature and precipitation changes. Uncertainties of the NPP prediction were apparent, owing to spatial resolution of the climate variables. The remote sensing study on hurricane disturbance to coastal forests found that increases in the intensity of severe weather in the future would likely increase the turn-over rate of coastal forest carbon stock. Forest attributes and site conditions had a variety of effects on the vulnerability of forests to hurricane disturbance and thereby, spatial patterns of disturbed landscape. Soil groups and stand factors, including forest types, forest coverage, and stand density contributed to 85% of accuracy in the modeling probability of Hurricane Katrina disturbance to forests. In conclusion, this research demonstrated that quantification of forest

biomass carbon, using geo-referenced datasets and GIS techniques, provides a credible approach to increase accuracy and constrain the uncertainty of large-scale carbon assessment. A combination of ecosystem modeling and GIS/Remote Sensing techniques can provide insight into future climate change effects on forest carbon change at the landscape scale.

CHAPTER 1 INTRODUCTION

Forest ecosystems in the United States were estimated to contain about 53 Pg of carbon, of which 41% is stored in biomass. Spatial and temporal changes in this large carbon storage are complex and can be a result of (1) local site conditions such as climate, geomorphology, and soil that determine long-term carbon sequestration potential; (2) disturbances such as changes in land use, previous and current forest management practices, and natural disasters, e.g., forest fire and disease that alter carbon pools; (3) vegetation types, a consequence of local site conditions and disturbances; and (4) forest growth phases, which determine temporal biomass accumulation rates. In the context of global climate change, substantial challenges have been shown to maintain and increase the forest carbon storage, and to predict its future change, given the large uncertainties of the variability inherent in forest ecosystems.

During the past three decades, many studies were conducted on carbon accounting of forest ecosystems. During the late 1990s and early 2000s, intensive efforts in field experiments (e.g., Free-Air Carbon Dioxide Enrichment program; DeLucia et al. 1999; Hendrey et al. 1999) and large scale modeling approaches (e.g., Vegetation-Ecosystem Modeling and Analysis Project; Kittel et al. 1995; Schimel et al. 1997), were undertaken to understand the mechanisms of forests as a terrestrial carbon sink. Processes studied ranged from carbon dioxide, climate change, and nitrogen fertilization effects on vegetation growth (Bazzaz et al. 1990; Kauppi et al. 1992; Nilsson and Wiklund 1992) to historical land use (Caspersen et al. 2000; Houghton et al. 1999; Schimel et al. 2001). While the mechanisms and the detailed spatial pattern of this sink remain elusive (Field and Fung 1999), Schimel et al. (2001) concluded that forest regrowth and reversion of agricultural land contribute more to this terrestrial sink in the United States and other regions than carbon dioxide and climate effects. These findings reveal that our present understanding of the global carbon cycle is constrained by uncertainty over forest ecosystem carbon storage and changes.

Forests in Louisiana have been recognized as a carbon sink, contributing to offsetting anthropogenic carbon dioxide emissions and mitigating atmospheric carbon dioxide greenhouse effects (Birdsey 1996; Birdsey and Lewis 2002; Brown et al. 1999; McNulty et al. 2000; Mickler et al. 2004; Smith and Heath 2004; Smith et al. 2003; Xu and Wang 2006). However, global climate models have projected increased temperature and precipitation for Louisiana in the 21st century. Increases of these two critical weather factors may have significant effects on forest ecosystems, especially with regard to forest growth and carbon sequestration potential. In addition, global warming is predicted to result in a sharp increase in the intensity of tropical cyclones (Emanuel 2005; Webster et al. 2005), consequently causing an upward trend of destructive potential of hurricanes to Louisiana's forests. As a result, the induced carbon variation in the forest ecosystem by climate change and hurricane disturbance would affect carbon output from the forest ecosystem to aquatic environments as dissolved organic carbon.

With the above introduction in mind, this dissertation is organized by three interrelated research questions: (1) what is the current carbon stock in Louisiana's forest ecosystems? (2) how will the biomass carbon stock respond to future climate change? and (3) how will the coastal forest resources respond to natural disturbances, such as hurricanes. Specifically, the research objectives are to

(1) quantify forest biomass carbon across Louisiana at the grid and watershed scales;

(2) investigate the relationship of forest biomass carbon stock with watershed characteristics, such as watershed drainage density and watershed slope;

(3) assess changes in forest productivity and carbon stock in response to future climate change;

(4) determine an optimum remote sensing change detection technique for identifying hurricane damage to forests; and

(5) investigate associations of forest and site factors with hurricane disturbance at landscape levels.

The dissertation is divided into seven chapters. Starting with a brief introduction in Chapter 1, Chapter 2 provides a literature review emphasizing the current state of research and knowledge on the role of forest ecosystem carbon in global climate change. Chapter 3 presents the study on biomass carbon assessment using geospatial techniques and discusses how the carbon stock is spatially distributed across the landscape in Louisiana. Chapter 4 discusses the modeling assessment on the potential response of Louisiana's forest carbon stock to three climate change projections. Chapter 5 examines different remote sensing detection techniques to select an optimum method for identifying hurricane damage to forests. Chapter 6 focuses on the analysis of spatial associations of forests and site factors with hurricane disturbance at the landscape level. Chapter 7 summarizes relevant findings and identifies future research needs. Chapters 3, 4, 5, and 6 are written as stand-alone journal publications. They have their own introduction, methods, results, and discussion sections, and therefore, there will be some repetition between the chapters.

CHAPTER 2 LITERATURE REVIEW

Carbon Dioxide and Climate Change

Global climate has been changing at a rapid rate since the mid 19th century. In its latest global climate assessment, the Intergovernmental Panel on Climate Change (IPCC) reported that global mean temperature has increased 0.76 °C (0.57 – 0.95 °C) from 1850 – 1899 to 2001 – 2005, and that the temperature would continue to increase by 0.64 - 0.69 °C during 2011to 2030 and 1.79 - 3.13 °C during 2080 to 2099, in reference to the means observed between 1980 and 1999 (Fig. 1, Meehl et al. 2007). At the same time, global warming is expected to cause changes in distribution, intensity, and frequency of precipitation. The observed precipitation from 1900 to 2005 increased significantly in eastern parts of North and South America, northern Europe and northern and central Asia, whereas it declined in the Sahel, the Mediterranean, southern Africa and parts of southern Asia (IPCC 2007c). For future precipitation under scenario A1B in the Special Report on Emissions Scenarios (SRES), climate models predicted (Meehl et al. 2007) that annual precipitation at most high latitudes, as well as in eastern Africa, central Asia and the equatorial Pacific Ocean, would increase by 20% in the period from 2080 to 2099, in comparison with the precipitation observed in the regions between 1980 and 1999 (Fig.2).

The increase in global temperature may have caused sea level rise as evidenced by an average rate of 1.8 (1.3 to 2.3) mm per year of world's oceans over 1961 to 2003. The rising rate was accelerating over the period from 1993 to 2003, about 3.1 (2.4 to 3.8) mm per year. Under the SRES A1B scenario, the sea level from the present (1980 – 1999) will rise 0.21 to 0.48 m by the end of this century (2090–2099) (Fig. 3, Meehl et al. 2007). In addition, global warming is expected to increase the likelihood of tropical cyclone intensity (Fig. 4, Emanuel 2005; Webster et al. 2005) and, consequently, an upward trend in hurricane destructive potential (Emanuel 2005). The environmental changes induced by the global temperature increase and precipitation intensity will affect our human society and economic development directly or indirectly through

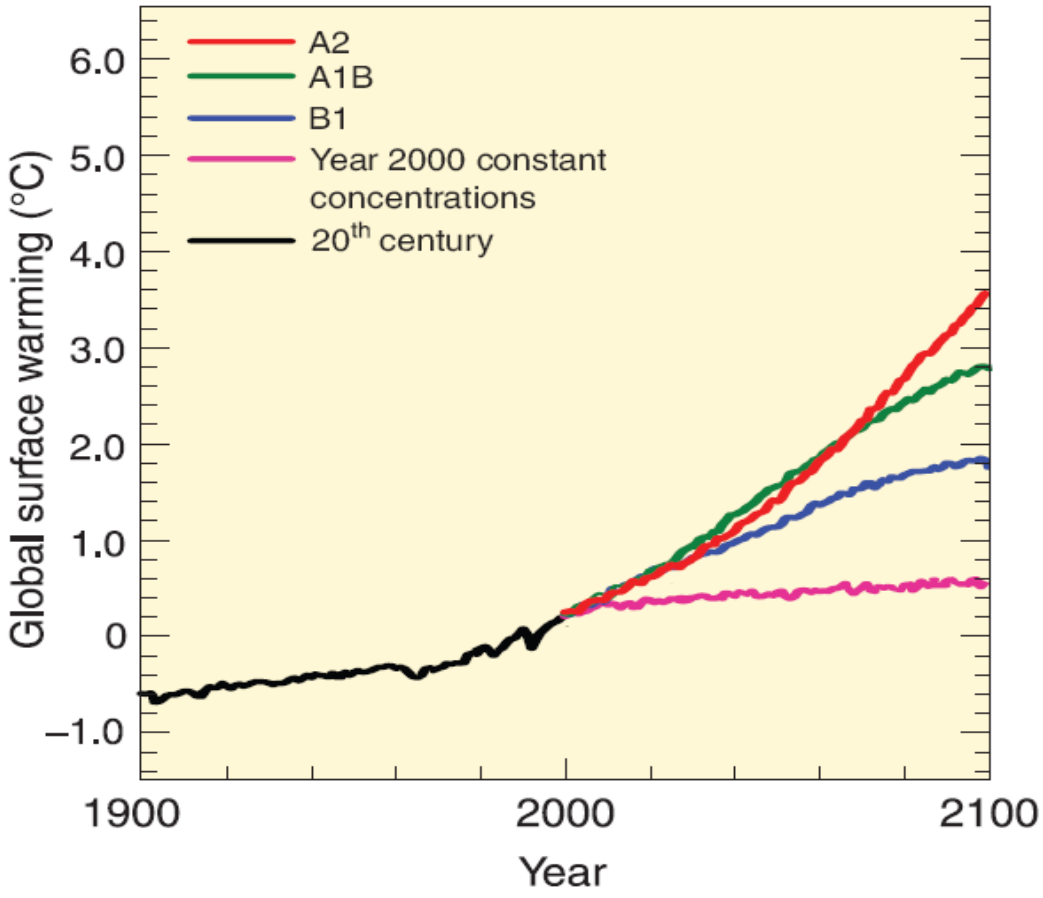

Fig. 1 Observed and multi-model predicted global surface temperature (relative to 1980–1999) for the A2, A1B and B1 scenarios, shown as continuations of the 20th century simulations. The orange line is for the experiment where CO_2 concentrations were held constant at year 2000 values (adapted from IPCC, 2007c).

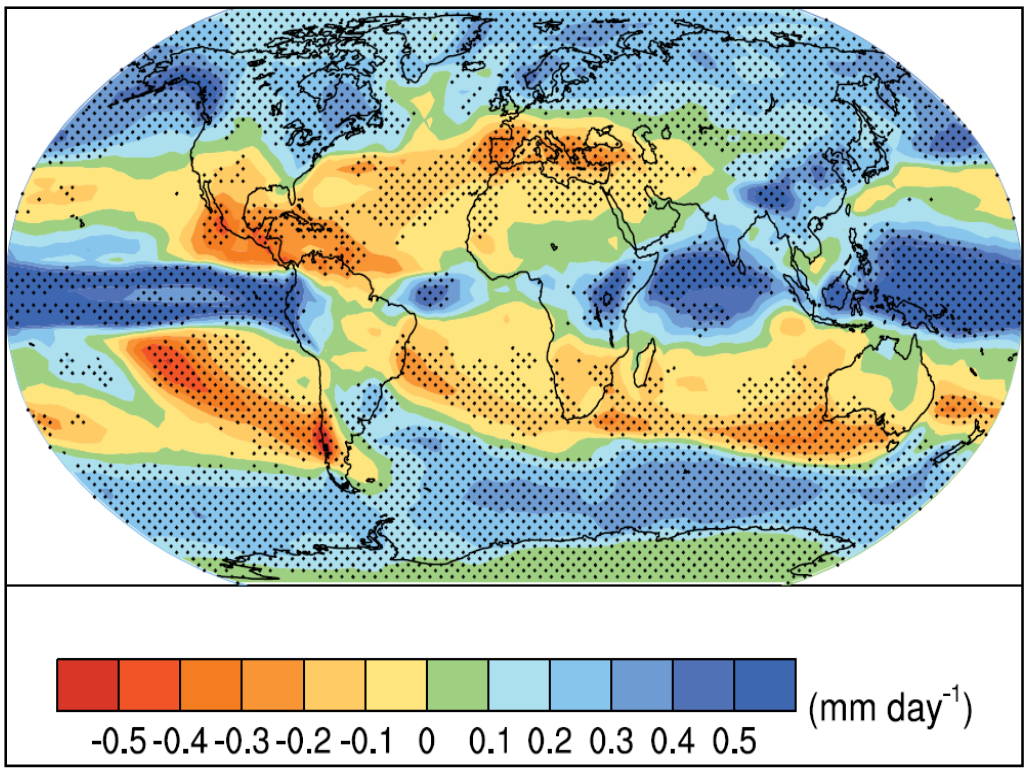

Fig. 2 Multi-model predicted changes in precipitation (mm/day) for the SRES A1B scenario for the period 2080 to 2099, relative to 1980 to 1999 (adapted from Meehl et al., 2007).

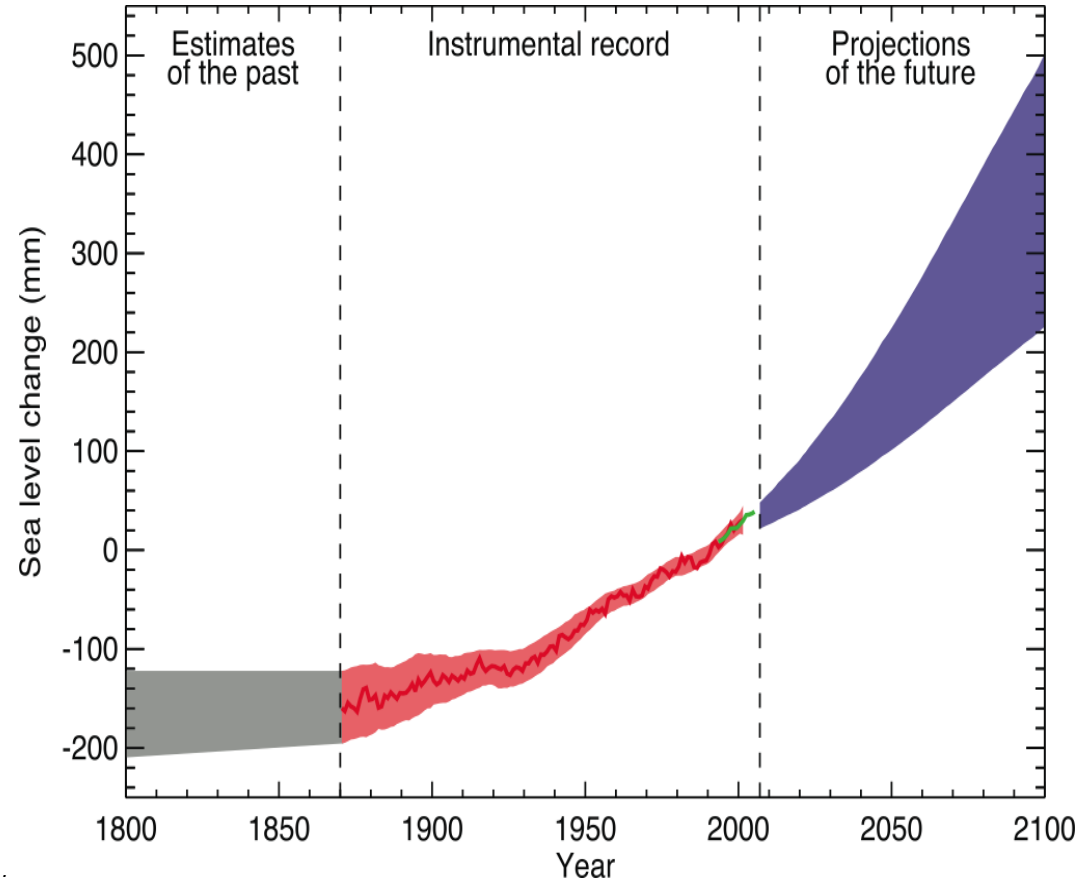

Fig. 3 Time series of global mean sea level (deviation from the 1980-1999 mean) in the past and as projected for the future. The grey shading shows the uncertainty in the estimated long-term rate of sea level change. The red line is a reconstruction of global mean sea level from tide gauges, and the red shading denotes the range of variations from a smooth curve. The green line shows the global mean sea level observed from satellite altimetry. The blue shading represents the range of model projections for the SRES A1B scenario for the 21st century, relative to the 1980 to 1999 mean (adapted from IPCC, 2007d).

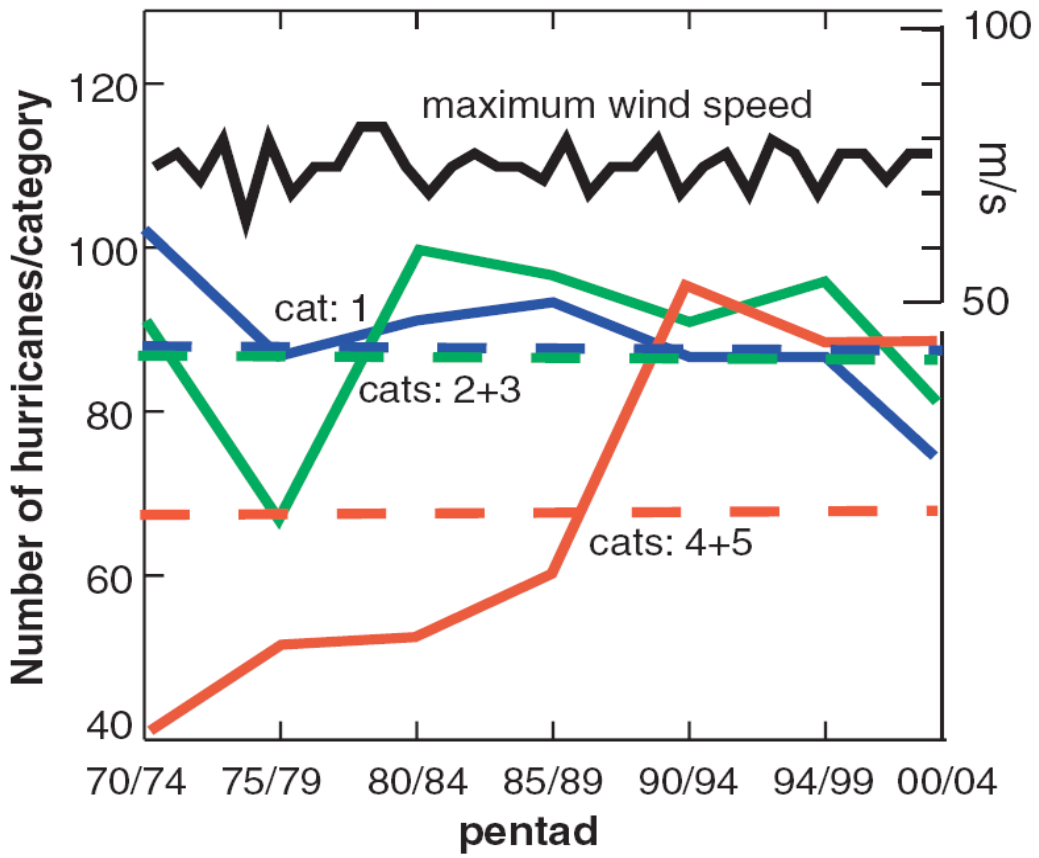

Fig. 4 Total number of category 1 (blue curve), categories 2 and 3 (green), and categories 4 and 5 hurricanes (red) in 5-year periods, according to the Saffir-Simpson scale (category 1 to 5). The bold curve is the maximum hurricane wind speed observed globally (measured in meters per second). The horizontal dashed lines show the 1970–2004 average numbers in each category (adapted from Webster et al., 2005).

the impacts on food, water, and ecosystem resources (IPCC 2007c).

The rapid global climate change has been attributed to the increase of greenhouse gases (GHG) in the atmosphere due to intensified industrialization, agricultural practices, and land use changes. Over geological time, the climate is mainly controlled by the earth's orbital characteristics, volcanic eruptions, variations of solar output, greenhouse gas effects, or any combination of these factors. However, since the Industrial Revolution and particularly since the mid-20th century, the global climate change has been likely due to an observed increase in anthropogenic greenhouse gas concentrations (IPCC 2007d). Abundance or properties of these

gases can lead to a warming or cooling of the climate system, depending on how the gases interact with incoming solar radiation and out-going infrared (thermal) radiation. Among the four principal greenhouse gases of carbon dioxide (CO_2), methane (CH_4), nitrous oxide (N_2O) and the halocarbons (a group of gases containing fluorine, chlorine, or bromine, such as fluorocarbon) emitted due to human activities, carbon dioxide is the second-most important greenhouse gas after water vapor (IPCC 2007c). Since the Industrial Revolution in the 1700s, the atmospheric carbon dioxide concentration increased from a range of 275 to 285 ppm in 1700 to 1850, to 379 ppm in 2005. In the recent decade between 1995 and 2005, the atmospheric carbon dioxide has experienced the highest average growth rate of about 19 ppm, when compared to records for any decade since direct atmospheric carbon dioxide measurements began in the 1950s (Forster et al. 2007). Carbon dioxide has increased energy at the top of the atmosphere (radiative forcing) 1.66 w/m^2 in 2005, relative to the start of the industrial era. The radiative forcing of carbon dioxide accounts for 72% of the total forcing of CO_2, CH_4, and N_2O (Forster et al. 2007).

The effects of CO_2 on climate change and their covariation relationship was revealed through instrumentally measured CO_2 and derived from proxies, such as ice cores. The potential effects of human activities on carbon cycle and climate change were noticed as early as 1896 by Svante Arrhenius (Arrhenius 1896), who postulated that a doubling of CO_2 in the atmosphere could lead to a temperature rise of 4 – 5°C. In the late 1950s, Charles David Keeling began monitoring atmospheric CO_2 at the Mauna Loa Observatory in Hawaii. The records, subsequently named Keeling's curve, showed a steady rise of the carbon dioxide level, with seasonal variations and peak levels reaching into the late northern hemisphere winter (Fig. 5, Keeling et al. 2009). The records from 1958 to 2004 show that the fluctuations of carbon dioxide concentrations from four months to eleven years were positively correlated in a power-law fashion (Varotsos et al. 2007). Atmospheric CO_2 concentrations before Keeling's records were

derived from proxies, such as ice cores. Ice cores have become a unique and powerful resource for studies of past climate and forcing factors, such as greenhouse gas concentrations, back for 800,000 years (Wolff 2005). Present-day atmospheric burdens of the two important greenhouse gases, carbon dioxide and methane, seem to be unprecedented during the past 420,000 years (Petit et al. 1999). The covariation of carbon dioxide in Vostok ice cores and a reconstructed temperature with an involvement of complex biogeochemical systems is highly correlated with R^2 of 0.89 for the past 150 kyr and R^2 of 0.84 for the period of 350± 150 kyr ago. The close relationship strongly supports the importance of carbon dioxide as a forcing factor of climate change (Cuffey and Vimeux 2001).

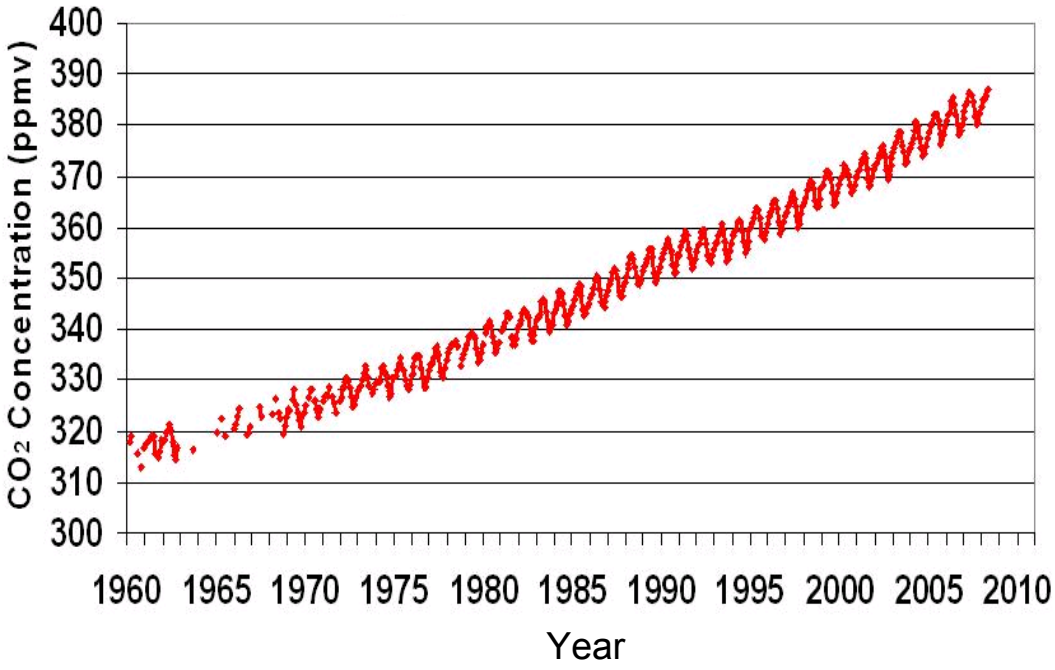

Fig. 5 Atmospheric carbon dioxide records from Mauna Loa (adapted from Keeling et al., 2009).

Emission of greenhouse gases will continue to exert a force on climate; the rate of climate change has been projected by models from perspectives of divergent emission scenarios. Up to now, there are over 20 models from different centers, available to project climate continentally or

regionally. For instance, model HADCM3 (developed in UK Met Office), CCSM3 (National Centre for Atmospheric Research), and CGCM3 (Canadian Center for Climate Modelling and Analysis) predict a climate change at spatial resolutions of 2.5° x 3.75° (HADCM3), 1.4° x 1.4° (CCSM3), and 3.75° by 3.75° (CGCM3). The models consist of components of atmospheric, oceanic, and land surface processes, as well as other components. The model predictions are generally based on scenarios of greenhouse gas emissions, including four families of A1, A2, B1, and B2, which differ by driving forces, such as demographic and socio-economic development and technological change (Fig. 6). The scenarios are described in the following excerpt from IPCC report Climate Change 2007: Mitigation (IPCC 2007b, p7):

> A1 – The A1 storyline and scenario family describes a future world of very rapid economic growth, global population that peaks in mid-century and declines thereafter, and the rapid introduction of new and more efficient technologies. Major underlying themes are convergence among regions, capacity building and increased cultural and social interactions, with a substantial reduction in regional differences in per capita income. The A1 scenario family develops into three groups that describe alternative directions of technological change in the energy system. The three A1 groups are distinguished by their technological emphasis: fossil intensive (A1FI), nonfossil energy sources (A1T), or a balance across all sources (A1B) (where balanced is defined as not relying too heavily on one particular energy source, on the assumption that similar improvement rates apply to all energy supply and end use technologies).
>
> A2 – The A2 storyline and scenario family describes a very heterogeneous world. The underlying theme is self reliance and preservation of local identities. Fertility patterns across regions converge very slowly, which results in continuously increasing population. Economic development is primarily regionally oriented and per capita economic growth and technological change more fragmented and slower than other storylines.
>
> B1 – The B1 storyline and scenario family describes a convergent world with the same global population, that peaks in midcentury and declines thereafter, as in the A1 storyline, but with rapid change in economic structures toward a service and information economy, with reductions in material intensity and the introduction of clean and resource efficient technologies. The emphasis is on global solutions to

> economic, social and environmental sustainability, including improved equity, but without additional climate initiatives.
>
> B2 – The B2 storyline and scenario family describes a world in which the emphasis is on local solutions to economic, social and environmental sustainability. It is a world with continuously increasing global population, at a rate lower than A2, intermediate levels of economic development, and less rapid and more diverse technological change than in the B1 and A1 storylines. While the scenario is also oriented towards environmental protection and social equity, it focuses on local and regional levels.

Scenarios of B1, A1B, and A2 usually represent low, moderate and high greenhouse gas emissions in the future. The approximate CO_2 equivalent concentrations for the three scenarios are projected to be 600, 850, and 1250 ppm in 2100, respectively (Nakicenovic et al. 2000). Climate variation in the 20th century is simulated by the 20th Century Climate in Coupled Models (20C3M) experiment, using historical records of external forcing. The results from the 20C3M experiment are used as initial states for other SRES scenario experiments.

In the state of Louisiana, climate has been changing as in other parts of the world. CCSM3 has projected an increased mean annual temperature, starting late in the 20th century and early 21st century, with the recorded highest temperature (19.51 °C) in 1999 and the lowest (17.69) in 1928 before 2000, as well as the highest temperature (20.90 °C) in 2094 and the lowest (19.19) in 2003 after 2000 (Fig. 7a). The annual precipitations before 2000 show slight changes with the highest (1114 mm) in 1966, and the lowest (847 mm) in 1999 before 2000 (Fig. 7b), and then after 2000, the precipitations gradually increase with the highest (1187mm) in 2088.

Carbon Storage in Forest Ecosystems

Occupying one-third of the earth's land surface, forests play a critical role in the global carbon stock and cycling. It is estimated that the world's forests store 283 Pg of carbon in their biomass alone (FAO 2006). Forests exchange carbon dioxide with the atmosphere through

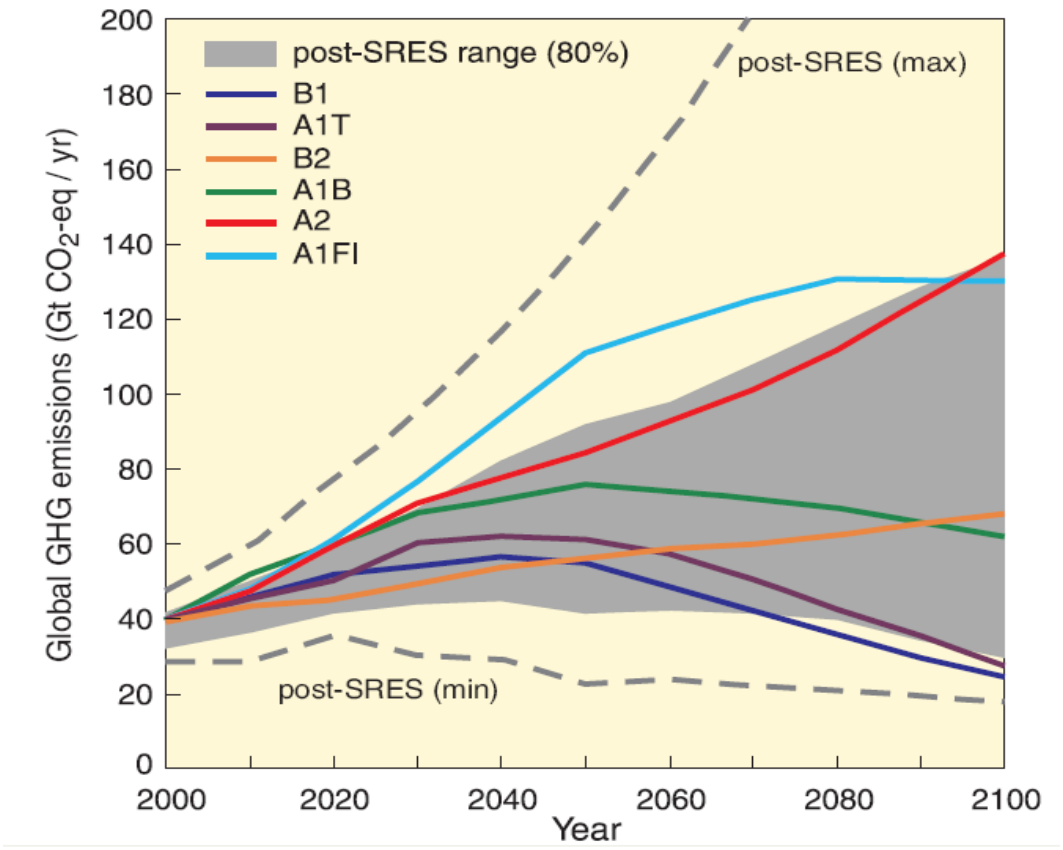

Fig. 6 Global greenhouse gas emissions (in $GtCO_2$-eq per year) in the absence of additional climate policies: six illustrative SRES marker scenarios (colored lines) and the 80th percentile range of recent scenarios published since SRES (post-SRES) (gray shaded area). Dashed lines show the full range of post-SRES scenarios. The emissions include CO_2, CH_4, N_2O and F-gases (adapted from IPCC, 2007c).

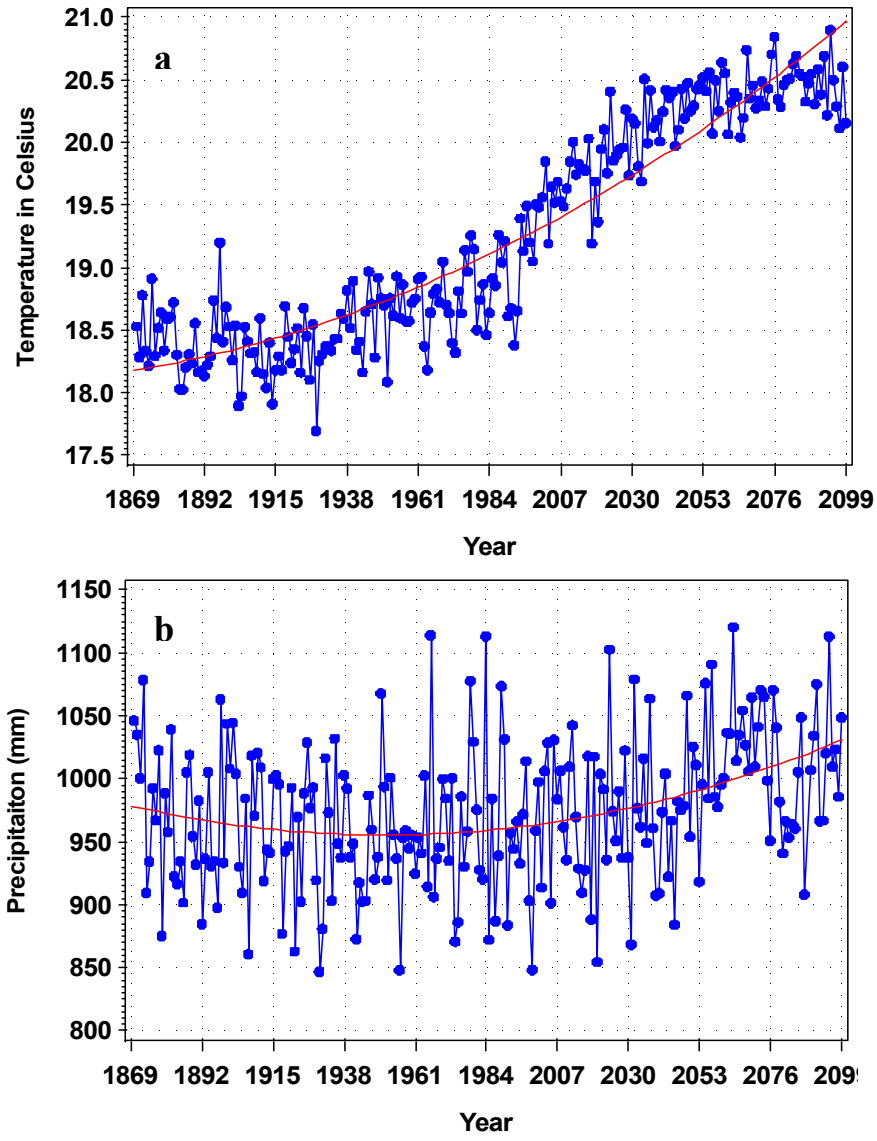

Fig. 7 CCSM3 simulated Louisiana annual (a) mean temperature and (b) annual precipitation for 1870 to 1999 with the 20C3M scenario and for 2000 to 2099 with the B1 scenario. Atmospheric carbon dioxide concentrations and other input data in 20C3M experiment are based on historical records or estimates beginning around the time of the Industrial Revolution. The IPCC SRES B1 experiment is based on projected low population growth, high GDP growth, low energy use, high land-use changes, low resource availability, and medium introduction of new and efficient technologies. For the B1 scenario, atmospheric carbon dioxide reaches 550 ppm by the year 2100. Data source: EOS-WEBSTER (http://eos-webster.sr.unh.edu/home.jsp).

photosynthesis and respiration processes (Fig. 8). The total amount of carbon captured via photosynthesis, the main entry of carbon into forest ecosystem, is gross primary productivity (GPP). Approximately half of it is lost back to the atmosphere through forest growth and maintenance respirations (autotrophic respiration). The balance between GPP and the respiration is net primary productivity (NPP), a net flux of carbon from the atmosphere into forests per unit time. Through allocation process, the carbon captured by photosynthesis is partitioned in proportion to all tissues (e.g., stem, branch, foliage, coarse roots, fine roots, mycorrhizae, and reproduction). As a result of fallen foliage, branches, and root turnovers, carbon is transferred to soils from above- and below-ground biomass, thereafter to be released back to the atmosphere by decomposition (heterotrophic respiration) or lost as either dissolved organic or inorganic matter into the aquatic ecosystem. Only the carbon that is stored in woody biomass, such as roots, stems, and branch material, is sequestered for a longer term.

Globally, forest and soils contain about 1146 Pg of carbon with over two-thirds of the carbon contained in soils and associated peat deposits (Dixon et al. 1994). Forests in the northern hemisphere, particularly between latitude 37N and 64N, have been identified as a sink of carbon due to regrowth on abandoned agricultural land, reduced fire frequency, longer growing seasons, and fertilization by carbon dioxide and nitrogen (Ciais et al. 1995; Fan et al. 1999; Goodale et al. 2002; Houghton and Hackler 2000; Houghton et al. 1999; Nishizono et al. 2005; Schimel et al. 2001; Turner et al. 1995a). In the United States, forests occupied 251 million hectares of land in 2002. These forests contained approximately 52.5 Pg of carbon in their above- and below-ground biomass, with a carbon density of 17.7 kg/m^2 (Birdsey 1992). Since 1952, carbon stored in U.S. timberland has increased by 38% or 8.8 Pg. Carbon storage is expected to increase until 2040, but at a slower rate than at present (Birdsey et al. 1993). The U.S. forests are removing 10% carbon (200 Tg) of fossil fuel emissions annually from the atmosphere (Birdsey et al. 2005),

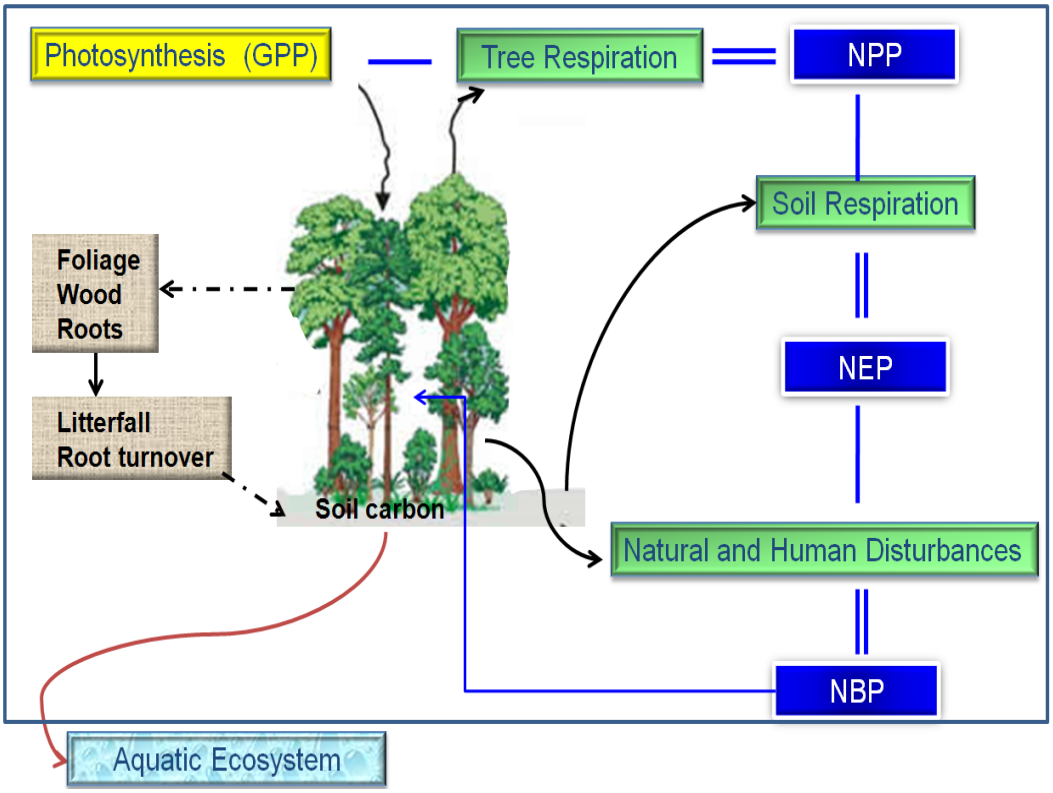

Fig. 8 Net primary productivity (NPP), net ecosystem productivity (NEP), net biome productivity (NBP), and carbon cycling in forest ecosystems.

thereby mitigating the atmospheric carbon dioxide concentrations. Forests in Louisiana cover 48% of the state's area. The total above-ground forest biomass carbon in Louisiana, including live and dead trees, understory vegetation, downed dead wood and the forest floor was increased from about 300 Tg in 1950 to about 460 Tg in 2000 with a mean annual change of 3.9 Tg per year from 1953 to 1997 (Mickler et al. 2004).

Spatial and temporal changes in carbon in forest ecosystems have been documented. In the United States, carbon stocks vary at a regional scale with 39% of U.S. forest carbon is stored in Pacific Coast forests, 15% in the Rocky Mountains and the Northeast regions, and 10% in the Southeast, South Central, and North Central regions (Birdsey 1992). The Northeast region gains the largest carbon accumulation (Turner et al. 1995b). Most of the individual states show

increases in the ecosystem and wood products carbon but a few states show a decreasing trend (Birdsey and Lewis 2002). The carbon storage also differs by ownerships, forest types, and class-age (Birdsey and Lewis 2002; Guldin and Kaiser 2004; Smith and Heath 2002; Turner et al. 1995a). Non-industrial private owners gain the most carbon by a significant margin, followed by National Forests from 1987 through 1997. In contrast, the forest industry and other public ownership groups lose carbon (Birdsey and Lewis 2002). Among forest types, oak-hickory contains the highest carbon storage in the Eastern United States (Guldin and Kaiser 2004). Douglas - fir contains the highest storage in the Western United States. Pinyon - juniper has the lowest amount of carbon because it occurs in dry climates that support lower vegetation densities (Birdsey 1992). The amount of carbon stored in the forest ecosystem is strongly related to class-age (Guldin and Kaiser 2004; Turner et al. 1995a). In young forest land, as the tree bole volume rapidly accumulates, the forest ecosystem become a strong carbon sink. In contrast, rates of mature forest gains are less, due to more stem respiration and a possible reduction of photosynthetic rates (Turner et al. 1995a). Therefore, for a particular year, a mature or old-growth stand may be a carbon source (Song and Woodcock 2003). However, more of the total carbon is significantly stored in a living old forest ecosystem. For instance, the total ecosystem carbon content (vegetation, detritus and soil) of an old ponderosa pine forest (250 years old) in Oregon is about twice that in the young forest (50 years old; 21 vs. 10 kg C m^{-2}) (Law et al. 2001). Conversion of old-growth forests to young fast-growing forests will not decrease atmospheric carbon dioxide in general (Harmon et al. 1990).

In the U.S., total carbon stored in forest ecosystems has been estimated by several researchers using Forest Inventory and Analysis (FIA) data (Birdsey 1992; Birdsey 1996; Birdsey and Lewis 2002; Johnston et al. 1996; Mickler et al. 2004; Schroeder et al. 1997; Smith and Heath 2004; Smith et al. 2003; Van Tuyl et al. 2005). The estimations are often implemented

at county and state scales (Birdsey and Lewis 2002; Brown et al. 1999; Smith and Heath 2004). The major procedure in estimating carbon with FIA data is to convert derived growing-stock volume into the biomass content of all forest components: above-ground, below-ground, understory, and forest floor. Factors to convert tree volume to carbon have been documented by Birdsey (1992), Turner (1995a), Smith and Heath (2002), and Jenkins (2003).

The Role of Forest Dynamics in Global Carbon Cycling

The rates of carbon fixation and release in forest ecosystems via photosynthesis and respiration are subject to climate change, because climate variables have profound effects on forest function and productivity. Temperature, precipitation, nutrients, and soil water are key factors controlling forest growth processes: photosynthesis, respiration, carbon allocation, and evapotranspiration. Temperature impacts photosynthesis, respiration, and evapotranspiration by regulating rates of metabolism and altering water vapor deficit in the air. A warming temperature increases the photosynthesis rate to an optimum, except in regions where it is already close to the optimum temperature, and /or it accentuates water stress (Saxe et al. 2001). Water is a principal requirement for photosynthesis and the main chemical component of most plant cells, thus high levels of precipitation could result in increased growth (Aber et al. 2001). In terms of effects of climate change on forest productivity globally, climate change is believed to have a generally positive impact on forest productivity, if water supply is not limited (Boisvenue and Running 2006). In the U.S., generally, north central and northeastern forests may gain biomass, but forests growing farther south could lose varying amounts of biomass (Winnett 1998). In Florida, as monthly minimum and maximum temperatures are increased by 2°C, the net primary productivity (NPP) of loblolly pine forests has been predicted to decreases by 30% (McNulty et al. 1996b).

Process-based forest growth models can be useful for predicting long term effects of climate

change on forest NPP. It is a measurement of plant growth obtained by calculating the quantity of carbon absorbed and stored by vegetation per unit of area and time. Comprehensive reviews of field methods for estimates of NPP can be found in Clark et al. (2001). However, at a regional scale, the process-based ecosystem models were recognized as the appropriate tool for an estimation of the NPP. Process-based models generally describe key ecosystem processes or simulate the dependence of growth on a number of interacting processes, such as photosynthesis, respiration, decomposition, and nutrient cycling. The main advantage of the models is their capability to generate long-term forecasting through numeric integration of the processes and effects of natural and human-induced changes on carbon budgets (Peng et al. 2002). Over the past three decades, a series of process-based models were developed to simulate NPP and the effects of environmental changes on forest ecosystem dynamics, such as the Net Photosynthesis-Evapotranspiration model (PnET; Aber and Federer 1992), BioGeochemical Cycles model (Biome-BGC; Band et al. 1993; Running and Coughlan 1988; Running and Gower 1991), and the Physiological Processes Predicting Growth model (3-PG;Landsberg and Waring 1997).

PnET has been widely used to predict forest net primary production in foliage, wood and roots, nitrogen, and soil water carbon and water balances of forest ecosystems, as well as environmental effects on forest production at stand and regional scales (Aber and Federer 1992; Aber et al. 1995; McNulty et al. 2000; McNulty et al. 1996a; McNulty et al. 1996b; McNulty et al. 1994; Mickler et al. 2002a; Mickler et al. 2002b; Mickler et al. 2004; Ollinger et al. 1998). Carbon in foliage (bud), wood, and root is allocated from the carbon captured by photosynthesis. The photosynthetic rate is simulated, starting from leaf level, via processes shown by the purple boxes in Figure 9. The whole canopy photosynthesis is computed by these processes, seen as the dark green boxes, also presented in Figure 9. The maximum net photosynthetic rate is assumed as a function of foliar nitrogen concentration. Maximum gross photosynthesis per unit leaf area

is computed as 110% of the max net photosynthesis. Gross photosynthesis is the max gross photosynthesis, modified by the direct effect of vapor pressure deficit on stomatal conductance (D_DVPD), temperature (D_Temp) and soil water stress on stomatal closure (D_water). T_Temp are calculated by temperatures at which photosynthesis starts and the mean day temperature. D_water is determined by transpiration (Trans), potential transpiration (PotTrans), water in soil (water), soil water release parameter (f), potential gross photosynthesis, and water use efficiency (WUE). As photosynthesis is simulated at canopy level, the canopy is divided into 50 layers. The gross photosynthesis in each layer is the photosynthesis on the top of the canopy, modified by light effect (LightEff), a function of half saturation light level (HalfSat) and radiation on the top of the canopy ($\mathbf{I_0}$) , and leaf area index (LAI). The whole canopy photosynthesis per ground area is an integration of the photosynthesis at all 50 layers. PnET input data include a monthly mean maximum and mean minimum temperature, precipitation, radiation, and soil water holding capacity. In order to run the model, 36 variables are required to be parameterized (see Table 1 in (Aber et al. 1995).

Forest Disturbance by Severe Weather

Global warming is expected to change intensity, although not the frequency, of tropical cyclones (Emanuel 2005; Webster et al. 2005); consequently, global warming creates an upward trend in the destructive potential of severe weather. The change possesses a great environmental threat especially to low latitude coastal regions, such as Louisiana.

In the United States, hurricanes are responsible for an annual average of $1.6 billion damage for the period 1950-1989, $2.2 billion for 1950-1995, and $6.2 billion for 1989-1995 (Jarrell et al. 2001). On average, about 10.6 major hurricane (Saffir Simpson scales greater than 2) each decade from 1896 to 1995 made landfalls along the northern Gulf of Mexico (Bove et al. 1998); from 1901 through 1992, 11 of the 50 strongest storms impacted Louisiana (Stone et al. 1997).

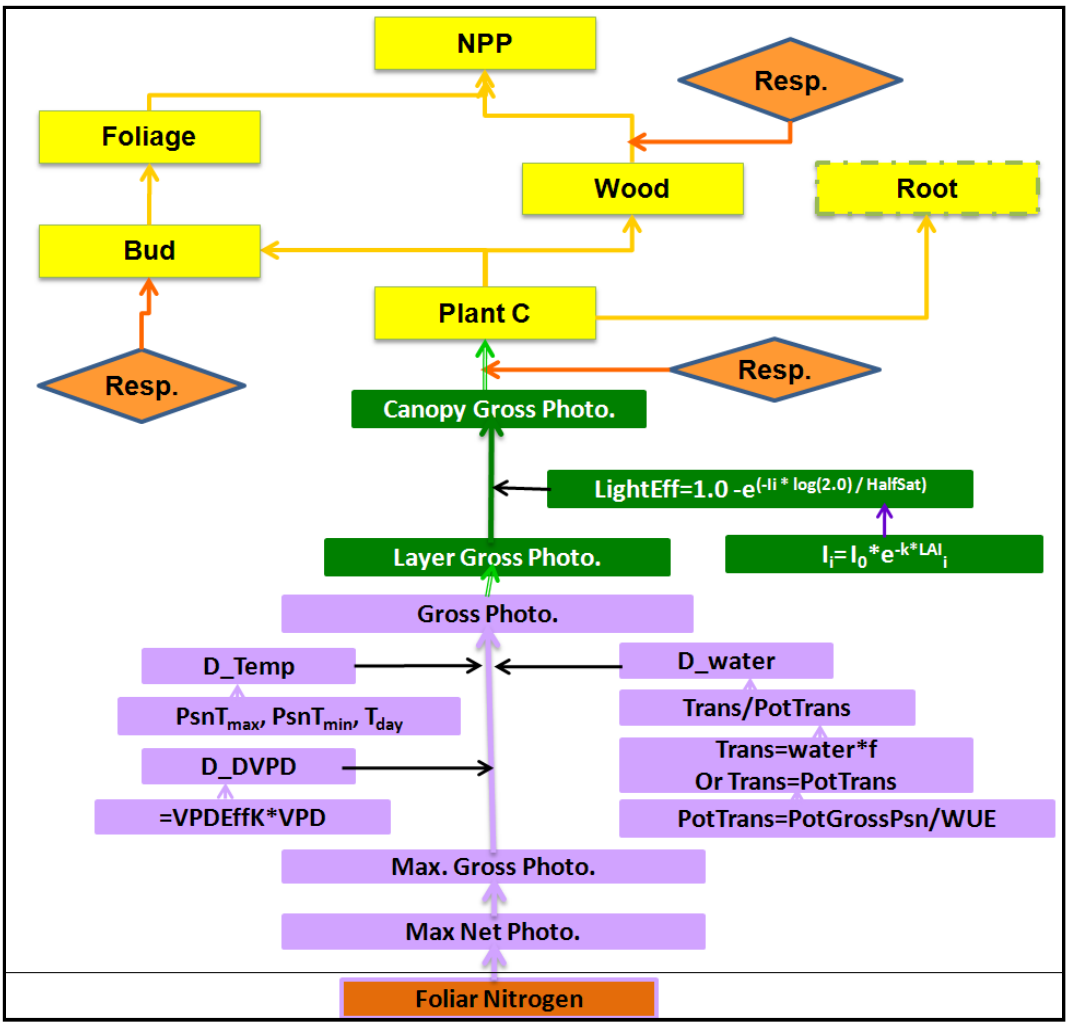

Fig. 9 Flowchart of the simulation procedure in the PnET model.

Three recent dreadful hurricanes, Katrina, Rita, and Gustav made their landfalls in 2005 and 2008, presenting a vivid reminder that the level of destruction from hurricanes is widespread and staggering. Hurricanes often leave a highly heterogeneous landscape, characterized by a mosaic of undisturbed forests with completely and partially uprooted and broken trees, as well as an additional dieback of trees in the lowlands. An accurate determination of area and the severity of disturbed forests and identification of factors contributing to spatial patterns of the hurricane disturbance are essential to allow forest managers and scientists to take short-term actions on salvage harvesting, wood industry, and habitat protection, as well as to make assessments on

long-term environmental effects and forest ecosystem recovery.

Remote sensing techniques supply a time- and cost-saving approach to identify hurricane damage to large area forests, and even to forests inaccessible to ground investigators. Remote sensing usually repeatedly acquires images or information of a phenomenon, object, or material by a recording device without physical, intimate contact with the targets at pre-determined spatial, temporal, and spectral scales. The information on the images can be correlated to properties of the objects and make it possible to inventory, monitor, and research changes of the objects and phenomena. Accuracies of processing and interpretation of the images for deriving understandable information and products depend on the quality of the images and the degree of knowledge possessed by the researchers.

Change detection, one of the remote sensing techniques, has been utilized to detect forest disturbance by harvesting, insect and disease defoliation, and forest fires (Coppin et al. 2004). The change detection procedures detect forestland modifications over a period of interval through application of change detection algorithms to a change index derived from two or multi-date images. Various change indices, such as six Tasseled Cap transformations and NDVI, and different algorithms including univariate image differencing (UID), selective principal component analysis, and change vector analysis have been applied (Coppin et al. 2004). To detect hurricane disturbance to forest, Ramsey et al. (2001) and Ayala-Silva and Twumasi (2004) have applied a UID algorithm to Advanced Very High Resolution Radiometer NDVI values between pre- and post- hurricane.

Severity and landscape patterns of a hurricane disturbance to forests are associated with a series of biotic and abiotic factors including stem size, species, canopy structure, stand density, intensity of the wind, topography, and soil characteristics. Cypress (*Taxodium distichum*) (Putz and Sharitz 1991; Touliatos and Roth 1971) and tupelo (*Nyssa aquatic*) (Gresham et al. 1991) are

reported to be highly resistant to strong winds. Southern red oak (*Quercus falcate*), water oak (*Quercus nigra*), and sweetgum (*Liquidambar styraciflua*) are found to be more susceptible to strong tornado winds, compared to loblolly (*Pinus taeda*) and longleaf pines *(P. palustris*) (Glitzenstein and Harcombe 1988). Shorter trees with smaller diameters are usually less severely damaged than taller trees with larger diameters (Francis 2000; Lugo et al. 1983; Ostertag et al. 2005; Reilly et al. 2002). Poor drainage and seasonal water logging (Mayer 1989; Ray and Nicoll 1998) can lead to lower stand stability against wind damage. Forests growing on windward slopes are more vulnerable to windthrow than those on leeward slopes (Bellingham 1991; Foster and Boose 1992; Lugo et al. 1983; Reilly 1991), and forests in lower elevations receive more damage than those in higher elevations (Reilly et al. 2002).

In order to assess an association of hurricane disturbance, together with a series of ecological factors at a regional scale, remote sensing techniques integrated with geographic information systems (GIS) could be applied for explanation and prediction of the cause-effect between the factors and the disturbance. The value of GIS applications lies in the ability to analyze spatial data using spatial analysis methods and involving integration of spatially referenced data in a problem-solving environment. Integration of GIS and remotely sensed data, a major GIS data source, offers a tool for extending the knowledge gained from intensive in-situ investigations to larger geographic areas at more frequent intervals and for a longer period of time. Based on an empirical function of wind damage with forest exposure, tree height, and species composition, Foster and Boose (1992) constructed a GIS framework to analyze forest responses to strong wind at landscape level and concluded the predicted results were in good agreement with the field measurements. Boose et al. (1994) demonstrated that wind velocity gradients, variation in site exposure, local topography, and forest species composition and structure controlled hurricane damage to forests at landscape scale through assessment of actual

forest damage with remotely sensed data. Furthermore, McMaster (2005) predicted forest areas would be damaged by a severe storm by using slope, aspect, soil moisture, relative elevation, and land cover as predictors, thus achieving an overall prediction accuracy of 60%.

CHAPTER 3 SPATIAL DISTRIBUTION OF FOREST BIOMASS CARBON IN LOUISIANA AND ITS RELATIONS TO WATERSHED CHARACTERISTICS

Introduction

Forests have been recognized as playing a critical role in global carbon cycle by offsetting anthropogenic carbon dioxide emission into the atmosphere (IPCC 2007b). Forests exchange carbon with the atmosphere through photosynthesis and respiration processes. These processes and the rate of global carbon exchange can be affected by a number of anthropogenic activities and natural disturbances, such as timber harvest, conversion of forest land to other land uses, wildfires, disease, and hurricanes. Under severe circumstances, human activities and natural disturbances can completely turn forests from a carbon to an atmospheric carbon dioxide source. Consequently, forest carbon storage fluctuates over time and across the landscape. As global climate change research intensifies its focus on regional and local levels, an accurate estimation of carbon storage in the forest ecosystem at various temporal-spatial scales increasingly gain global attention (Brown 2002). Particularly, spatial estimates of carbon storage, coupled with mapping forest biomass, can supply knowledge for land-owners and policy-makers to monitor changes in forest ecosystems, and thus manage forests for carbon sequestration, as well as the sustainable development of forest industry (Labrecque et al. 2006).

Forests in Louisiana cover an estimated 48% (or 5.2 million hectares) of the state total land area. In addition to an economic contribution as the second largest industry in the state ($4.4 billion in 2007), Louisiana's forests also are a tremendous carbon sink, converting considerable amounts of carbon dioxide into biomass. Forest carbon storage in Louisiana has been estimated with Forest Inventory and Analysis (FIA) data by several researchers (Birdsey 1996; Birdsey and Lewis 2002; Brown et al. 1999; Mickler et al. 2004; Smith and Heath 2004; Smith et al. 2003; Xu and Wang 2006). However, because the researchers used the FIA data collected from different inventory dates and applied different spatial aggregation, different carbon storage data has been reported. In a recent study, Xu and Wang (2006) found that from 1991 to 2003, biomass

carbon stocks in forest groups of elm-ash-cottonwood, oak-hickory, oak-gum-cypress, loblolly-shortleaf pine and oak-pine decreased by 18.4, 13.8, 10, 9.6, and 2.7%, respectively. In contrast, carbon storage in longleaf-slash pine forests increased 11.8%, which may be due mainly to the native pine restoration effort since the early 1990s. Although the total carbon storage in Louisiana forests declined 9.3%, the forested land area increased by 1.7%, showing the dynamic relation among reforestration, growth, and carbon stock. During 2000-2006, the USDA Forest Service completed another FIA assessment for Louisiana. As more timely data via a five-year annual inventory strategy become available, there exists a great need for a spatial modeling tool that is readily conducive to large-scale analysis of carbon storage.

As a unit of management, watershed facilitates an examination of interrelationships between land and water use, and multiple environmental effects of these relationships on the terrestrial ecosystem. Watershed characteristics, such as drainage density and average watershed slope, represent a variability of soil physical, biogeochemical, and microclimate variables among watersheds. Drainage density is probably the parameter which most globally represents the interaction between climate and geomorphology in the development of the drainage network (Rodrigueziturbe and Escobar 1982). Topographic features such as slope and aspect have also been found to be important watershed characteristics for determining nutrient export rates (Sonzogni 1980) and radiation (Piedallu and Gegout 2007), and thus species of richness and diversity (Olivero and Hix 1998). In a recent study, Zhong and Xu (2009) reported that soil organic carbon density at the watershed scale reflected a close relationship with the drainage density and average watershed slope. This finding suggests that positive relations between forest biomass carbon and watershed features may exist, and that such relationships may be useful for developing large landscape carbon prediction models.

This study was conducted to (1) produce spatially explicit estimates of forest biomass

carbon storage in Louisiana with a fine grid (30 by 30 m) and watershed scales with FIA data; (2) assess relationships of two watershed features of drainage density and he average watershed slope with carbon storage; and (3) create a spatial modeling system that is conducive to assessing forest biomass carbon changes using FIA information. Furthermore, the results coupled with the technical approach of this study build a foundation for two other studies on climate change and extreme weather effects on forest biomass carbon dynamics, which are reported and discussed in Chapters 4, 5, and 6.

Methods

Study Area

Louisiana is situated on the lower course of the Mississippi river. The state is located between 89° W and 94º W in longitude and between 29° N and 33º N in latitude. It is a low-lying state with an average elevation of 30.5 m, ranging from 2.4 m below and 163.0 m above sea level. The land surface is divided naturally into two major parts – the uplands, and the alluvial and coast swamp regions. Louisiana has a relatively constant, semitropical climate, mainly determined by its subtropical latitude and its proximity to the Gulf of Mexico (National Climatic Data Center 2009). In summer, the moist and semitropical weather often proves favorable for afternoon thunderstorms. In the colder season, the tropical air and cold, continental air alternately occupies the state for a period of time. Based on long-term records, the state experiences an average annual temperature and precipitation of 19.2 °C and 1562 mm.

Forests in the state cover 5.17 million hectares of land, or 48% of the state's total land area. Broadly, these forests are classified into four categories of deciduous, evergreen, mixed and woody wetland forests with an area of 0.22, 2, 0.37, and 2.58 million hectares, respectively, as computed from 2001 National Land Cover Dataset (NLCD) (Multi-Resolution Land Characteristics Consortium 2001). Spatially, the predominant forest type groups in Louisiana are

oak-gum cypress and elm-ash-cottonwood in the north and south Deltas (Rosson Jr. 1995). The second in dominance is the loblolly-shortleaf pine, distributed in southwest and northwest portions of the state. For longleaf-splash pine, 83% of this species distribute in the southwest part of Louisiana. In terms of forest coverage in parishes, the forest coverage changes parish to parish, with over 60% forested land in 27 parishes, and less than 20% forest coverage in nine parishes. In terms of ownership, nonindustrial private forest ownership is the dominant land ownership.

Forest Biomass Carbon Estimation

The carbon stored in the forest biomass at the watershed scale was estimated through four steps. First, the forest biomass carbon in each plot, designed and inventoried by the USDA Forest Service, was computed with the FIA dataset. The dataset was collected by the agency, beginning in 1930 and presenting a continuous cycle of about 10 years. In Louisiana, the latest inventory was conducted during 2000-2006. The 2006 dataset includes 12 attribute tables, listing attributes of tree and site information of 6589 plots established across the state. Of all the plots, 2,899 plots are identified as plots representing forestlands (Fig. 10). Each plot occupies 0.4 hectare (1 acre) forest land and represents about 2428 hectares (6000 acres) of land. If the plots are forested strips, then these must be 37 m (120.0 ft) wide for a continuous length of at least 111 m (363.0 ft) in order to meet the one acre threshold for a plot. The biomass carbon in each plot was calculated as 50% of the sum of the dry biomass of all trees, with a diameter at breast height equal to or larger than 1 inch within the plot (Alerich et al. 2006). The reported biomass represents an oven-dry weight of the total above-ground biomass, including all tops and limbs (but excluding foliage). Specifically, the equation for the computation is listed below:

$$c = tpacurr * drybiot * 0.5$$

where c (pound/acre) is carbon storage in each plot; *tpacurr* is the number of trees per acre that

the tree represents for calculating current estimates of the number of trees, volume, and biomass on forest land; *drybiot* in pound is the oven-dry biomass weight of the representative tree; and 0.5 is the conversion factor of dry biomass to carbon.

Secondly, each plot was assigned a forest type of evergreen, deciduous, mixed, or wetland Forests, which were derived from NLCD 2001 (Fig. 11). NLCD 2001 was created by the Multi-Resolution Land Characteristics (MRLC) Consortium, a group of federal agencies. In 2000, the MRLC consortium purchased three dates of Landsat 7 imagery to coordinate the production of a comprehensive land cover database for the nation. The land was classified into 29 covers nationwide with four forest classes: evergreen, deciduous, mixed, or wetland forests.

Thirdly, four Thiessen polygon GIS layers for the four forest types of FIA plots were generated in order to interpolate carbon storage from plot level to the entire forested lands in the state (Fig. 12). Thiessen polygon is one of methods of spatial interpolation, which assigns values of the observed point to unsampled locations within the polygon. Unique properties of the polygons are that each polygon is created by only one point, and any location within a polygon is closer to the point than to points in any other polygon. It is used widely to provide a simple overview of the spatial distribution of values. In this study, carbon storage in each plot (centroid of the Thiessen polygon) was assigned to all forested cells within the Thiessen polygon. The forested cells are determined, based on the 2001 NLCD (Fig. 11).

Eventually, carbon storage in all cells within a watershed was summarized as the total carbon storage in the watershed (Fig. 13). The watershed spatial layer, "Dataset Watershed Subsegments for Louisiana," was developed for the Louisiana Department of Environmental Quality Office of Water Resources' watershed assessment and management tasks. The watershed boundaries were hand-delineated on the USGS 15-minute Topographic Map, and then digitized (Louisiana Geographic Information Center 2004). Certain drainage boundaries were updated, using USGS

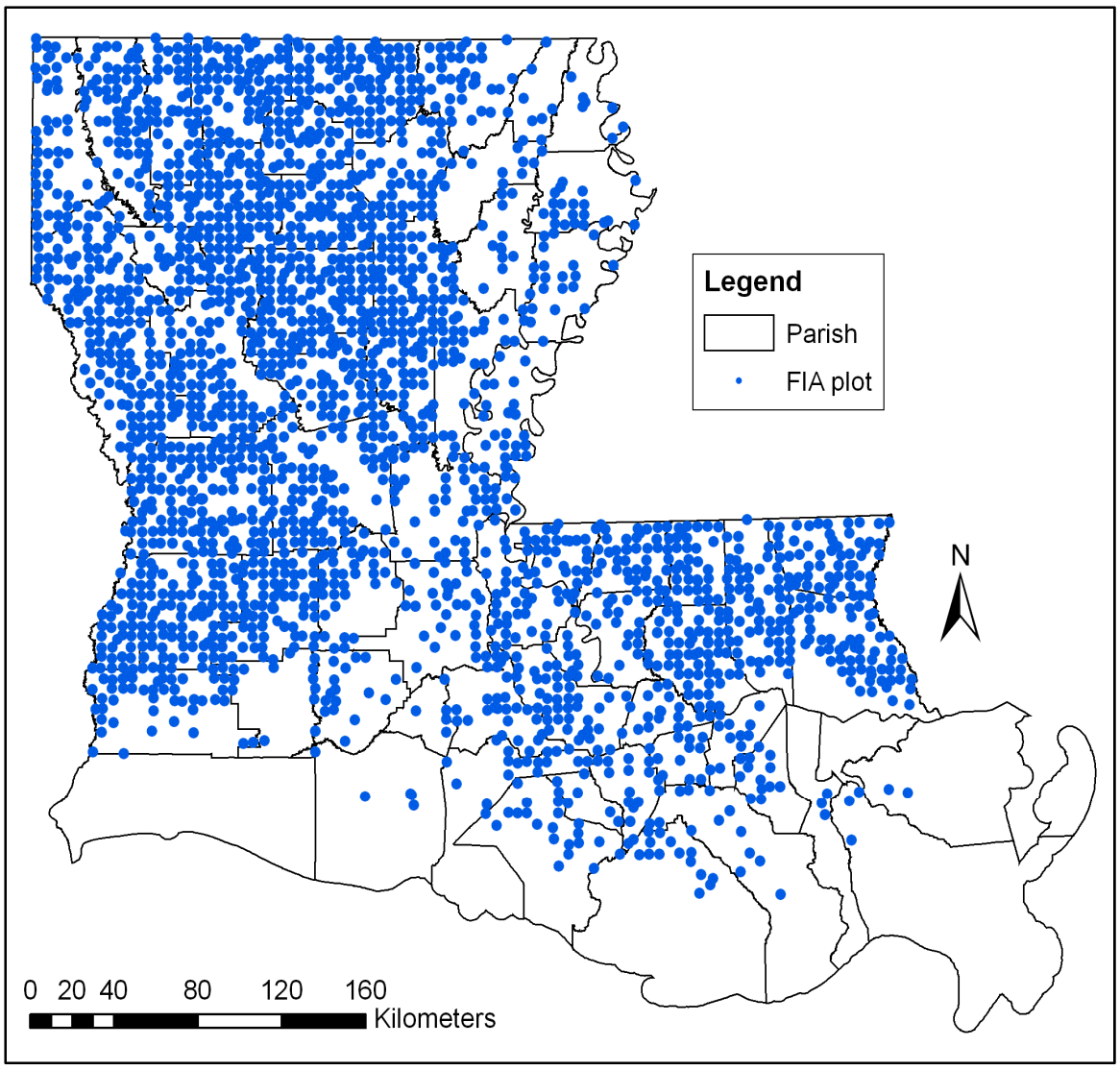

Fig. 10 Field plots in Louisiana established by the Forest Inventory and Analysis (FIA) Program of the U.S. Department of Agriculture Forest Service.

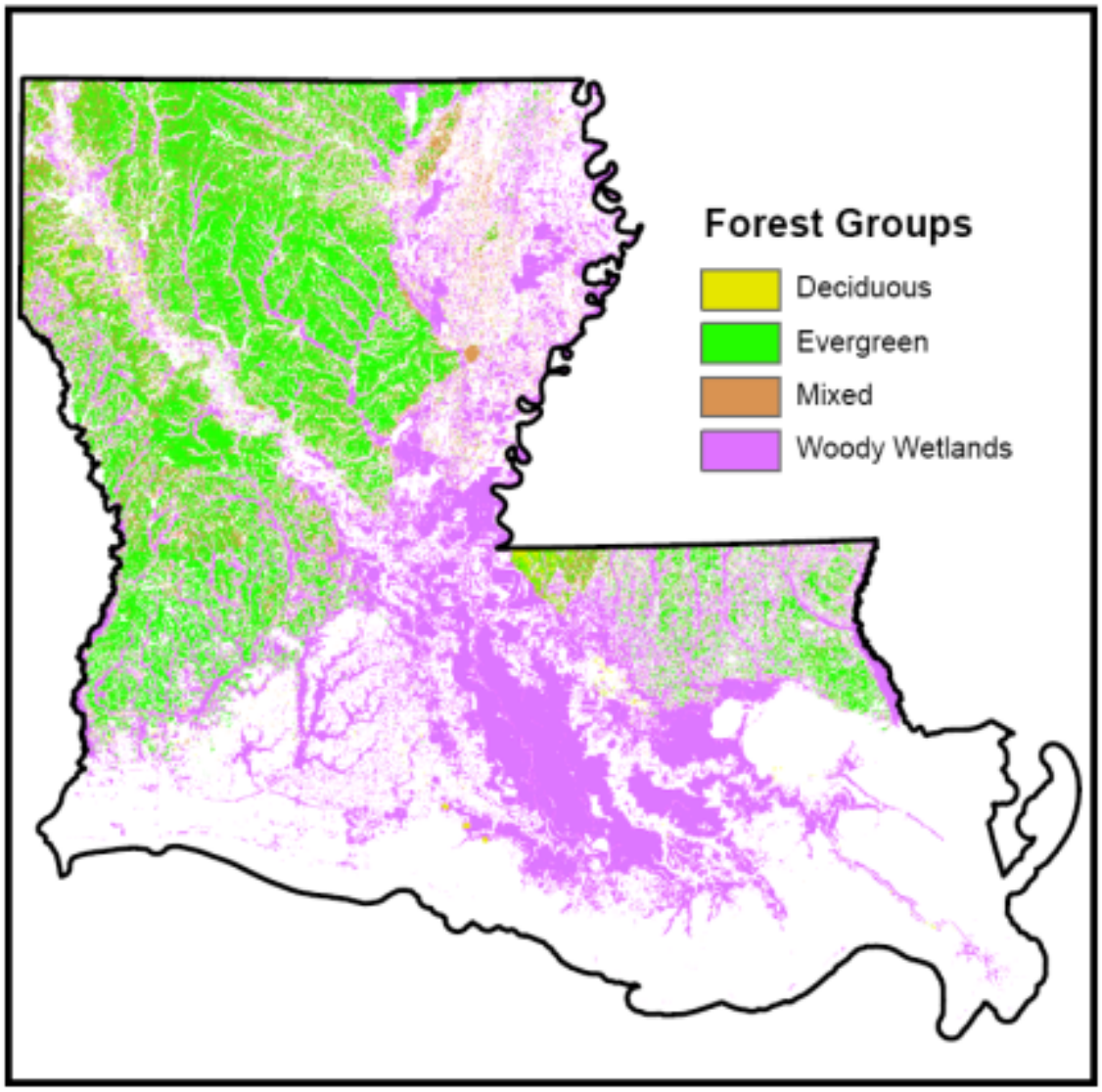

Fig. 11 Forest distribution in Louisiana generated from 2001 National Land Cover Dataset.

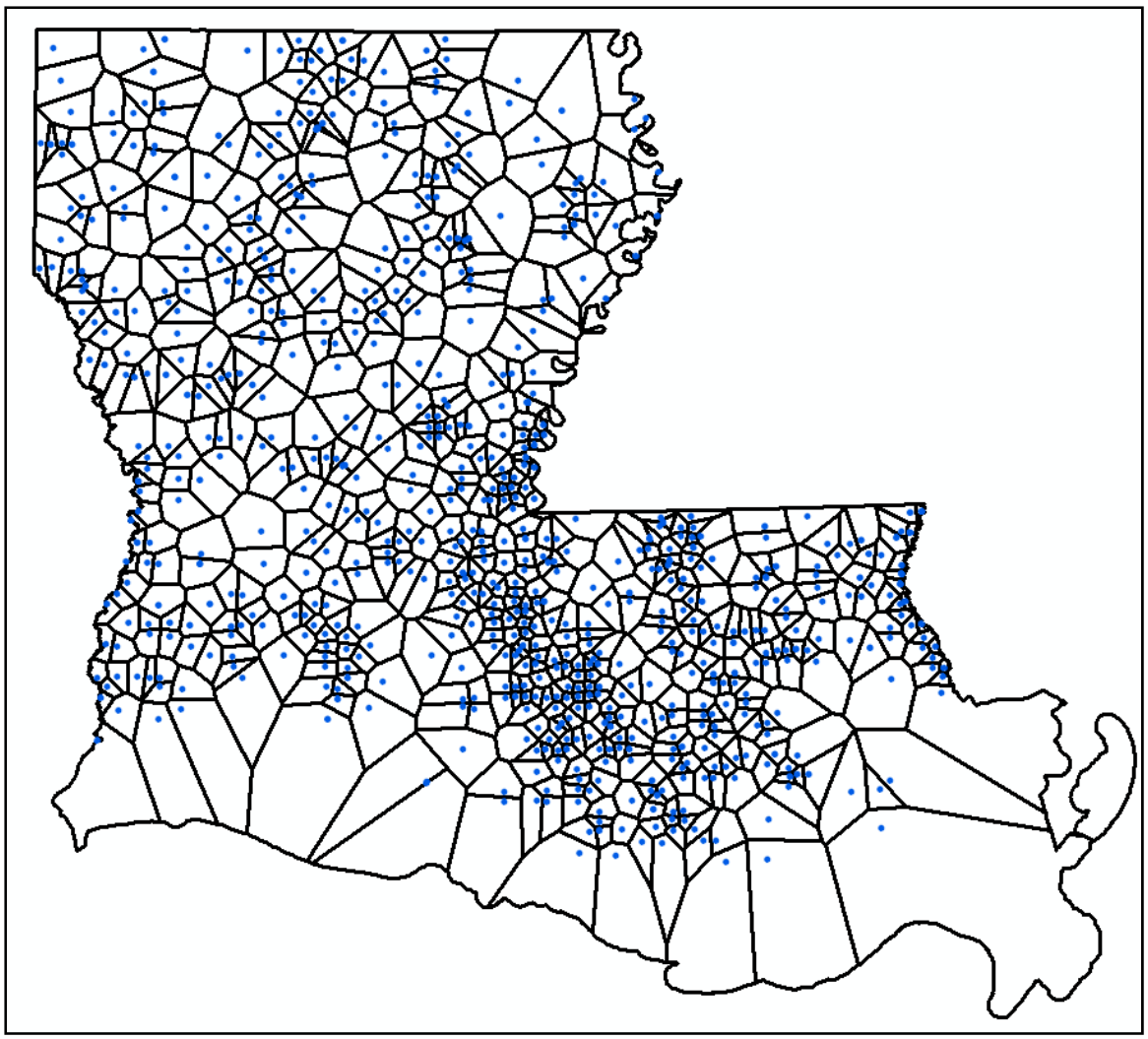

Fig. 12 Thiessen polygons created for forest inventory plots across Louisiana.

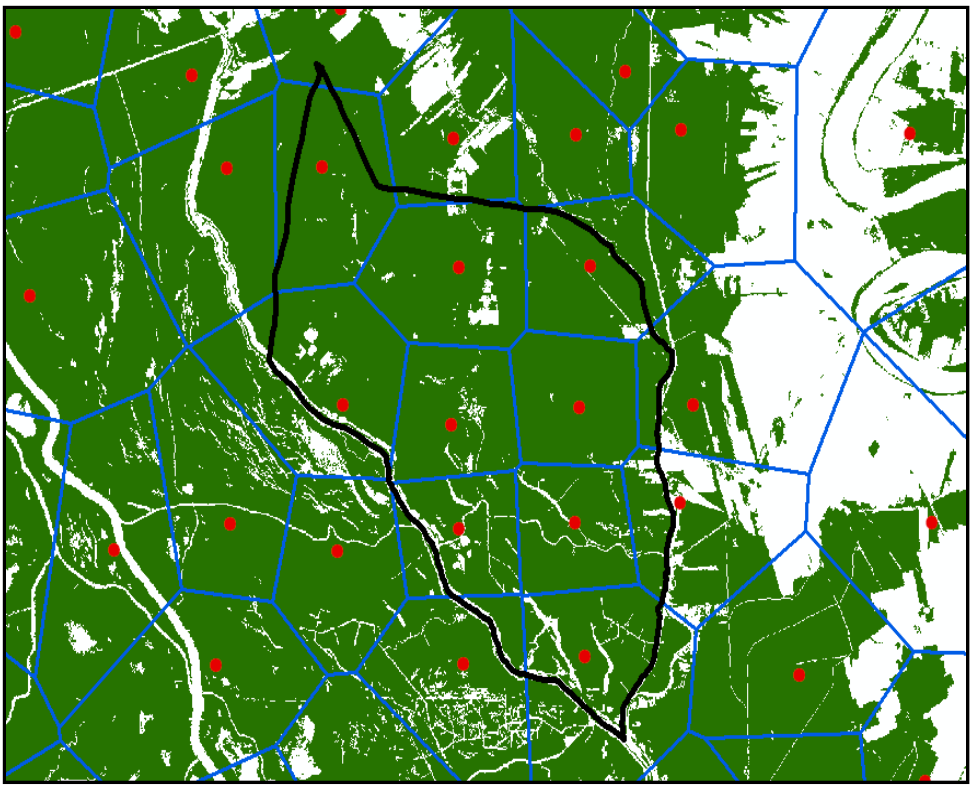

Fig. 13 Assignment of forest biomass carbon from a plot (red dot) to all forest cells (green, 30 m by 30 m) within a Thiessen polygon of the plot (blue). Carbon storage in a watershed is a sum of the carbon in all cells within the watershed boundary (black).

2400 Topographic Maps. A total of 484 watersheds were delineated with an average area of 267 km^2 varying from 0.23 km^2 to 3115 km^2.

Relationship between Carbon Storage and Watershed Features

Relationships of two watershed features of drainage density and average watershed slope with carbon storage in watersheds were assessed through a regression analysis. Drainage density is a ratio of the total length of streams within a watershed to the total area of the watershed. The length of streams and rivers in a watershed was calculated by overlaying "National Hydrography Flowlines Data" over the watershed boundary layer. The average watershed slope was computed as a mean of slopes of all digital elevation model cells (30 m × 30 m) in a watershed.

Results

Carbon Storage and Spatial Distribution

Forests in Louisiana, occupying 5.2 million hectares land, stored 219.2 Tg of carbon with an average of 43.2 Mg/ha (Table 1). Among the four types of forests, wetland and evergreen forests accounted for 89% of the forested land, and stored over 90% of the carbon. Mixed and deciduous forests stored less than 10% of the carbon on about 11% forest areas, which indicated that forest area was the most important factor in determining fractions of total carbon storage in each type of forest across the state. Among the forest groups, carbon density tended to vary with wetland forests having the highest carbon storage capacity. However, the slight difference of carbon density among the forest types indicated that the carbon density was not a factor in determining the wide range of carbon storage among the forest types.

Table 1 Carbon storage in Louisiana forests

Forest Type	Forest Area		Carbon Density	Carbon Storage	
	$*10^3 km^2$	(%)	(Mg/ha)	(Tg)	(%)
Deciduous	2.2	4.2	33.6	7.2	3.1
Evergreen	20.0	38.8	39.4	77.4	35.3
Mixed	3.7	7.2	37.2	13.8	6.3
Woody wetlands	25.8	49.9	47.8	120.8	55.1
LA state	51.7		43.2	219.2	

Spatial distribution of forest carbon density in Louisiana presented apparent variability with a range of 1- 234 mg/ha (Fig. 14). The pixels with high carbon density mainly were distributed along the Red River, and in the Atchafalaya River and Lower Pearl River valleys. As the pixel size was raised from 30 m by 30 m (Fig. 14) to 12 km by 12 km (Fig. 15), a clearer pattern of the carbon density with three categories was displayed. An analysis of the area percentages of the four forest types in the three carbon density categories (Table 2) revealed that the pixels associated with high carbon density more likely could be wetland forests, as carbon density

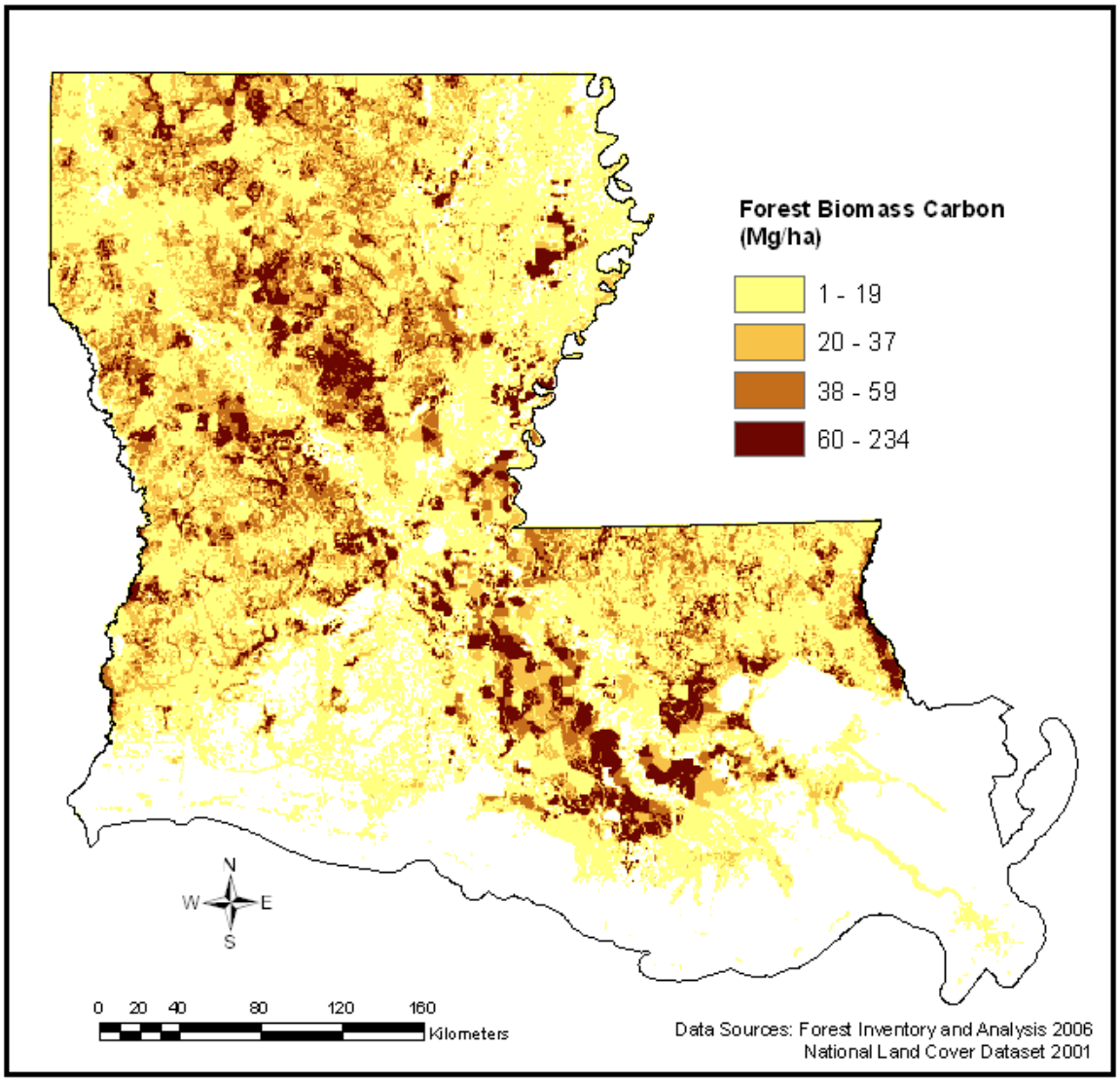

Fig. 14 Distribution of forest biomass carbon density at pixel size of 30 m by 30 m across Louisiana.

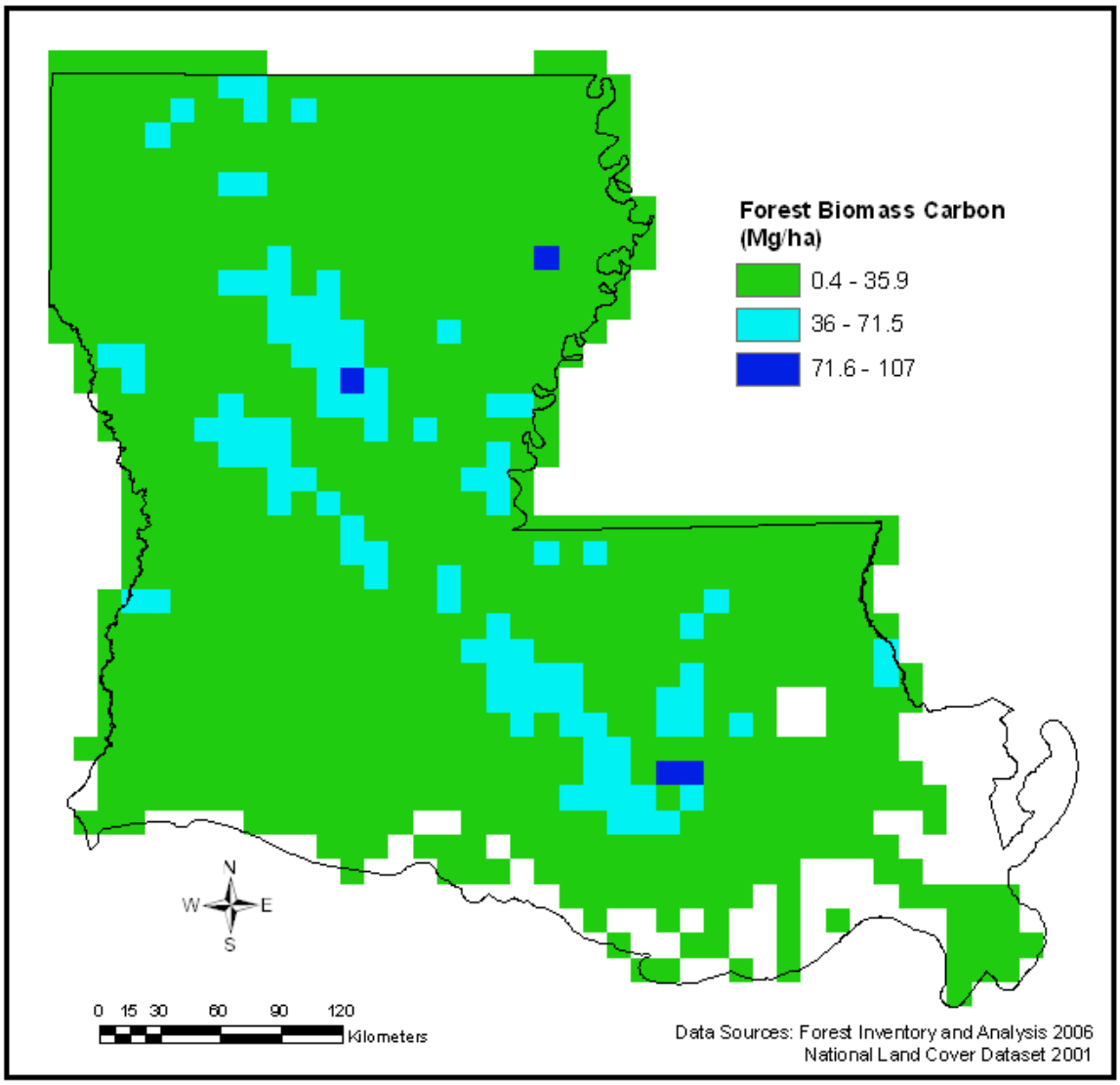

Fig. 15 Distribution of forest biomass carbon density at pixel size of 12 km by 12 km across Louisiana.

Table 2 Area fractions of the four forest categories in the carbon density classes

Carbon range (Mg/ha)	Deciduous (%)	Evergreen (%)	Mixed (%)	Woody wetlands (%)
0.4-35.9	4.6	39.9	8.0	47.5
36-71.5	2.8	36.4	4.5	56.2
71.6-107	1.0	20.2	1.6	77.2

increased from categories 1 to 3, the area percentages of deciduous, evergreen, and mixed forests decreased dramatically, while the percentage of woody wetlands noticeably rose.

Biomass Carbon Storage on Watersheds

The average biomass carbon storage on Louisiana's watersheds was 0.5 Tg with a standard deviation of 0.9 Tg. The average carbon density in watersheds varied by 19.9 Mg/ha with a standard deviation of 17.3 Mg/ha. Although the spatial distribution of total carbon storage and carbon densities across all watersheds in the state varied, no noticeable trends were presented (Figs. 16 - 18). An analysis of the correlation of total carbon storage and forest area in the watersheds showed that these two were highly correlated (R^2=0.93; Fig. 19), indicating that the forest area was the main factor in determining the quantity and spatial pattern of carbon in the watersheds.

Watershed Features and Its Relation to Carbon Storage

In Louisiana, the 484 watersheds had an average watershed degree of 2.7 degrees and a range from 0 to 14.6 degrees (Fig. 20). The watersheds with a slope degree of less than one were mainly distributed in coastal areas and the Mississippi River Valley (Fig. 20). The mean drainage density was 1.7 km/km^2 with a maximum of 8.9 km/km^2 and a minimum of 0. A map of drainage density showed that watersheds with a higher drainage density clustered and mainly distributed at three locations: the southeast coast, the east Florida parishes, and the middle of the upper part of Louisiana (Fig. 21). No correlations were identified between the total carbon storage in the watershed with drainage density (R^2=0.004; Fig. 22a) and watershed slope (R^2=0.09; Fig. 22b).

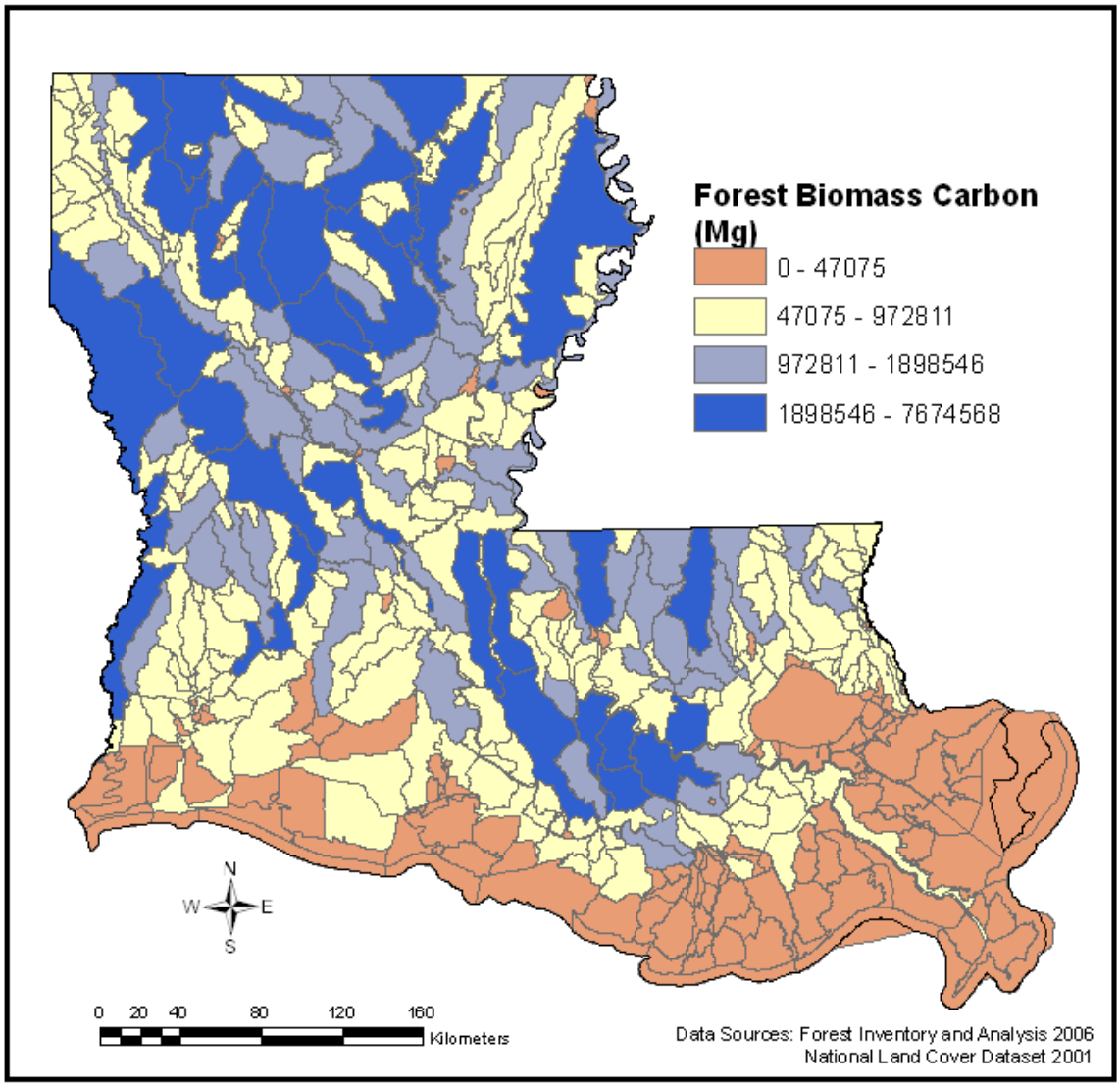

Fig. 16 Total forest biomass carbon stock across Louisiana's watersheds.

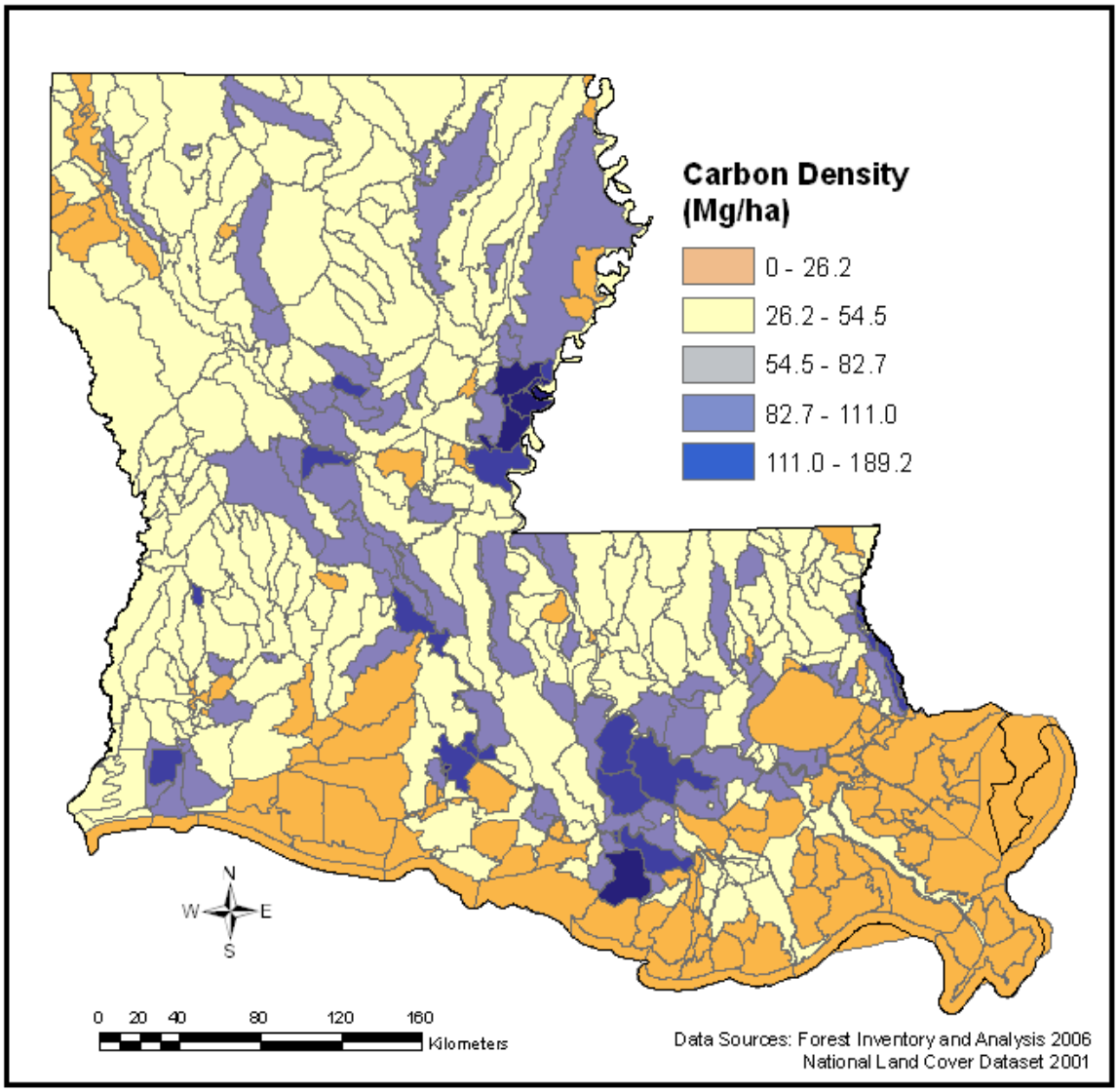

Fig. 17 Forest carbon density (total carbon divided by forest area) across Louisiana's watersheds.

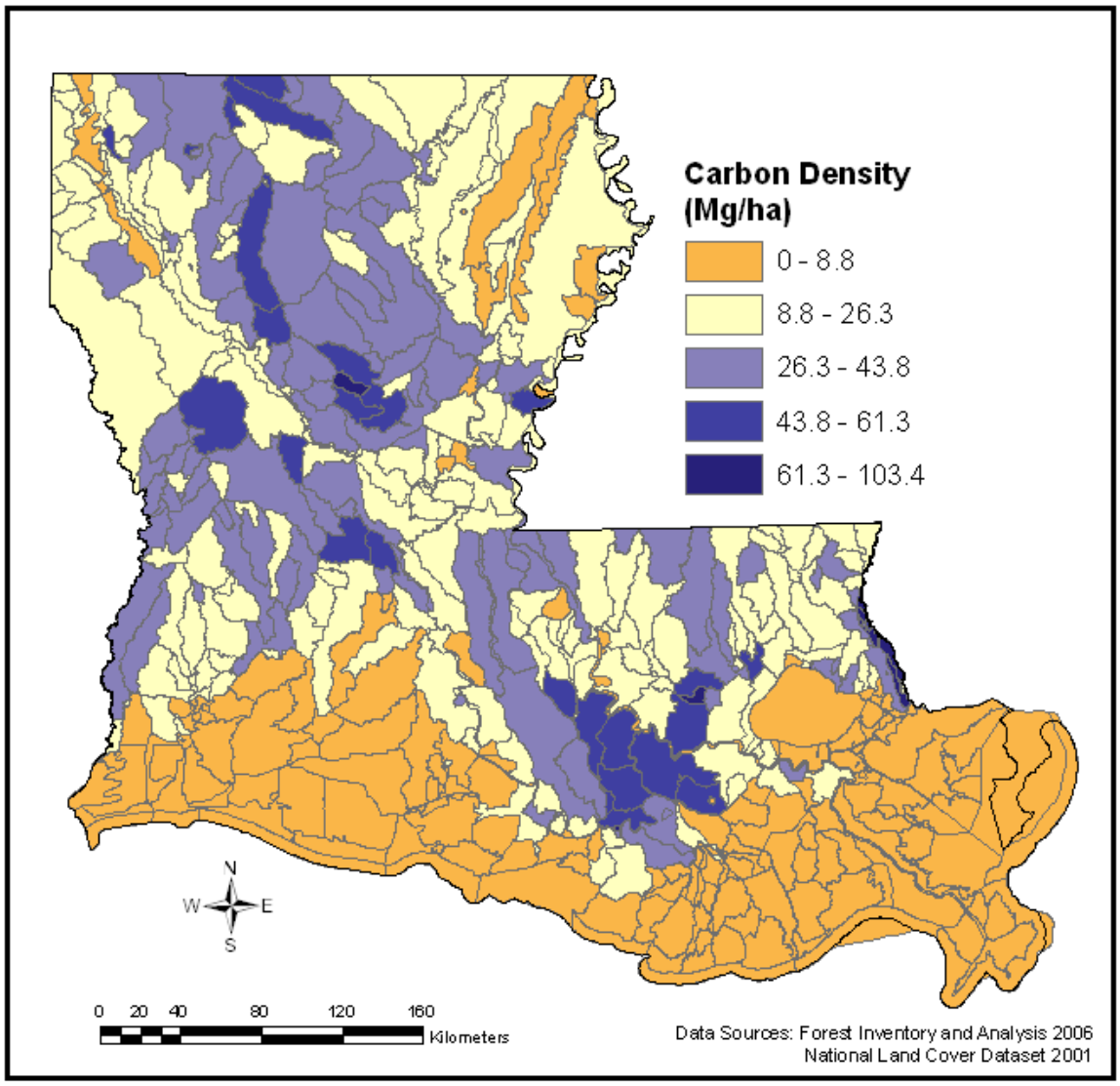

Fig. 18 Forest biomass carbon density (total carbon divided by total watershed area) across Louisiana's watersheds.

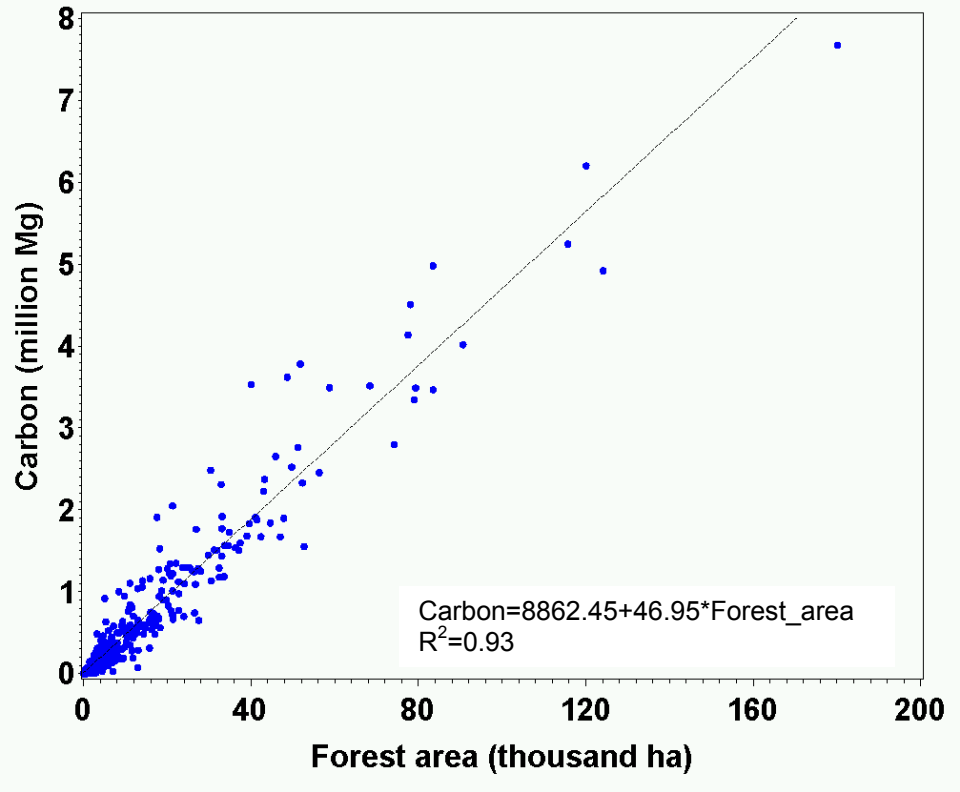

Fig. 19 Relationships of forest biomass carbon stock at the watershed scale with the total forested land area.

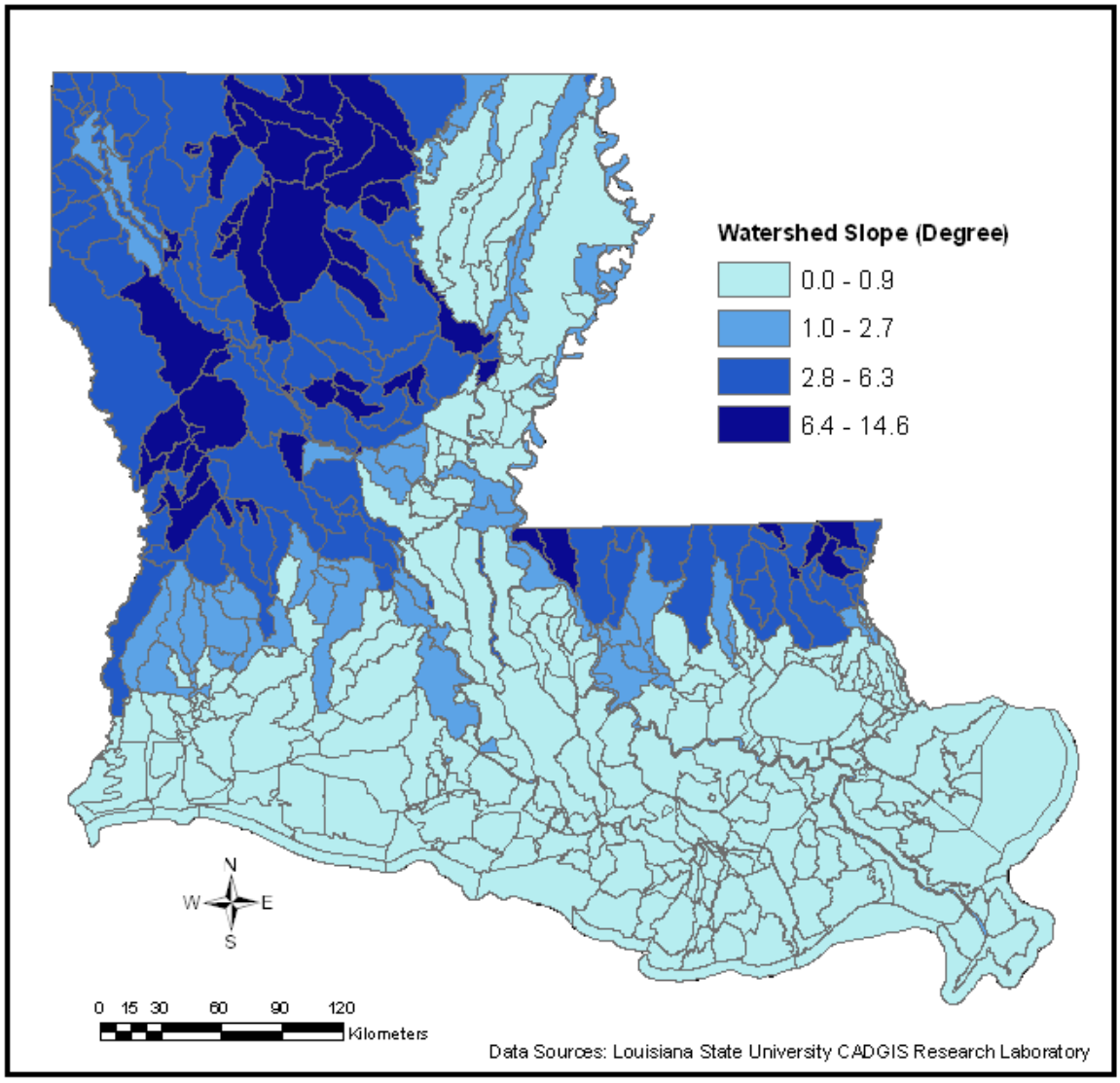

Fig. 20 Average slope degree of Louisiana's 484 watersheds.

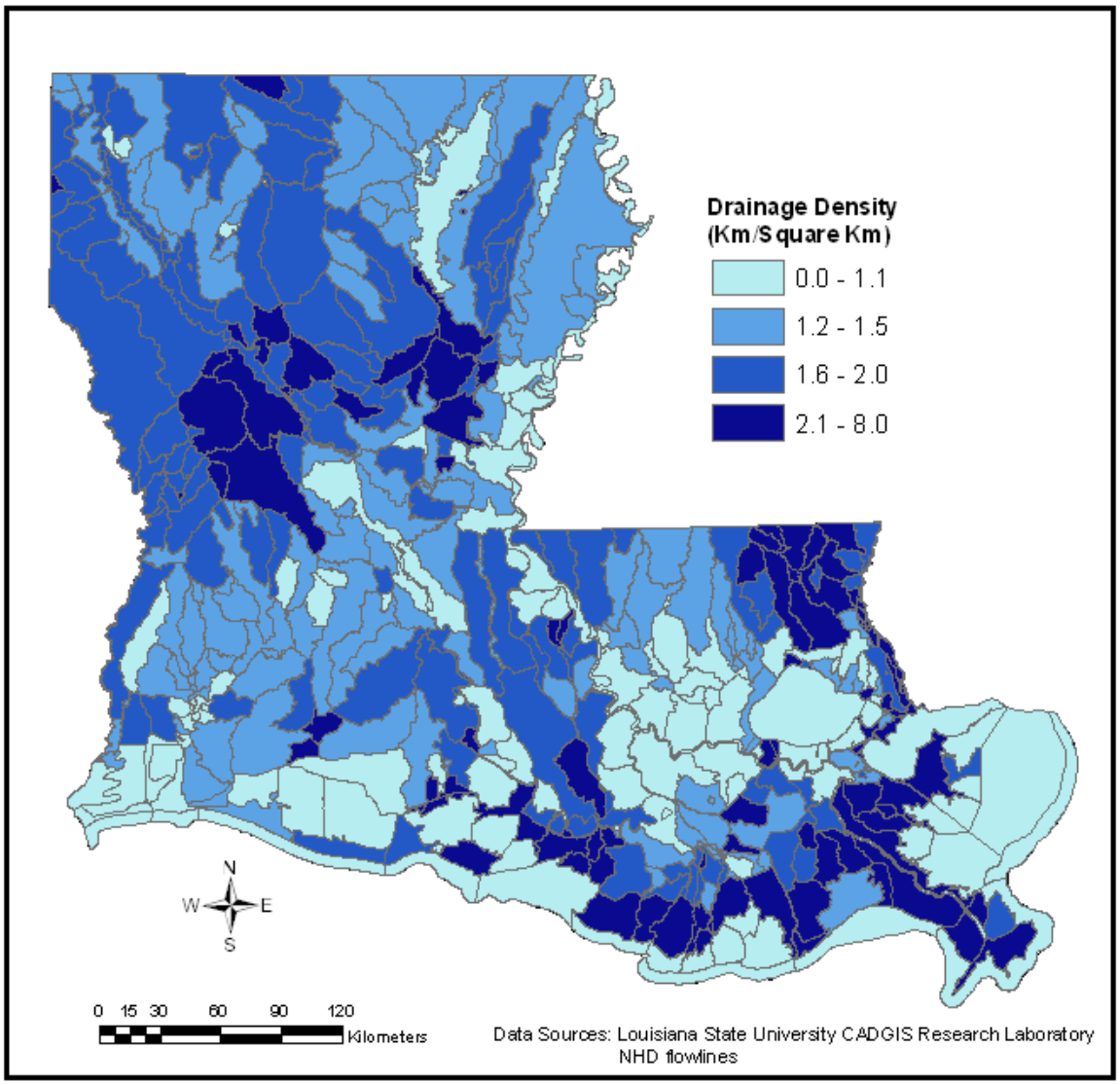

Fig. 21 Drainage density of Louisiana's 484 watersheds.

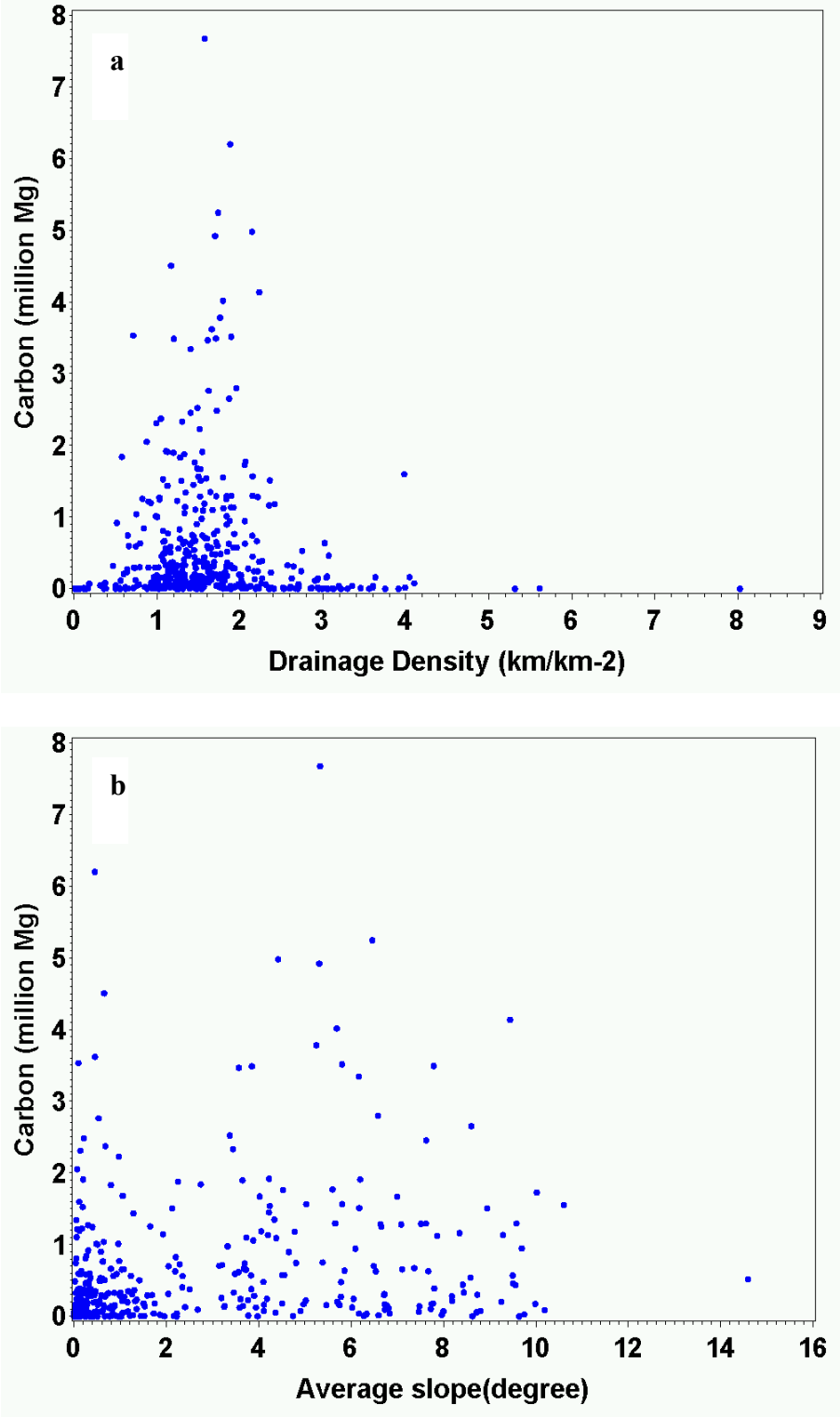

Fig. 22 Relationships of watershed carbon storage with (a) drainage density and (b) average watershed slope.

Discussion

Mapping Forest Biomass Carbon

This study computed carbon storage in each FIA plot from the FIA dataset 2006 for Louisiana, and interpolated the carbon storage from the inventory plots to a fine grid spatial scale (30 m by 30 m) with the Thiessen polygon approach. The generated map explicitly represented the spatial variation of carbon in the state. The map not only showed the smooth variation of the carbon storage in some areas but also the contrast changes in other areas. The variations are a representation of spatial composition, as well as a configuration of the four forest types of evergreen, deciduous, mixed, and woody wetland forests in the state. Overall, this study demonstrated that the Thiessen polygon approach is a good method for interpolation of the forest carbon from plot to grid level for large areas. However, for adjacent plots with a wide range of biomass values, the method may result in biased estimates in pixels along the borders of Thiessen polygons. Therefore, an interpretation of the carbon density with apparent contrast changes at the boundaries of some Thiessen polygons should be cautious.

In addition to the Thiessen polygon, other spatial analyses approaches, e.g., K-nearest neighbors (KNN) and geospatial statistics, have been extensively studied and reviewed (Fournier et al. 2003; Holden et al. 2003; Labrecque et al. 2006; Maselli and Chiesi 2006; Zheng et al. 2007). Of these, KNN provides the good spatial distribution estimates for all biomass ranges (Labrecque et al. 2006). To conduct the KNN approach, an accurate location of the FIA plot is required to determine the nearest neighbors, based on the distance (spectral) between the plots. Unfortunately, in order to enforce the Food Securities Act to ensure that the FIA plot data cannot be linked to its owner, coordinates of the plots were fuzzed within 1.6 km of the exact plot location and up to 20% of the private plot coordinates were swapped with another similarly private plot within the same county (Alerich et al. 2006). The fuzzed and swapped FIA plots

presented a difficulty in the application of alternative spatial analysis methods. Therefore, for a wide application of FIA data in forestry and ecosystem management, a release of FIA data with accurate location information to scientific communities is required.

Relations between Carbon Storage and Watershed Features

Correlations of drainage density and watershed slope with forest biomass carbon storage in watersheds were not significant in this study. However, several studies reported that forest biomass is correlated to watershed features, in that some factors (e.g., soil water content) controlling forest growth processes are highly affected by watershed features (Abrahams and Ponczynski 1984; Meynendonckx et al. 2006; Piedallu and Gegout 2007; Prasad et al. 2005; Talling and Sowter 1999; Zushi 2006). These studies noted that drainage density is negatively correlated to precipitation intensity and mean annual precipitation (Abrahams and Ponczynski 1984) and is positively correlated to slope angle, if the overland flow is dominant (Talling and Sowter 1999). A high value of the drainage density can increase the level of nutrient accession in waterways, owing to a relatively high density of streams, and thus a rapid storm response (Prasad et al. 2005). As the watershed slope is steeper, it is more likely that overland flow and surface soil erosion will occur, and that consequently, more soil organic matters will move toward the drainage network (Meynendonckx et al. 2006), contributing to lower carbon storage in the soil (Zushi 2006). Watershed features, such as slope and aspect also affect radiation distribution in watersheds. A GIS program calculated solar radiation for the whole of France, demonstrating that radiation values increase with a slope for southern exposure, except in summer, and decrease with a slope for north, east, and west exposures (Piedallu and Gegout 2007). Some other studies also reported that along with radiation changes, the vegetation of northwest-facing plots differed from that of the southeast aspect in species richness and diversity, canopy cover, and canopy height, yet differences between northeast and southwest aspects were significant for fewer

attributes (Bale et al. 1998; Olivero and Hix 1998).

The low correlation between forest biomass carbon in watersheds and watershed characteristics identified in this study could be due to human and natural disturbances to forests at landscape level. In the 2004 planting season, Louisiana landowners reforested the land with over 128 million seedlings. Meanwhile, 1.2 billion board feet of sawtimber and 6.3 million cords of wood were harvested (Frey 2005). In addition, from 1988 through 1997, an average of 3,822 wildfires burned 18,606 hectares of forestland each year, releasing a vast amount of carbon dioxide back to the atmosphere (Louisiana Department of Agriculture & Forestry). All these facts demonstrated that human activities and natural disturbances alter carbon storage in forest ecosystems. In contrast, the watershed features can remain unchanged over an extensive period of time. Therefore, significant relationships were not identified between watershed carbon storage and features.

Conclusions

This study quantified forest biomass carbon storage at grid and watershed scales in Louisiana with the latest (2006) Forest Inventory and Analysis dataset and the National Land Cover Dataset. In addition, the study examined effects of watershed features on forest biomass carbon storage at landscape level. Forest biomass carbon in Louisiana showed spatial changes across the landscape, apparently reflecting human activities and natural disturbances. The carbon density map could be used by a carbon credit exchange program (e.g., the Chicago Climate Exchange) to verify carbon stored in forests on small patches of lands. At the watershed level, carbon storage is mainly determined by the areas of forest within the watershed, which suggests that afforestation would be a management strategy to sequester carbon for mitigating atmospheric carbon dioxide concentration. As a natural boundary and link of both forest and aquatic ecosystems, carbon storage in the watershed may facilitate examination of the carbon flux between forest ecosystems

and aquatic environments and an assessment of the effects of hydrological properties on carbon assimilation and accumulation at broad scales. If the FIA program could release data with original coordinates of the inventory plots to the research community, accuracy of the estimate and prediction of carbon across the state could be improved through applying other analysis approaches, or FIA could incorporate the analysis.

CHAPTER 4 MODELING VARIATIONS AND UNCERTAINTIES OF LOUISIANA FOREST NET PRIMARY PRODUCTIVITY IN RESPONSE TO CLIMATE CHANGE

Introduction

Since effects of the global climate change on forest ecosystems and the roles of forests in the global carbon cycle cause concern worldwide, an accurate prediction of spatial and temporal responses of forest productivity to future climate change is necessary for resources managers and policy makers to develop strategies and plans for sustainable forest management, carbon sequestration, and a mitigation of greenhouse gas effects. Global climate has been changing since the Industrial Revolution. It is highly possible that the rapid change in the past 50 years was caused by significant increases of greenhouse gas (GHG) concentrations in the atmosphere (IPCC 2007d). GHG emission scenarios in the 21st century have been published by the Intergovernmental Panel on Climate Change (IPCC) (Nakicenovic et al. 2000). According to the IPCC, the GHG emission scenario is driven by forces inclusive of demographic and socio-economic developments, and technological change, containing four families of A1, A2, B1, and B2. Among these, A1 is subset into A1F1, A1B, and A1T. Scenarios of B1, A1B, and A2 usually represent low, moderate, and high greenhouse gas emissions in the future. The carbon dioxide equivalent concentration for three scenarios in 2100 is predicted to be about 600, 850, and 1250 ppm, respectively. Based on the emission scenarios, the global mean surface air temperature has been predicted to rise by 1.8°C (1.1 - 2.9°C) for B1 scenario and 4.0°C (2.4 - 6.4°C) for A1F1 scenario for the period 2080 to 2099 relative to 1980 to 1999 (Meehl et al. 2007). In addition, global warming is expected to cause changes in distribution, intensity, and frequency of precipitation. The precipitation would increase over 20% at most high latitudes, as well as in eastern Africa, central Asia, and the equatorial Pacific Ocean for the A1B scenario for the period 2080 to 2099 to be relative to 1980 to 1999 (Meehl et al. 2007).

Climate change may have affected many ecosystems in the world and are expected to have potential wide-ranging effects on human societies (IPCC 2007a). For forest ecosystems, the

increase of the atmospheric CO_2 concentration has been reported to have a generally positive influence on forest productivity, providing water and nutrient supplies are not limited (Boisvenue and Running 2006). About 20% of the current forest area in the conterminous United States would experience some level of carbon loss, should temperature and precipitation be increased by 3.3°C and 23% from 2000 to 2099, in reference to 1961 to 1990 (Aber et al. 2001). In turn, forests affected by the climate change in turn can exert feedbacks to the climate owing to the role of forests in global carbon cycling, as well as having a direct effect on solar radiance (albedo). For instance, U. S. forests have been identified as a net carbon sink (Ciais et al. 1995; Fan et al. 1999), sequestering 200 Tg carbon annually from the atmosphere, or 10% of U.S. fossil fuel emissions (Birdsey et al. 2005).

Predicting effects of climate change on forest productivity over a long period of time requires the application of process-based forest growth models, owing to the complexity of climate-forest interactions (Aber et al. 2001). Forest growth can be affected by site factors that include climate conditions and water and nutrient supplies, as well as by physiological processes, such as photosynthesis, respiration, carbon allocation, and evapotranspiration. Process-based models incorporating these factors and processes can generate a long-term forecasting of forest productivity under various natural and human induced-changes (Peng et al. 2002). A series of process-based models have been developed to simulate net primary productivity (NPP) dynamics and effects of environmental changes on NPP with different approaches (Aber and Federer 1992; Landsberg and Waring 1997; Running and Coughlan 1988; Running and Gower 1991). Net photosynthesis- evapotranspiration (PnET) model has been widely used to predict forest net primary production in foliage, wood, and roots, as well as environmental effects on forest production at stand and regional scales (Aber et al. 1995; Campbell et al. 2009; McNulty et al. 2000; Mickler et al. 2004; Ollinger et al. 1998).

Forests in Louisiana, covering 48% of the state's land area, provide a variety of commercial products that support local economies and habitats, which in turn propagate diverse plant and animal species associated with particular landforms, soils, and hydrologic regimes. In addition, Louisiana's forests are still a tremendous carbon sink even though Xu and Wang (2006) found that from 1991 to 2003, biomass carbon stocks in Louisiana forests decreased 9.3%. Among the forest types, only the longleaf-slash pine type showed a carbon increase of 11.8%; carbon in the remaining forest types decreased by 2.7% to 18.4%. These changes have been attributed mainly to forest management practices. It is uncertain how these forests, in addition to management and land use change, will respond to future climate change.

Global climate models have projected increased temperature and precipitation for Louisiana in the 21st century. The climate changes may have a significant effect on the forest ecosystems, especially with regard to the potential of a forest to sequester carbon. McNulty et al. (2000) predicted that southern pine productivity in Louisiana would increase by 2.5% between 1990 and 2040, and would decrease by 6% from 2040 to 2100 under the Hadley2Sul climate change scenario. Mickler et al. (2002b) forecasted that the average NPP for evergreen, deciduous, and mixed forest types would decrease 13%, 2%, and, 7%, respectively, under the same climate change scenario. However, these predictions were made for only one climate change scenario. The prediction results may not reveal the actual effects of climate change on Louisiana's forests, due to the large spatial resolution and high uncertainty of climate change predictions. This study will 1) develop a spatially explicit modeling framework for forest biomass carbon prediction; 2) predict responses of forest biomass carbon to three commonly used climate change scenarios (IPCC SRES B1, A1B, and A2) at the higher spatial resolution of 4980 m by 4980 m; and 3) assess uncertainties associated with the NPP prediction at the grid and state levels.

Methods

Modeling Approach

Forest NPP in the entire state of Louisiana for 2000 to 2050 was predicted with a forest growth model, PnET-II (Aber and Federer 1992; Aber et al. 1995), under three climate change scenarios: B1, A1B, and A2. Spatial distribution of forests including deciduous, evergreen, mixed and woody wetland forests were determined from 2001 National Land Cover Data (Multi-Resolution Land Characteristics Consortium 2001). In order to predict forest NPP for the entirety of Louisiana with the canopy- to stand-level model PnET-II, the forest lands were aggregated into 2711 pixels with size of 4980 m by 4980 m. Each pixel within a forest type was considered a stand. PnET-II was run twice at each pixel, one with parameters of evergreen forests and another one with parameters of deciduous forests. Then the two sets of PnET-II outputs were summarized by multiplying area fractions of the evergreen and deciduous forests in each pixel to compute the NPP in each pixel. If it were mixed forests as NLCD indicated, then a ratio of 60: 40 for evergreen and deciduous was assumed to calculate the mixed forests NPP (Ollinger et al. 1998), and a ratio of 75:25 for the wetland forests (Rosson Jr. 1995; USDA Forest Service 2007). The model run began from 1960 and ended in 2050, and was calibrated for the 14-year period from 1991 to 2003. In the following sections, details on running the model are described starting with a brief introduction of PnET-II, followed by model input data preprocessing and parameter preparation, model calibration, and final sensitivity and uncertainty analysis.

PnET- II: a Forest Growth Model

The PnET-II model simulates the NPP of foliage, wood, and roots by tracking carbon fixed during photosynthesis, allocated to foliage, wood, and roots, and respired from leaf, stem, and roots (Aber and Federer 1992; Aber et al. 1996). The model assumes that the maximum photosynthetic rate is a function of foliar nitrogen concentration. Maximum gross photosynthesis

per unit leaf area is 110% of the max net photosynthesis. Gross photosynthesis is the maximum gross photosynthesis modified by effects of temperature, soil water stress on stomatal closure, and the direct effect of the vapor pressure deficit on stomatal conductance. The whole canopy photosynthesis integrates photosynthesis per ground area basis by stratifying the canopy into 50 layers through incorporating specific leaf weight and light attenuation with canopy depth. The model assumes that the leaf area is equal to the maximum amount of foliage that could be supported with the given soil water holding capacity, species, and climate limitations.

Model Input Data Sets

The input data sets for PnET-II include climate, forest spatial distribution, attribute parameters, soil water holding capacity, and site attributes, such as latitude.

Climate scenarios – Monthly precipitation, maximum and minimum temperatures, and solar radiation data for the three climate change scenarios of B1, A1B, and A2 between 1960 and 2050 were derived from CCSM3 model outputs. The outputs were downloaded from the disseminator of CCSM 3 outputs: the Earth System Grid (ESG) and the Eos-Webster. A total of 13 pixels with a size of 1.4° x 1.4° were subset for Louisiana from the raw dataset covering the entire globe. The data during 1960-1999 were the same among the scenarios and simulated with the 20C3M experiment. For the experiment, the atmospheric carbon dioxide concentrations and other input data were based on historical records or estimates beginning around the time of the Industrial Revolution. In contrast, the climate variables data during 2000-2050 varied by the three scenarios (IPCC 2007c).

Site variables – Latitude, forest types, area percentages of evergreen and deciduous forests, and water holding capacity (WHC) were input variables for each grid. Forest types and area percentages of each type in each grid were determined from NLCD 2001 (Multi-Resolution Land Characteristics Consortium 1992). NLCD was derived from Landsat TM and ETM imagery, and

four forest types (deciduous, evergreen, mixed, and wetland forests) were classified for pixels with a size of 30 m by 30 m. The 30 m by 30 m pixels were aggregated into 4980 m by 4980 m and then the area percentage of each forest type in each pixel was computed. At the scale of 4980 m by 4980 m, there were in total 2,711 forest pixels in Louisiana.

Soil water holding capacity (WHC), the total depth of water that a soil can store within its entire vertical profile, was calculated from the Soil Survey Geographic (SSURGO) database developed by the USDA Natural Resources Conservation Service (Soil Survey Staff 2004). The geospatially referenced data is the most detailed level (1:12,000 to 1:163,360) of soil mapping. A map unit, polygon on the map, is the fundamental graphic feature in SSURGO spatial data. Attributes of the map units include the proportionate extent of the component soils and the physical and chemical properties for each soil. WHC was computed via two steps. The first step was to calculate the water storage within a given component:

$$component\_whc = \sum((hzdepb\_r - hzdept\_r) * \text{ awc\_r })$$

where hzdepb_r is the distance from the top of the soil to the base of the soil horizon, hzdept_r is the distance from the top of the soil to the upper boundary of the soil horizon, and awc_r is the amount of water that an increment of soil depth, inclusive of fragments, can store that is available to plants (Soil Survey Staff 2004) .

The second step was to compute the weighted mean value of the profile water storage for a given map unit:

$$WHC = \frac{\sum\left(\frac{comppct\_r}{100} * component\_whc\right)}{\sum\left(\frac{comppct\_r}{100}\right)}$$

where comppct_r is the percentage of the component of the map unit (Soil Survey Staff 2004) .

Forest parameters – Thirty-six parameters were required to run the model. However, it was not necessary for all of them to change with forest sites (Aber et al. 1995). In this study, four parameters including intercept (AmaxA) and slope (AmaxB) of relationship between foliar N concentration (FolNCon) and max net photosynthesis rate, foliage retention time (FolReten), and specific leaf weight (SLWmax) were drawn from published values (Ellsworth and Reich 1992; Maier et al. 2008; Reich et al. 1995; Springer et al. 2005; Tang et al. 2004).

Model Calibration

Model calibration is a critical step for model applications. In general, it is an iterative procedure of parameter evaluation and refinement as a result of comparing simulated and observed values. Unfortunately, field observations of carbon fluxes neither from eddy convariate towers nor free air carbon enrichment (FACE) programs were available for calibrating the carbon accounting model PnET-II in Louisiana. In this study, The FIA database 1992 and 2006 were used as an alternative independent dataset for PnET-II calibration. The FIA data tables include attributes of tree and site information for about 3000 plots in the entire state. Each plot is one acre in size and represents about 6000 acres of land. From the FIA data sets, the forest biomass carbon in 1991 (C91) and 2003 (C03), and yearly mortality (M9103) and removals (R9103) between 1991 and 2003 for each plot were derived. The mortality and removals were losses of biomass carbon owing to mortality and removals including harvests between these two inventories. PnET-II was calibrated for Louisiana forests with an assumption during these years (Fig. 23)

$$C03 = C91 + PnETNPP - M9103 - R9103$$

where PnETNPP was the sum of the predicted annual NPP by PnET-II for the year of 1991 through 2003.

The calibration was conducted at parish level. Within each parish, even though coordinates

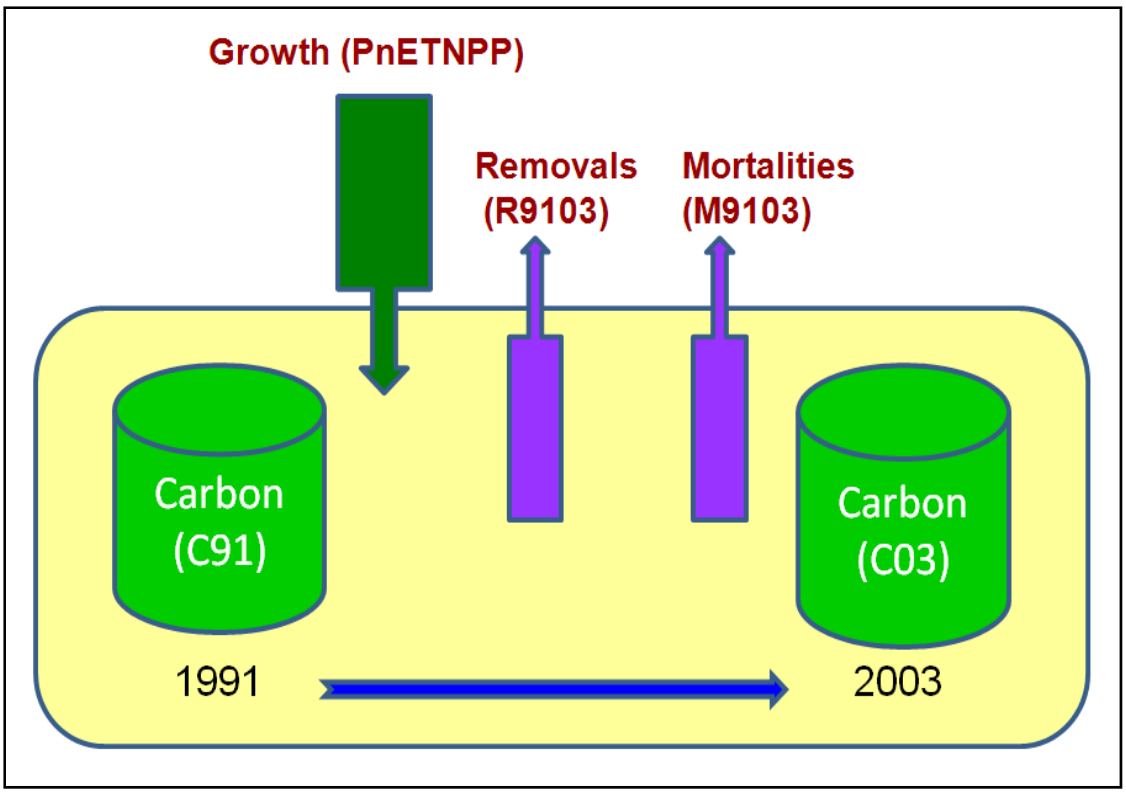

Fig. 23 PnET calibration with carbon storage in 1991(C91) and 2003 (C03), removals (R9103) and mortalities (M9103) between 1991 and 2003, as well as forest growth predicted by the PnET-II model (PnETNPP). The mortality and removals were losses of biomass carbon owing to mortality and removals, including harvests between these two inventories.

of individual plots were swapped and fuzzed, the summarization of forest attributes at the parish level is not affected by the hidden location of the plots (Alerich et al. 2006).

Sensitivity and Uncertainty Analysis

Sensitivity analysis is an investigation of the importance of the imprecision or uncertainty in model inputs of the modeling process. The analysis describes how much the model output values are affected by changes in model input values. Sensitivity of PnET to a set of parameters have been assessed by increases of 10% of the parameter values (Aber et al. 1996), and the results show that the gross carbon exchange (GCE) is more sensitive to the foliar N concentration and the slope of the relationship between maximum net photosynthesis rate and foliage nitrogen

concentration, then followed by daily max net photosynthesis as a fraction of the early morning instantaneous rate, and specific leaf weight. In this study, sensitivity of these four parameters were analyzed by the Monte Carlo simulation. This simulation is a numerical method to propagate model uncertainty, which involves a large number of iterations of the basic deterministic model with parameters determined by probability distribution functions, usually normal distribution (Smith and Heath 2001). Normal distribution of an input parameter for sensitivity analysis was generated with an assumption that the standard deviation was 10% of the mean value of the parameter and a total of 100 values for each parameter was generated. For a sensitivity analysis of the model to climate inputs, four climate variables, including maximum and minimum temperatures, precipitation, and solar radiation were simulated. For each climate variable, the monthly input was the data during 2000 to 2050 that were subtracted or added one stand deviation of the monthly climate data between 1970 and 2000.

Results

Temporal Change in NPP

Model calibration procedure showed that the model achieved a high accuracy and reliability in predicting NPP at parish level. Therefore, it was not necessary to further refine or adjust the parameter values for NPP prediction during 2000 to 2050 (Fig. 24). As predicted NPP (Fig. 24a) was counted for quantifying the carbon balance between 1991 and 2003, a balance of carbon on both sides of the equation, C03 = C91 + PnETNPP - M9103 - R9103, with a strong agreement was achieved (R^2=0.9; Fig. 24b). Meantime, this residual analysis also revealed that in a parish, the studentized residual was greater than 3, and there was an increasing trend of the residual values with rising predicted values (Fig. 24c). This trend may imply an error aggregation effect in the carbon quantification and prediction processes.

The predicted NPP among the three scenarios over the years were divergent as shown by the

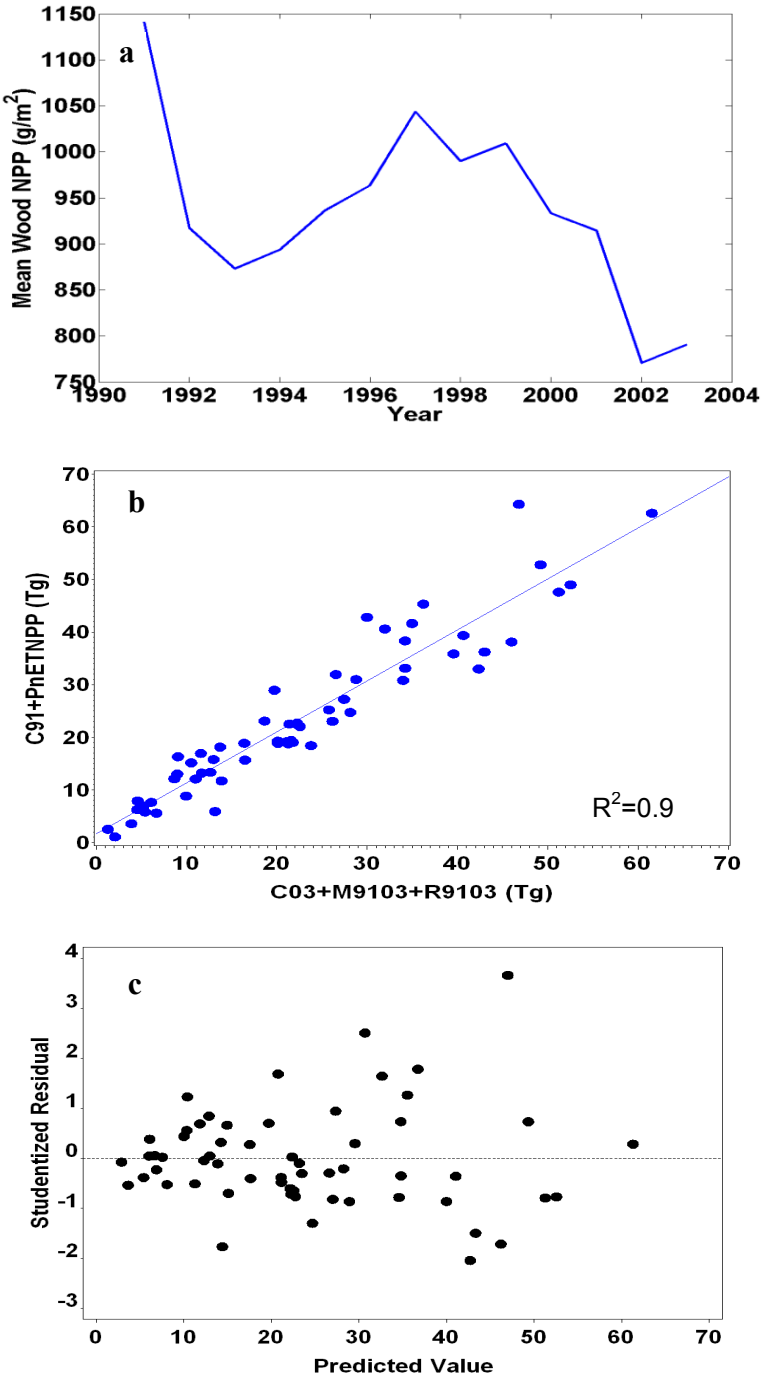

Fig. 24 (a) Predicted NPP during 1991 to 2003 by PnET-II, (b) calibration of PnET-II with independent data derived from FIA dataset at parish level, and (c) residual analysis of the predicted and the computed values. In figure b, C91 and C03 are forest biomass carbon in 1991 to 2003. M9103 and R9103 are losses of biomass carbon owing to mortality and removals, including harvests, between these two inventories. PnETNPP is the sum of the predicted annual NPP for the years of 1991 to 2003. The line and dots represent relationships as indicated by the equation: C03 = C91 + PnETNPP − M9103 − R9103.

10-yr moving average (Fig. 25a), the 10-yr average for the period of 2010 to 2050 relative to 2000 to 2010 (Fig. 25b), and the accumulated annual mean NPP during 2000 to 2050 (Fig. 25c). The 10-yr moving average displayed a wide range of difference in annual NPP values among the three scenarios during about 2010 to 2030, but afterward, the values noticeably converged to a narrow range. Compared to the mean NPP during 2000 to 2010 (Fig. 25b), the mean values in the remaining years showed that for the B1 scenario, the mean NPP between 2010 and 2020 was higher than the mean between 2000 and 2010. After 2020, even the NPP increased slightly, but the mean values at the 10-year period from 2020 through 2050 still were lower than in 2000-2010. For A1B and A2 scenarios, the 10-yr mean values showed overall increasing trends, and all values except for the value during 2010 to 2020 for the A2 scenario were greater than in 2000 to 2010. The accumulated annual mean NPP (Fig. 25c) also showed a difference among the three scenarios with an obviously higher accumulated NPP for B1 than for the A1B and A2 scenarios. For both the A1B and A2 scenarios, the accumulated trends were not distinguishable. In addition, an ANOVA analysis of the mean NPP values of the three scenarios for the years of 2000 through 2050 revealed that the mean value of B1 scenario significantly differed from those of A1B and A2 (Fig. 26). However, no significant difference was found between mean NPP values of A1B and A2 scenarios.

Spatial Change in NPP

At the grid scale, the predicted NPP from the selected years showed that in the entire state of Louisiana, NPP values presented a distinctly declining trend from south to north, but only small changes at the west-eastward dimension (Fig. 27). As a total of 11 climate grids (number 3 though 13), as shown in the NPP map in 1980, were categorized into three groups by latitude gradients (Fig. 27 and Table 3), the average NPP changed significantly from one group to the next. For instance,

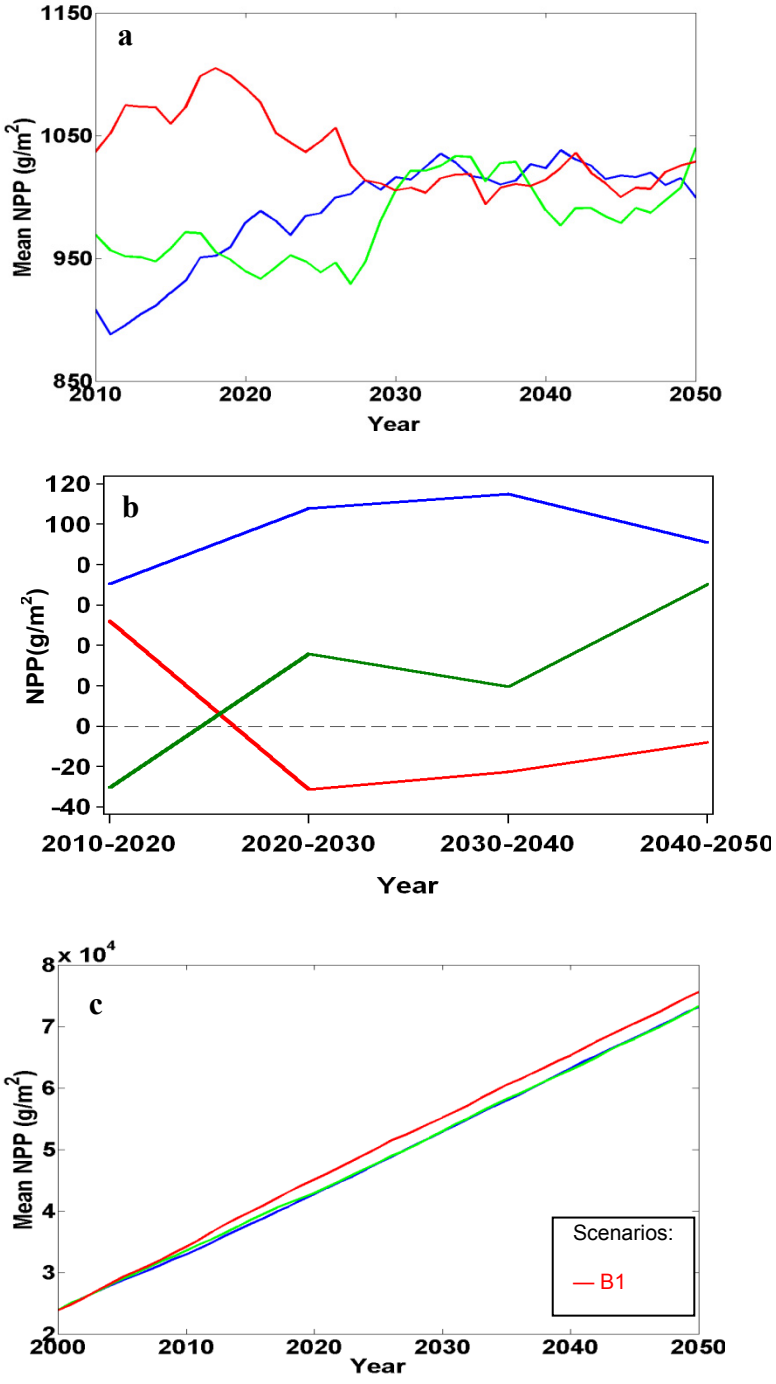

Fig. 25 (a) Predicted 10-yr moving average NPP in Louisiana during 2000 to 2050 by the three climate change scenarios of A1B (blue), A2 (green), and B1 (red), (b) 10-yr average for the period of 2010 to 2050, relative to 2000 to 2010, and (c) accumulated annual mean NPP.

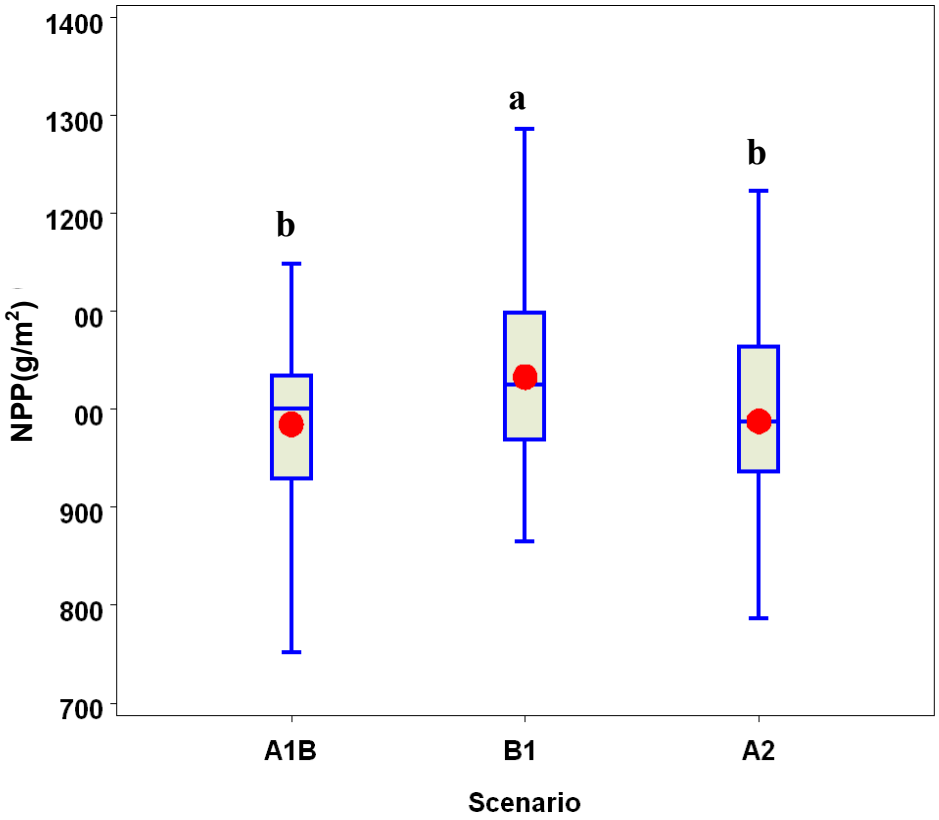

Fig. 26 ANOVA analysis of the predicted mean NPP values of the A1B, B1, and A2 scenarios during 2000 to 2050. The means followed by the same letter on top of the bars are not significantly different at the 0.05 level.

from north through south, the NPP changed from 864 g/m^2 to 1295 g/m^2, and then to 1720 g/m^2. However, the NPP was nearly homogeneous within each group, as evidential by the low standard deviation of 37 g/m^2, 53 g/m^2, and 77 g/m^2 in southern, central and northern groups, respectively.

Sensitivity Analysis

Sensitivity analysis of the four parameters (a) foliar N concentration (FolNCon), (b) slope of the relationship between maximum net photosynthesis and foliar N concentration (AmaxB), (c) daily max net photosynthesis as fraction of early morning instantaneous rate (AmaxFrac), and (d) specific leaf weigh (SLWMax) showed that PnET-II was more sensitive to FolNCon and AmaxB than AmaxFrac and SLWMax, in terms of changes in standard deviations (*s*) of the predicted NPP of the parameters (Fig. 28, Table 4). The mean percentage changes of *s* by the parameters,

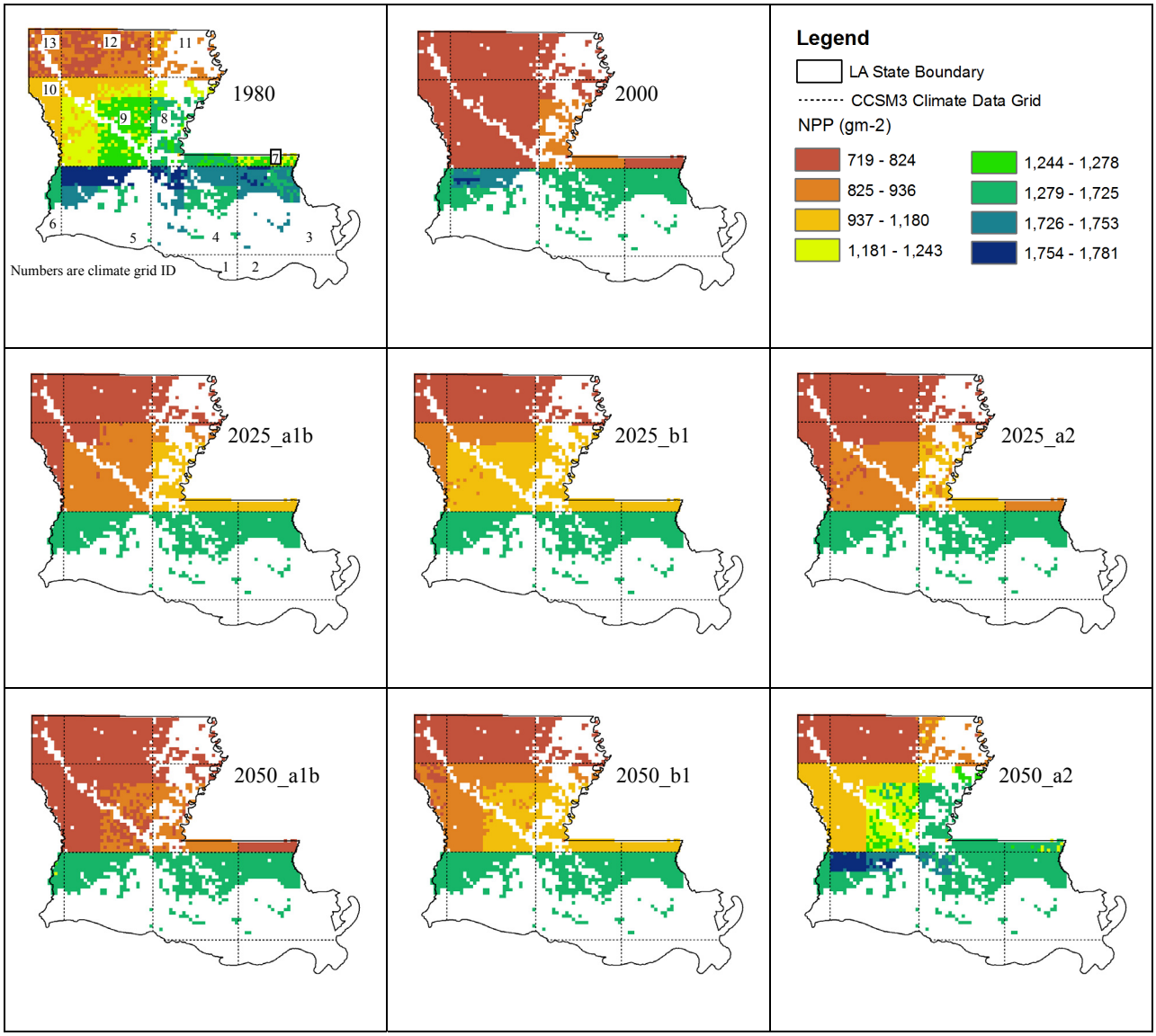

Fig. 27 Predicted NPP by PnET-II at grid scale (4980 m by 4980 m) for the four dates of 1980, 2000, 2025, and 2050 and the three climate change scenarios.

Table 3 Mean and standard deviation of NPP during the four years by the grid groups and the three climate change scenarios, and percentage changes of the mean NPP in 2025 and 2050 relative to 2000.

			1980	2000	2025			2050			
Group #	GRID #	Units			A1B	B1	A2	A1B	B1	A2	Mean
1	3,4,5,6	g/m^2	1720±45	1616±74	1584±69	1600±65	1549±54	1444±62	1605±50	1699±37	1602±57
		%			-2	-1	-4	-11	-1	5	-1
2	7,8,9,10	g/m^2	1295±59	850±73	1031±112	1106±101	947±81	855±76	1030±91	1302±85	1052±85
		%			21	30	11	1	21	53	24
3	11,12,13	g/m^2	864±50	560±48	622±83	704±57	558±76	414±70	474±101	767±125	620±76
		%			11	26	0	-26	-15	37	11
Mean		g/m^2	1293±51	1008±65	1079±88	1137±74	1018±70	904±70	1036±81	1256±82	
		%			10	18	2	-12	2	32	

relative to the mean 1030 g/m^2 (predicted by PnET-II without Monte Carlo simulation), showed an average of 23.3% and 23.4% for FolNcon and AmaxB, with 11.4% and 5.0% for amaxFrac and SLWMax, respectively. In addition, the mean NPP changed by the parameters showed a narrow range of 2.9% - 3.7%, indicating that mean values of predicted NPP was not good as an index to evaluate PnET-II sensitivity to the parameters. The mean NPP change and mean *s* change of the three climate scenarios for each parameter were too close to distinguish the difference of the model's sensitivity to the parameters by the scenarios (Table 4).

Sensitivity analysis of four climate inputs of mean maximum and minimum temperature, precipitation, and radiation showed that the model was more sensitive to temperature than the other two inputs (Fig. 29, Table 5). In terms of the percentage change of mean NPP during 2000 to 2050, relative to the mean of 1030 g/m2 predicted by PnET-II without Monte Carlo simulation, the opposite signs of the percentages for mean maximum temperature were identified as compared to the remaining parameters, indicating a negative effect of an increasing mean maximum temperature on NPP, with a positive response of NPP on rising mean minimum temperatures, precipitation, and radiation. Particularly, an increasing max temperature could reduce a mean NPP 19% for the entire state during 2000 to 2050. The sensitivity analysis indicated that small changes in temperature in the future could result in a high variability in forest NPP.

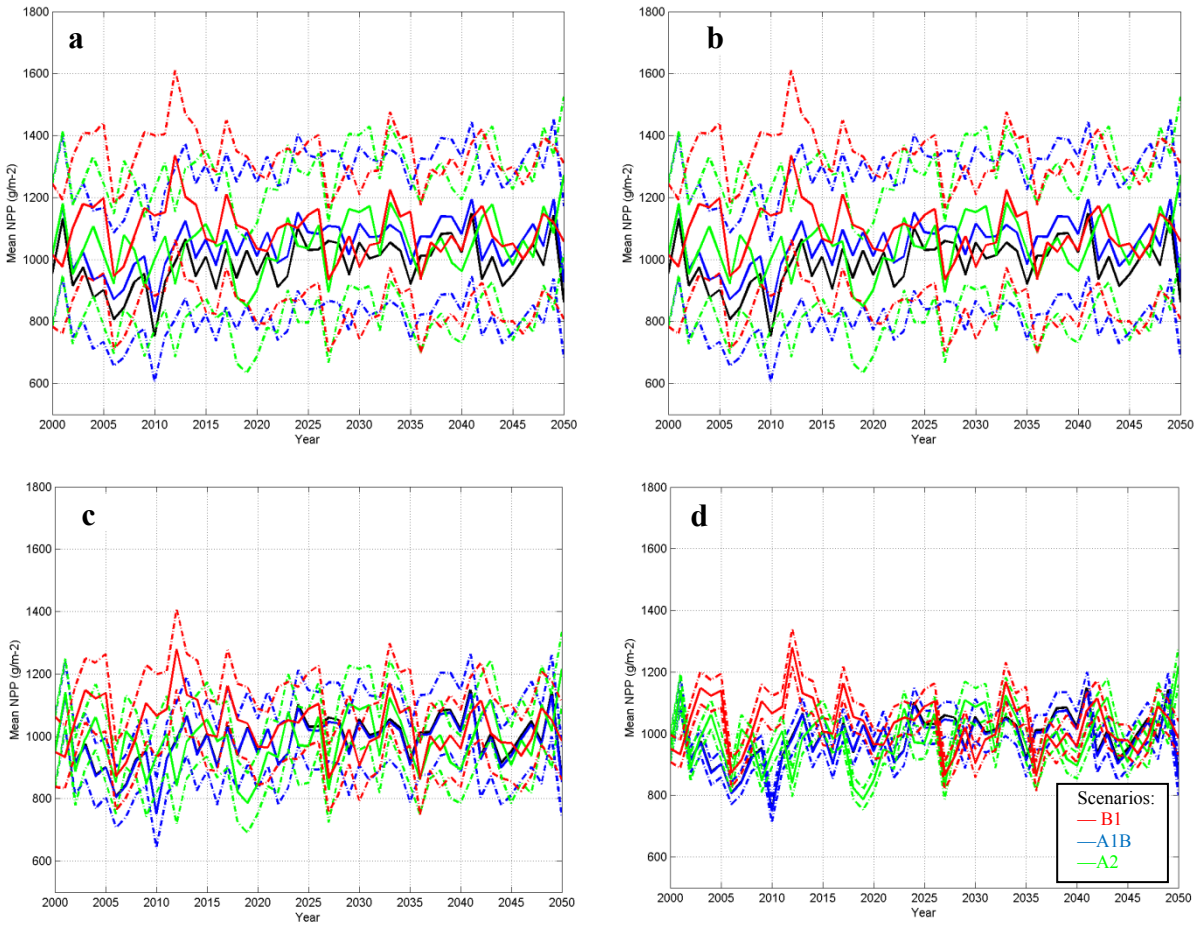

Fig. 28 Monte Carlo sensitivity analysis for PnET-II model parameters of (a) FolNCon, (b) AmaxB, (c) AmaxFrac, and (d) SLWMax in predicting forest NPP in Louisiana. Solid black line represents PnET-II prediction without application of Monte Carlo simulation. Solid blue, green and red lines represent average NPP values predicted by iterating PnET-II 100 times for each climate change scenarios of A1B, A2, and B1, respectively. The dashed lines display the mean NPP values with one standard deviation (*s*) for the climate change scenarios.

Table 4 Monte Carlo sensitivity analysis results for PnET-II model parameters of FolNCon, AmaxB, AmaxFrac, and SLWMax in predicting forest NPP in Louisiana.

Parameter	Climate scenario	Mean and *s* of NPP (g/m^2)[a]	Mean NPP change[b] (%)	Mean *s* change[c] (%)	Mean NPP change by the parameter (%)	Mean *s* change by the parameter (%)
FolNcon	A1B	1044±242	1.4	23.5	2.9	23.3
	B1	1090±242	5.8	23.5		
	A2	1045±236	1.5	22.9		
AmaxB	A1B	1053±243	2.2	23.6	3.7	23.4
	B1	1098±243	6.6	23.6		
	A2	1053±237	2.2	23.0		
AmaxFrac	A1B	978±120	-5.0	11.7	-3.3	11.4
	B1	1028±118	-0.2	11.5		
	A2	981±115	-4.8	11.2		
SLWMax	A1B	978±52	-5.0	5.0	-3.3	5.0
	B1	1028±52	-0.2	5.0		
	A2	983±50	-4.6	4.9		

[a] Mean and standard deviation of the NPP predicted by iterating 100 times of the PnET-II for all cells in Louisiana.

[b] Percentage of the mean NPP relative to the mean of 1030 g/m^2 predicted by PnET-II without Monte Carlo simulation.

[c] Percentage of the *s* relative to the mean of 1030 g/m^2 predicted by PnET-II without Monte Carlo simulation.

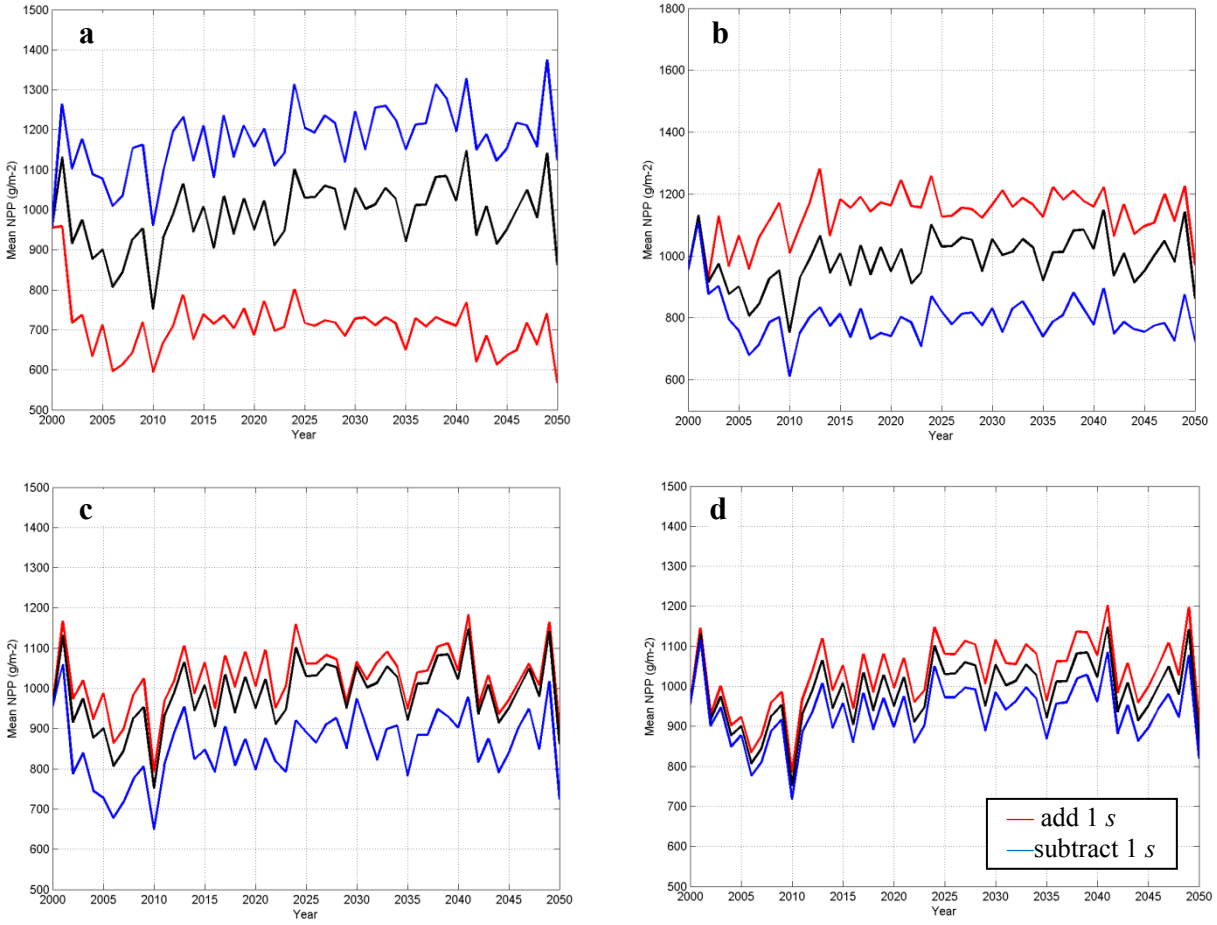

Fig. 29 Monte Carlo sensitivity analysis of PnET-II model to climate inputs of (a) maximum and (b) minimum temperature, (c) precipitation, and (d) radiation of A1B scenario in prediction of NPP in Louisiana. The solid black line represents PnET-II NPP predictions with raw CCSM3 climate data. The red and blue lines represent NPP, predicted by adding or subtracting the A1B climate data one standard deviation (*s*) of the corresponding climate variable data during 1970 to 2000.

Table 5 Monte Carlo sensitivity analysis of PnET-II model for climate inputs of the A1B scenario in forest NPP prediction in Louisiana.

Parameters	Input changes[a]	Mean output NPP during 2000-2050 (g/m^2)	NPP chang[b] (%)	Mean of the percentage changes by parameters (%)
Max. Temp.	+	831	-19	16
	-	1167	13	
Min. Temp.	+	1137	10	12
	-	895	-13	
Precipitation	+	1057	3	6
	-	938	-9	
Radiation	+	1061	3	3
	-	994	-3	

[a] + and - represent adding and subtracting A1B climate data one standard deviation of the corresponding climate variable data during 1970 to 2000.

[b] Percentage changes of mean NPP during 2000 to 2050 relative to the mean of 1030 g/m^2 predicted by PnET-II without Monte Carlo simulation.

Discussion

Temporal Effects of Climate Change on NPP

The modeling results of this study suggest that forest growth and biomass carbon will respond to long-term climate change. The results for scenario B1 showed an increasing trend of forest NPP from 2000 through 2020, but a sharply decreasing trend between 2000 and 2030. For both A1B and A2 scenarios, the predicted forest NPP showed increasing trends over the 50 years (Fig. 25b). The accumulated NPP for B1 scenarios was higher than NPP for A1B and A2. For the B1, A1B, and A2 scenarios, approximate carbon dioxide equivalent concentrations corresponding to the computed radiative forcing due to anthropogenic greenhouse gases and aerosols in 2100 would be 600, 850, and 1250 ppm (IPCC 2007c). Therefore, from the trends of NPP and the greenhouse gas emissions, we could conclude that a climate change associated with higher emission scenarios would be favorable to forest growth.

The correlation of higher emissions with the rising trends of NPP could be due to the changes in mean maximum and mean minimum temperatures and precipitation as projected by

CCSM3. Temperature controls the rates of metabolism and alters water vapor deficits in the air, which in turn determines the amount of photosynthesis, respiration, and evapotranspiration that can take place. With increasing temperature, vapor pressure deficits of the air may increase, with a concomitant increase in the transpiration rate from plant canopies (Kirschbaum 2004) . However, these increases in transpiration are likely to be reduced by stomatal closure in response to increasing CO_2 concentration (Kirschbaum 2004). In a short term, respiration is exponentially related to temperature increases, but in the long term, respiration rate may be limited by substrate supplication or gross primary production. In addition, water is a principal requirement for photosynthesis as well as the main chemical component of most plant cells. Along with temperature, precipitation mainly controls vegetation distribution and soil water content.

In Louisiana, for the B1 scenario, the 10-yr mean precipitation between 2000 and 2050 predicted by CCSM3 showed a decreasing trend with the highest mean during 2000-2010 and the lowest mean during 2010-2020 (Fig. 30a). For A1B and A2 scenarios, the 10-yr mean precipitation between 2000 and 2050 displayed increasing trends with the lowest mean precipitation during 2000 and 2010. According to sensitivity analysis, an increasing monthly average precipitation by one standard deviation could result in a 3% increase in NPP, but decreasing by one standard deviation would bring about a 9% decline (Fig. 29c). Therefore, changing precipitation in Louisiana would be a limiting factor on NPP for the B1 scenario, but a favorable factor for the A1B and A2 scenarios. In contrast, both 10-yr mean maximum and mean minimum temperatures between 2000 and 2050 would increase as compared to the means in 2000 to 2010 for the three scenarios (Fig. 30b and c). As indicated by the sensitivity analysis, an increasing mean maximum temperature would decrease NPP 19%, and an increasing mean minimum temperature would raise NPP 10%. Therefore, the projected increases in NPP for A1B and A2 could be a duo to an effective increase in minimum temperature and precipitation. In

addition, the less-than-one-degree increases in mean maximum temperatures for A1B and A2 did not constrain NPP via the temperature's effects on photosynthesis, respiration and evapotranspiration processes. Therefore, according to PnET-II, changes in minimum temperature and precipitation were the dominant factors in forest growth in Louisiana. In the B1 scenario, particularly, the smallest increase in mean minimum temperature and a decrease in mean precipitation as compared to those in 2000 to 2010 contributed to the predicted decline in NPP for the B1 scenario.

In addition to the influences of temperature, precipitation, and radiation on forest NPP, studies have found that an increase of atmospheric CO_2 concentration has different effects on NPP; a consensus conclusion on the effects has not been reached. Therefore, in this study, effects of increasing atmospheric CO_2 concentration on forest growth were not incorporated into the PnET for NPP prediction. The effect of CO_2 on NPP occurs mainly through reducing stomatal conductance and transpiration and improving water use efficiency; at the same time, it stimulates higher rates of photosynthesis and increases light-use efficiency (Drake et al. 1997). Without competition, elevated CO_2 typically increases leaf area, leaf mass, and numbers of produced branches (Saxe et al. 1998; Tissue et al. 1997). Sufficient nutrient provisions can also significantly amplify the effects of elevated CO_2 on carbon gain and biomass increment (Winter et al. 2001). Four FACE experiments representing a broad range of productivity, climatic and soil conditions, stand developmental history, and life history characteristics of the dominant species have demonstrated that NPP is highly conserved across a broad range of productivity, with a stimulation at the median of 23 +/- 2% (Norby et al. 2005).

However, questions remain as to whether the forest growth stimulated by elevated CO_2 will persist in a long experimental period, or whether such an effect is occurring on a large scale in natural forest stands. Some longer-term exposure studies suggest a reduction in carbon gain due

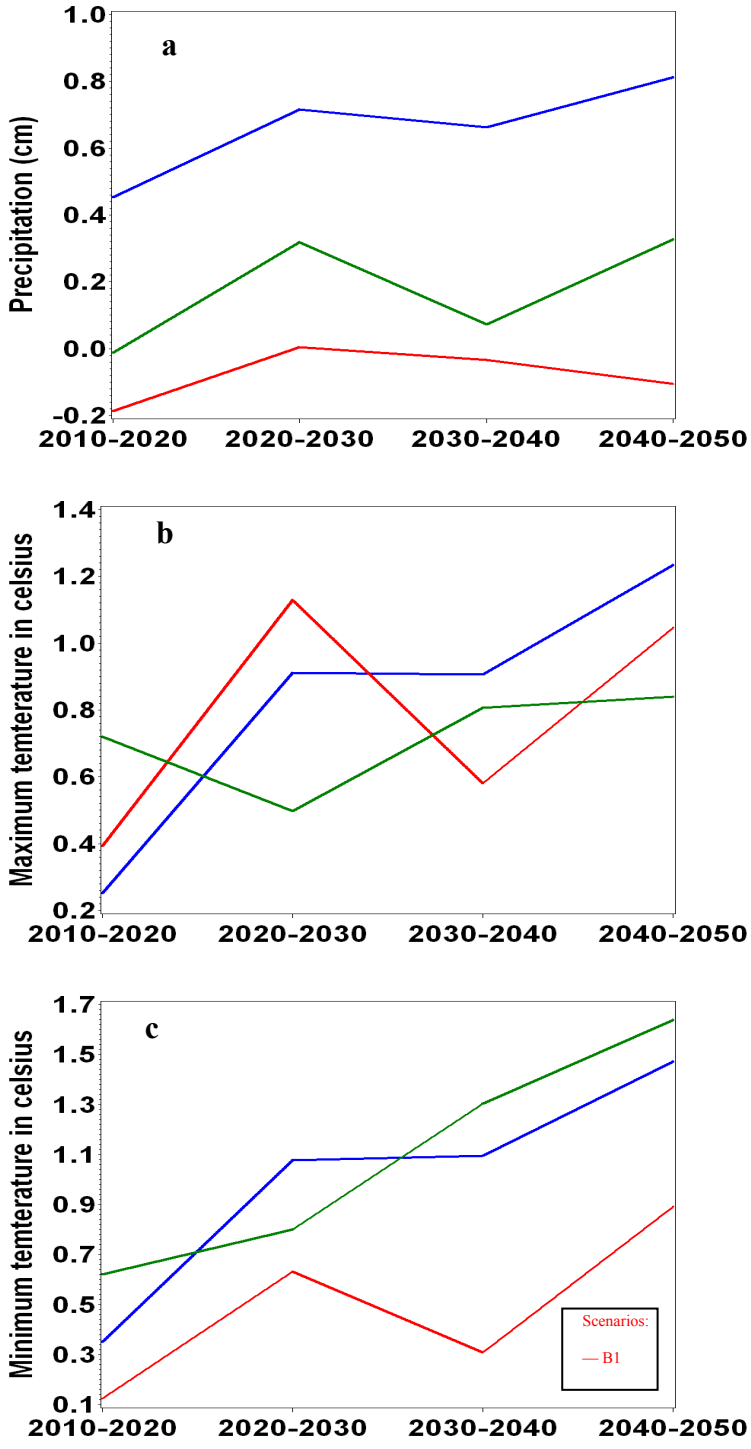

Fig. 30 Changes in 10-yr average (a) precipitation, (b) maximum temperatures, and (c) minimum temperatures during 2010 to 2050, relative to the 2000-2010 mean by the climate change scenarios.

to nutrient limitations, or end-product inhibition occurs over time (down-regulation of photosynthetic rates) (Tissue et al. 1993; Tissue et al. 1996; Tissue et al. 1997; Vivin et al. 1995). In addition, Asshoff et al. (2006) documented that after four years of exposure of 100-year-old temperate forest trees to elevated CO_2, the stem growth did not support the notion that mature forest trees will accrete wood biomass at faster rates in a future CO_2-enriched atmosphere. Korner et al. (2005) also found there was no overall stimulation in stem growth and leaf litter production of 35-meter-tall temperate forest trees after four years of exposure to elevated CO_2. Kiensat and Luxmoore (1988) obtained tree cores from 34 sites in four different climatic regions in the northern hemisphere, and concluded that increased growth in any of the tree-ring chronologies could not be solely attributed to higher atmospheric CO_2 concentrations. Jozsa and Powell (1987) analyzed boreal forest growth and found no an indication that there was a systematic growth trend related to CO_2 fertilization. In complicated real-world situations, the CO_2 fertilization effects in natural forest stands may be relevant to many factors other than CO_2 alone.

Uncertainties in Spatial Estimation of NPP

Spatial variations of predicted NPP over the years of 1980 through 2050 indicated a notable dependence of NPP on climate (Fig. 27). The prediction at the large pixel size of 1.4° by 1.4° of climate input data can result in high NPP changes (about 490 g/m^2) between one latitudinal climate zone to the next one. In contrast, within each climate zone, the standard deviation of NPP for all pixels was quite low, about 73 g/m^2. The small change of NPP within each climate zone and the jump of the mean NPP from one latitudinal climate zone to the next one, indicates a larger control of climate on NPP with relatively minimal effects of site conditions, such as soil water holding capacity or lengths of day and night.

Sensitivity analysis revealed that NPP prediction was most sensitive to foliar N concentration,

the slope of the linear relationship between maximum net photosynthesis and foliar N concentration, and daily max net photosynthesis as a fraction of the early morning instantaneous rate. In this study, values of these three parameters were kept unchanged for all pixels in the entire state. Therefore, the effects of these three parameters on spatial patterns of NPP were not determined. In order to reduce uncertainties of NPP over space, two steps may be required. First, climate models may need to produce products with a finer spatial scale. For instance, 4 km by 4 km climate data have been created for historical climate data, using the PRISM (Parameter-elevation Regressions on Independent Slopes Model) climate mapping system. Second, given the importance of parameters in spatial forecasting with an ecosystem model, the uncertainty caused by parameterization should be minimized through generating spatial layers of the parameters at a fine spatial scale. In some cases, the use of hyperspectral remotely-sensed data to generate spatial parameter layers, such as foliar N concentration, is possible (Ollinger and Smith 2005). However, in other cases, such an approach is impracticable, due to a limited availability of hyperspectral data. Therefore, spatial layers of the parameters should be generated by incorporating multispectral remotely-sensed data, inventory data (e.g., forest inventory and analysis data, and SSURGO soil data), field investigations and long-term records with geospatial techniques, such as k-nearest neighbors, segmented regression, and geospatial statistics. The generated spatial data layers will represent variations of vegetation parameters at a local scale. Particularly, such datat would be a better choice for heterogeneous landscape that has various vegetation types. Even though it is possible to derive values of some parameters, such as foliar N concentration for each species at landscape level, the determination of the values for broad forest groups of deciduous, evergreen, mixed, and woody wetland forests may be more practicable for applications. The reason is that the relationship of photosynthesis and foliar N concentration may highly vary when individual species or narrow species groupings are compared, but a positive linear trend should

be clearly viewed across a broad range of species (Peterson et al. 1999).

Conclusions

This study predicted NPP changes in Louisiana forests in response to three climate change scenarios with low, moderate, and high emissions (A1B, A2, and B1) for the period from 2000 through 2050. The modeling results indicate that a future climate change would increase forest productivity under scenarios A1B and A2, but they would reduce forest productivity under scenario B1. The mean forest NPP of B1 scenario over the years from 2000 to 2050 was significantly different from those of A1B and A2 scenarios. According to PnET-II, forest NPP appears to be primarily a function of minimum temperature and precipitation, rather than maximum temperature. The uncertainty of NPP over the space was noticeably related to spatial resolution of the climate variables. The study demonstrated that Louisiana forest ecosystems could be a carbon sink in the 21st century as long as the forest NPP is greater than the carbon loss duo to soil heterotrophic respiration, natural disturbances, and human activities. Decision makers necessitate to make long-term plans to reduce the carbon loss, and thus utilize the forests as a carbon sink to mitigate carbon dioxide greenhouse effects.

CHAPTER 5 COMPARISON OF REMOTE SENSING CHANGE DETECTION TECHNIQUES FOR ASSESSING HURRICANE DAMAGE TO FORESTS[1]

[1] With kind permission from Spring Science + Business Media: Environmental Monitoring and Assessment, comparison of remote sensing change detection techniques for assessing hurricane damage to forests, doi: 10.1007/s10661-009-0798-8, Fugui Wang and Y. Jun Xu.

Introduction

Hurricanes frequently cause extensive windthrow of trees, damage forest structures (Imbert et al. 1996), and fragment the forested landscape (Boose et al. 1994; Foster and Boose 1992). Such disturbances not only impact timber industry (Leininger et al. 1997) and wildlife habitats directly (Conner et al. 2005) but also often have long-term effects on forest succession (Vandermeer and Granzow De La Cerda 2004), nutrient cycling (Van Bloem et al. 2005), site productivity (Wang and Hall 2004), and drainage (Peierls et al. 2003). Hurricane Katrina, the third strongest storm to hit the USA coast during the last 100 years, made its landfall on 29 August 2005 near the border of the Louisiana and Mississippi. With sustained winds of 195 km/h hour and a storm surge level up to 7 m, the hurricane caused catastrophic damage in the coastal region of these two Gulf States. Large areas of the region's forests across the wind swath were severely damaged. Accurate determination of areas and severities of disturbed forests and identification of factors contributing to spatial patterns of the hurricane disturbance are essential for forest managers and scientists to take short-term actions on salvage harvesting, wood industry, and habitat protection, as well as to make assessments on long-term environmental impacts and forest ecosystem recovery. However, with much of the Katrina-affected region under permanent or seasonal inundation on the coastal lowlands, a full-scale ground-based assessment is technically difficult and economically challenging.

Remote sensing technique using change detection algorithms along with vegetation indices have been proven in many studies to be an effective means for large-scale assessment on forest disturbances by insect defoliation, clearcuts, and forest fires (Ayala-Silva and Twumasi 2004; Coppin et al. 2004; Coppin and Bauer 1994; Franklin et al. 2000; Hegarat-Mascle et al. 2006; Kwarteng and Chavez 1998; Lyon et al. 1998; Nackaerts et al. 2005; Ramsey et al. 1997). Change detection in remote sensing involves the use of two or multi-dates aerial or satellite

images covering the same geographic area to discriminate changes associated with land use and land cover properties between dates of imaging. Processes of change detection in general include pre-processing satellite imagery, detecting changes with change detection methods, and accuracy assessment. Image pre-processing commonly comprises a series of sequential operations, such as minimizing atmospheric effects on radiance, accurate spatial registration of the various dates of imagery, and transformation of satellite images to indices that are known to have a strong relationship between the index values and properties of land cover. Most documented change detection methods are based on per-pixel classifiers, such as post-classification comparison (PCC) method, and pixel-based change information contained in the spectral domain of the images (e.g. vegetation indices) (Coppin et al. 2004). In order to detect changes from the pixel-based change information on images, change detection algorithms, such as univariate image differencing (UID), are required.

The widely used indices in remote sensing change detection consist of Tasseled Cap index of greenness (TCG), brightness (TCB) and wetness (TCW), ratios of near-infrared to red image (RVI), normalized difference vegetation index (NDVI), and soil-adjusted vegetation index (SAVI). TCG, TCB, and TCW are three of six Tasseled Cap transformation bands calculated from data in the six Landsat TM bands (Crist et al. 1986). The indices are able to measure presence and density of green vegetation, overall reflectance (e.g. differentiating light from dark soils), and soil moisture content and vegetation density (structure) (Crist et al. 1986; Horler and Ahern 1986). Researchers have used TCW to estimate the age and structure complexity of mature and old growth forest stands (Hansen et al. 2001), and to detect forest changes due to mortality and timber harvesting (Collins and Woodcock 1996; Franklin et al. 2000). NDVI with a value range from -1 to +1 (Rouse et al. 1973) is probably the most often used index for detecting both seasonal changes in green biomass and changes to human activities and natural

disturbances. However, NDVI values asymptotically can reach a saturation level after a certain biomass density or leaf area index (LAI). Changes in land cover and biophysical vegetation parameters are difficult to detect in a 'saturated' mode (Huete et al. 1997a). The saturation problem of NDVI may limit its ability to detect relatively low-level damage in high density forests. High soil-induced "noise" in NDVI values could also result in inaccurate interpretation of the vegetation cover (Huete et al. 1994). RVI, the first ratio-based vegetation index (ratio of near-infrared to red) described by Jordan (1969), is a very similar index to NDVI but with higher sensitivity to dense forests. RVI has been found to have the highest sensitivity when LAI is greater than 1.8, while NDVI has the highest sensitivity when LAI is less than 1.8 (Ji and Peters 2007). Therefore, RVI may better differentiate levels of damage to wind-disturbed forests, as opposed to timber harvesting or fire disturbed forests. SAVI is a transformation technique that minimizes soil brightness influences on spectral vegetation indices involving red and near-infrared wavelengths, such as NDVI and RVI (Huete 1988). The use of SAVI can significantly reduce the error in estimation of vegetation coverage caused by soil brightness as compared with NDVI when percentage of vegetation cover is low (Purevdorj et al. 1998).

A variety of change detection algorithms including UID, selective principal component analysis (selective PCA), change-vector analysis (CVA), and post-classification comparison (PCC) have been developed and reviewed (Coppin et al. 2004; Lu et al. 2004). UID is a procedure that pixel value of vegetation index or satellite image from one date is simply subtracted from this of the other. The difference in areas of no change will be very small and areas of change will be the large positive or negative values. Selective PCA analysis is a special case of principal component analysis with only two input variables: pre- and post-events. The information that is common to both is mapped to the first component and that is unique to both is supposed to be mapped to the second component (Chavez and Kwarteng 1989; Coppin et al.

2004). Coppin and Bauer (1994) have successfully detected forest changes by applying UID and the second principal component of selective PCA algorithms to Tasseled Cap bands and NDVI values. Ramsey *et al.* (2001) and Ayala-Silva and Twumasi (2004) identified impacts of hurricane winds on forests through applying UID algorithm to Advanced Very High Resolution Radiometer NDVI values between pre- and posthurricane. CVA processes and analyses changes in all multi-spectral/multi-temporal data layers so as to ensure detection of all changes presented in the data, not just a previously defined change event (Fung 1990; Johnson and Kasischke 1998). Through CVA, spectral changes between two or more dates are separated into two output components: magnitude and direction component. Change magnitude is useful for relative comparisons within and among change types, and computed by determining the Euclidean distance between the two change index images (pre- and post-events). Change direction is a useful aid in discrimination of different phenomenological types of changes and is specified by whether the changes are positive or negative in each band. Allen and Kupfer (2001) have demonstrated that application of CVA provided the ability to summarize spectral changes (magnitude and direction) in high elevation Fraser fir forests due to mortality and regeneration processes. PCC procedure detect changes through classifying two or multi-dates images independently, and then comparing the land cover changes between the dates of imaging. Ucuncuoglu (2006) has demonstrated application of PCC method in detecting changes in coastal wetland and woody vegetation.

Collectively, these previous studies demonstrate the great utilities of using the vegetation indices and the algorithms to detect changes in vegetative surface caused by human activities or natural disturbances. However, strong hurricane winds can modify forest structures in a much different way from a complete timber harvest or insect defoliation. Katrina has left coastal Louisiana and Mississippi with a highly heterogeneous mosaic of completely and partially

uprooted and broken trees. After the hurricane, much of the coastal river floodplains were inundated, causing additional dieback of trees in the lowlands. Therefore, the change detection algorithms successfully applied to other forest disturbances may not be applicable to the hurricane damage. The ultimate goal of the present study was to identify the most appropriate vegetation index and change detection algorithm for assessment of the forest damage caused by Hurricane Katrina in the Lower Pearl River Valley and the surrounding area. We compared four change detection algorithms combined with six vegetation indices and a composite of the TM band 4, 5 and 3. The algorithms included UID, selective PCA, CVA, and PCC. The vegetation indices consisted of TCG, TCB, TCW, RVI, NDVI, and SAVI.

Methods

Study Area

In this study, we assessed forest damage caused by Hurricane Katrina in the Lower Pearl River Valley and surrounding area in St. Tammany and Washington Parish, Louisiana and counties of Hancock and Pearl River in Mississippi. The study area covered a geographic region between 90°21′ W and 89°19′ W, and 31°00′ N and 30°09′ N (Fig. 31). The center of Katrina passed through St. Tammany Parish, Hancock County, and Pearl River County. Pearl River, the largest river within the study area, travels southeasterly toward the Gulf of Mexico, forming an increasingly wide floodplain in the center portion of the area. Lake Pontchartrain, a 1,619-km^2 oligohaline estuary, is located in the southwest corner of the study area. The City of New Orleans is on the lake's south shore.

Forests in this region cover an area of about 370,000 ha, or 53% of the total area investigated. Bottomland hardwoods and upland pine forests are the two major forest types in this region. The upland forests mainly consist of loblolly-shortleaf pine, longleaf-slash pine and oak-pine groups (Wear and Greis 2002). The bottomland hardwoods are predominantly oak-

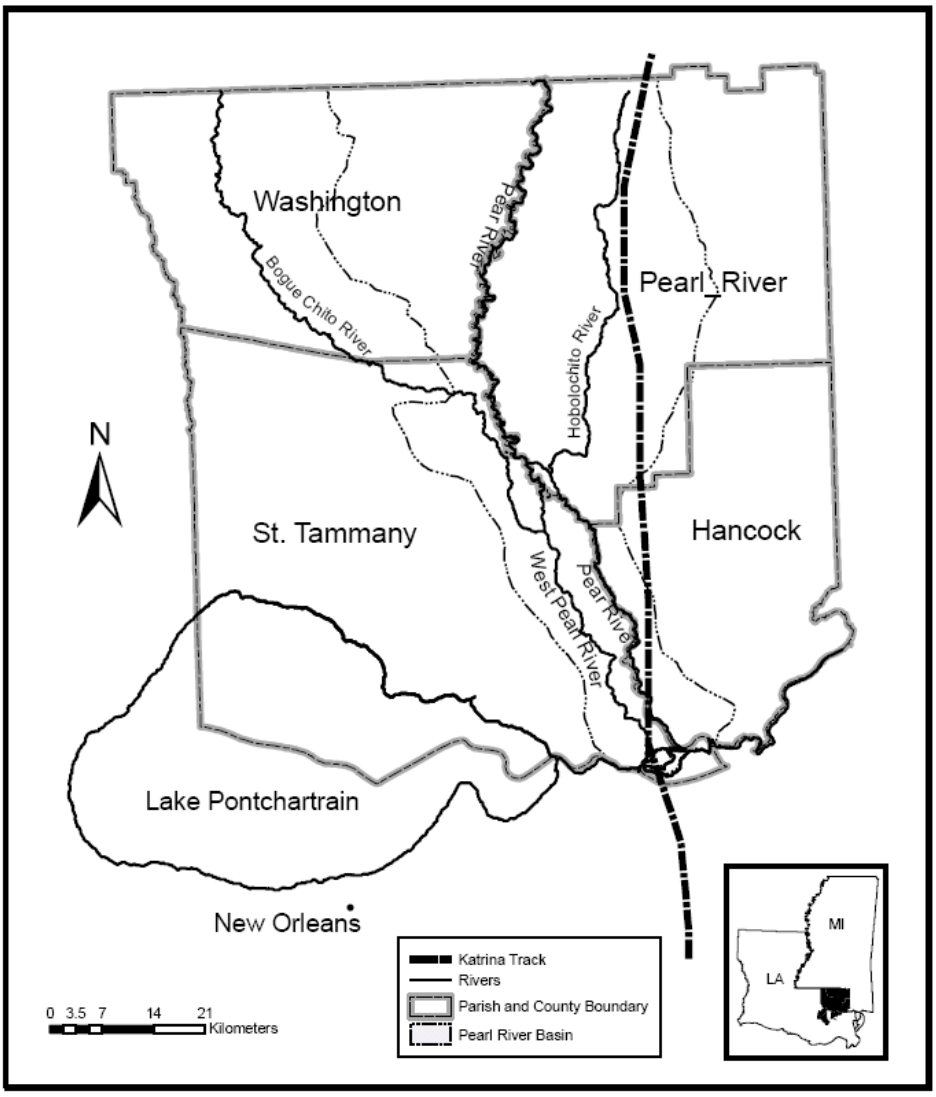

Fig. 31 Geographical location of the study area - The Lower Pearl River Valley and the surrounding area in the two parishes and two counties.

gum-cypress forests, in which over 50% of the canopy trees are tupelo, blackgum, sweetgum, oak, and southern cypress species, and less than 25% are southern pines. Besides timber production, these forests provide hunting, fishing and recreation opportunities, making an important contribution to the local economy and environmental well-being. The forests in the Bogue Chitto National Wildlife Refuge, the Pearl River and the Ben's Creek Wildlife Management Areas are of national importance for wildlife migration in North America.

The region has a subtropical humid climate characterized by an annual average temperature of 19°C, varying from 12°C in January to 28°C in July and by an annual average precipitation of 1,600 mm, ranging from 86 mm in October to 159 mm in July (Keim et al. 1995). Geologically, the region is dominated by Pleistocene river deposits that form terraces of decreasing elevation from approximately 122 m in the north to sea level in the southern portion, with dominant soil great groups of paleudults, fluvaquents and hydraquents (USGS 2002).

Data Collection

Geospatial data

The primary data sources used in this research were remotely sensed data including Landsat 5 TM imagery, Digital Orthophoto Quarter Quadrangles (DOQQ), and National Oceanic & Atmospheric Administration (NOAA) aerial photos. Two sets of the Landsat imagery were collected with the first taken on 22 August 2005, 7 days before Hurricane Katrina's landfall, and the second on 9 October 2005, 41 days after the hurricane. All the vegetation indices were derived from these two images. It was assumed that during this short period of time, no other disturbances occurred in the study area other than the damage from Katrina. It was also assumed that the changes detected by the change detection techniques were a direct result of the hurricane's impacts. The 2004 DOQQ imagery, supplied by Louisiana State University CADGIS Research Laboratory, has a spatial resolution of 1 m on the ground. The DOQQs were used as ground truth measurements to validate land cover classification of the pre-Katrina Landsat imagery. The NOAA aerial photos were acquired during the period between 30 August and 8 September 2005 by NOAA Remote Sensing Division, using an Emerge/Applanix Digital Sensor System from an altitude of 2,286 m. The photos were not georeferenced, but available in JPEG format with a shapefile depicting the approximate ground coverage of each photo.

To facilitate the image processing and execute change detection techniques, two other

geographically referenced data sets were collected: (1) Census 2000 TIGER/Road shapefiles, downloaded from the Environment Systems Research Institute and (2) political boundaries (parish, county and state boundaries), collected from Louisiana GIS May 2005 Supplemental DVD and University of Mississippi Geoinformatics Center.

Ground truth data

The ground truth data were generated through interpretation of NOAA aerial photos and field investigations. Initially, the aerial photos were rectified and registered to the road GIS layers and the TM imagery acquired on 9 October 2005 using a set of ground control points (GCP) for each photo correction, the first-order polynomial function, and a nearest neighbor resampling method. The location errors of the processed photos were controlled within 1 pixel of the satellite image. The disturbed and undisturbed forests were then labeled as polygons on the aerial photos using areas of interest tool in *ERDAS* IMAGINE 9.2 (Leica Geosystems Geospatial Imaging, LCC, Norcross, GA, USA).

Field surveys were conducted in April and June of 2006 for the two major forest categories in the study area. The first field inventory focused on damage in bottomland hardwoods along the coastal river floodplains, while the second field survey assessed disturbance conditions in the upland forests. Using a Trimble GPS receiver (Trimble Navigation Limited, Fremont, CA, USA), a laptop computer uploaded with the road data layer, and a set of pre-classified satellite imagery, forest damage levels were determined, recorded and georeferenced.

Through aerial photo interpretation and field investigation, a total of 6470 pixels (each in the size of 812 m2) were labeled as disturbed forests and a total of 4115 pixels were identified as undisturbed forests. Among all these pixels, 1592 pixels (952 pixels identified as damaged forests and 640 as undisturbed forests) were determined from the field investigations.

Image Preprocessing

Geometric and radiometric corrections were required for absolute comparison among the six vegetation indices and the composite. First, the image acquired on 22 August 2005 was rectified and registered to the image acquired on 9 October 2005 using a set of 42 GCP, the second-order polynomial function, and a nearest neighbor resampling method. The second-order polynomial function was used to correct slight distortion of the imagery. The processed imagery showed a location error of less than 1 pixel for these two images. Then, the two images were radiometrically corrected using the dark object subtraction model (Chavez 1996), which was recommended as one of the best atmospheric correction methods for change detection applications (Song et al. 2001). Through the radiometric correction, the impacts of sun angles and atmosphere factors on reflectance were minimized to a great extent and the digital imagery numbers were converted to reflectance from the ground.

Forested Land Identification

Pre-Katrina forested land areas were identified based on the 22 August 2005 image using ISODATA procedure (unsupervised classification method) and the maximum likelihood method in ERDAS IMAGINE 9.2 (Leica Geosystems Geospatial Imaging, LCC, Norcross, GA, USA). First, the imagery was classified into 250 categories for complex land covers including upland and wetland habitats in the region and a signature file was created by using the ISODATA procedure. Then, the imagery was reclassified into 250 categories using the signature file and maximum likelihood supervised classification method. Through visual inspection of the DOQQs, only the categories which apparently were forests or the categories which could be forests were carefully interpreted, determined, and grouped. The generated forestland imagery served as a mask of continuous change imagery and was applied as auxiliary data in detecting forest disturbance by PCC algorithm along with the composite imagery of bands 4, 5 and 3.

Generation of Vegetation Index Imagery

Images of vegetation indices including TCG, TCB, TCW, RVI, NDVI, and SAVI were derived from the satellite imagery through the equations given in Table 6. The adjustment factor (L) in the SAVI equation was set as 0.5. Setting L as 0.5 is an appropriate representation of the overall intermediate density of the forests in the area. Increases in *L* greater than 0.5 would introduce increasing soil background influences in SAVI (Huete 1988).

Table 6 Equations used to calculate the vegetation indices

Indices	Formulas[a]	Sources
RVI	TM4 / TM3	(Jordan 1969)
NDVI	(TM4 - TM3) / (TM4+TM3)	(Rouse et al. 1973)
SAVI	(TM4 - TM3) × (1+L) / (TM4+TM3+L)	(Huete 1988)
TCB	TCB = 0.3037 × TM1 + 0.2793 × TM2 + 0.4743 × TM3 + 0.5585 × TM4 + 0.5082 × TM5 + 0.1863 × TM7	(Crist et al. 1986)
TCG	TCG = - 0.2848 × TM1 - 0.2435 × TM2 - 0.5436 × TM3 + 0.7243 × TM4 + 0.0840 × TM5 - 0.1800 × TM7	(Crist et al. 1986)
TCW	TCW = 0.1509 × TM1 + 0.1973 × TM2 + 0.3279 × TM3 + 0.3406 × TM4 - 0.7112 × TM5 -0.4572 × TM7	(Crist et al. 1986)

[a]TM1, TM2, TM3, TM4, TM5, and TM7 stand for the six band images of Landsat TM from band 1 through band 5, and band 7.

Changed Feature Extractions

After the vegetation index imagery was created, algorithms of UID, selective PCA, and CVA were applied to the vegetation index imagery of TCG, TCB, TCW, RVI, NDVI, and SAVI for both pre- and post-Katrina to generate continuous change imagery for extracting the changed features.

Generation of continuous change imagery by UID algorithm was performed through subtracting the vegetation index (VI) imagery post-Katrina from pre-Katrina, by which the differences in the spectral responses to hurricane damage were emphasized and impacts of topographic effects were reduced (Lu et al. 2004) . In an ideal case, if forest cover was altered by Katrina, UID should generate a continuous change imagery in which negative values signify disturbed forests, and zero or positive values represent undisturbed forests.

Selective PCA analysis was applied to the bi-temporal vegetation index pairs (pre- and post-Katrina). A linear transformation routine was performed: selective PCA imagery= PCA ($VI_{post,}$ VI_{pre}), whereby the second principal component was assumed to represent the forestland changes from pre- to post-Katrina as recommended by literatures (Coppin et al. 2004).

In this study, it is known that type of changes in the forested land are forest damage by Katrina, which results in negative value changes for TCW, TCG, RVI, NDVI, and SAVI pixels of disturbed land, and positive for TCB pixels. Forest changes due to other reasons, such as forest growth in September, in such a short period interval (41 days) is not a major concern. Therefore, CVA was only applied for detecting the magnitude of changes in the forestlands. The magnitudes of forest changes were computed through a quadratic-square-root transformation of the vegetation indices between pre- and post-Katrina as follows:

$$\Delta M_{WB} = \sqrt{(post_{TCW} - pre_{TCW})^2 + (post_{TCB} - pre_{TCB})^2}$$

$$\Delta M_{GBW} = \sqrt{(post_{TCG} - pre_{TCG})^2 + (post_{TCB} - pre_{TCB})^2 + (post_{TCW} - pre_{TCW})^2}$$

$$\Delta M_{WNRS} = \sqrt{(post_{TCW} - pre_{TCW})^2 + (post_{NDVI} - pre_{NDVI})^2 + (post_{RVI} - pre_{RVI})^2 + (post_{SAVI} - pre_{SAVI})^2}$$

$$\Delta M_{WNR} = \sqrt{(post_{TCW} - pre_{TCW})^2 + (post_{NDVI} - pre_{NDVI})^2 + (post_{RVI} - pre_{RVI})^2}$$

$$\Delta M_{NR} = \sqrt{(post_{NDVI} - pre_{NDVI})^2 + (post_{RVI} - pre_{RVI})^2}$$

Where:

ΔM_{WB}: Magnitude changes of TCW and TCB

ΔM_{GBW} Magnitude changes of TCG, TCB, and TCW

ΔM_{WNRS} Magnitude changes of TCW, NDVI, RVI, and SAVI

ΔM_{WNR} Magnitude changes of TCW, NDVI, and RVI

ΔM_{NR} Magnitude changes of NDVI and RVI

The designs of these index combinations were for testing if the addition of extra pairs of indices could improve the detection accuracy, and if CVA with multiple indices is more powerful in detecting hurricane disturbance, compared to the UID algorithm. For instance, ΔM_{WB} can be compared to continuous TCW change imagery produced by UID because if change of TCB is 0, then the ΔM_{WB} is equivalent to UID.

Identification of the Disturbed Forests and Accuracy Assessment

There are a number of automatic, semiautomatic or manual trial-error approaches developed for identifying the land cover changes on continuous change imagery (Bruzzone and Prieto 2000; Chen et al. 2003; Ridd and Liu 1998). These approaches detect land cover changes based on threshold values determined either automatically by certain algorithms or by manual trial-error approaches, which are complicated to apply and may affect both accuracy and reliability of the change detection processes. In our study, along with reliable ground truth data, supervised classification method was used to classify the continuous change imagery, and composite imagery of TM bands 4, 5 and 3 post-Katrina into two categories: disturbed and undisturbed forests. For PCC algorithm, the classified image alone showed changes in the forested land caused by Katrina because the image pre- Katrina just has one class: undisturbed forests. About 15% of the ground truth pixels were randomly chosen as independent data for accuracy assessment. The error matrix, accuracy totals, and kappa statistics (KS) were computed to evaluate accuracies of the classifications.

Results

Area and spatial distributions of forests disturbed by Hurricane Katrina varied with the change detection techniques (Table 7; Fig. 32). Area of the disturbed forestland ranged from

85,861 ha detected by selective PCA of SAVI to 264,617ha by PCC with two noticeable area groups of greater than 180,832 ha and less than 124,205 ha. The landscape with disturbed forests also displayed two unique patterns, depending upon the area group. The spatial pattern of the landscape with larger disturbed areas showed that the disturbed forests were across the entire region with a mosaic of undisturbed and disturbed forest patches (Fig. 32a). On the contrary, the landscape pattern with lower disturbed area showed that disturbed forests were clustered in Pearl River valley and southern Hancock County (Fig. 32b).

Table 7 Disturbed forest areas and accuracy assessments of the change detection techniques

Algorithm	Vegetation index	Disturbed area (ha)	Overall accuracy (%)	Error I[f] (%)	Error II[g] (%)	Difference between errors I and II (%)	Overall kappa statistics	KS for the undisturbed forests	KS for disturbed forests
UID	TCW	186625	78.4	23.5	19.9	3.6	0.56	0.57	0.56
	NDVI	109458	66.4	45.2	24.1	21.1	0.31	0.27	0.36
	RVI	115399	67.5	52.4	16.4	36.0	0.32	0.25	0.46
	SAVI	108521	59.5	60.2	24.8	35.4	0.15	0.12	0.21
2nd component of selective PCA	TCW	206449	58.5	45.0	38.0	7.0	0.16	0.17	0.16
	NDVI	108611	66.7	44.3	24.2	20.1	0.32	0.28	0.36
	RVI	124205	69.5	41.4	21.8	19.7	0.37	0.33	0.48
	SAVI	106783	59.7	59.9	24.8	35.1	0.16	0.13	0.22
CVA	WB[a]	190891	80.8	22.1	16.7	5.3	0.61	0.61	0.61
	GBW[b]	180832	80.6	22.8	16.6	6.2	0.61	0.6	0.62
	WNRS[c]	109820	67.6	54.6	14.4	40.2	0.32	0.24	0.49
	WNR[d]	109858	67.6	54.6	14.4	40.2	0.32	0.24	0.49
	NR[e]	109853	67.6	54.6	14.4	40.2	0.32	0.24	0.49
PCC	B453	264617	86.4	13.9	13.4	0.5	0.72	0.74	0.71
1st component of selective PCA	TCW	198625	81.2	22	15.6	6.4	0.62	0.61	0.63
	NDVI	120281	60.4	47.6	33.0	14.6	0.19	0.18	0.21
	RVI	226072	60.9	20.2	53.9	33.7	0.24	0.42	0.17
	SAVI	85861	50.7	68.4	33.9	34.5	0.02	-0.02	-0.03

[a]TCW and TCB
[b]TCG, TCB, and TCW
[c]TCW, NDVI, RVI, and SAVI
[d]TCW, NDVI, and RVI
[e] NDVI and RVI
[f]Error of disturbed forests classified as undisturbed
[g]Error of undisturbed forests classified as disturbed

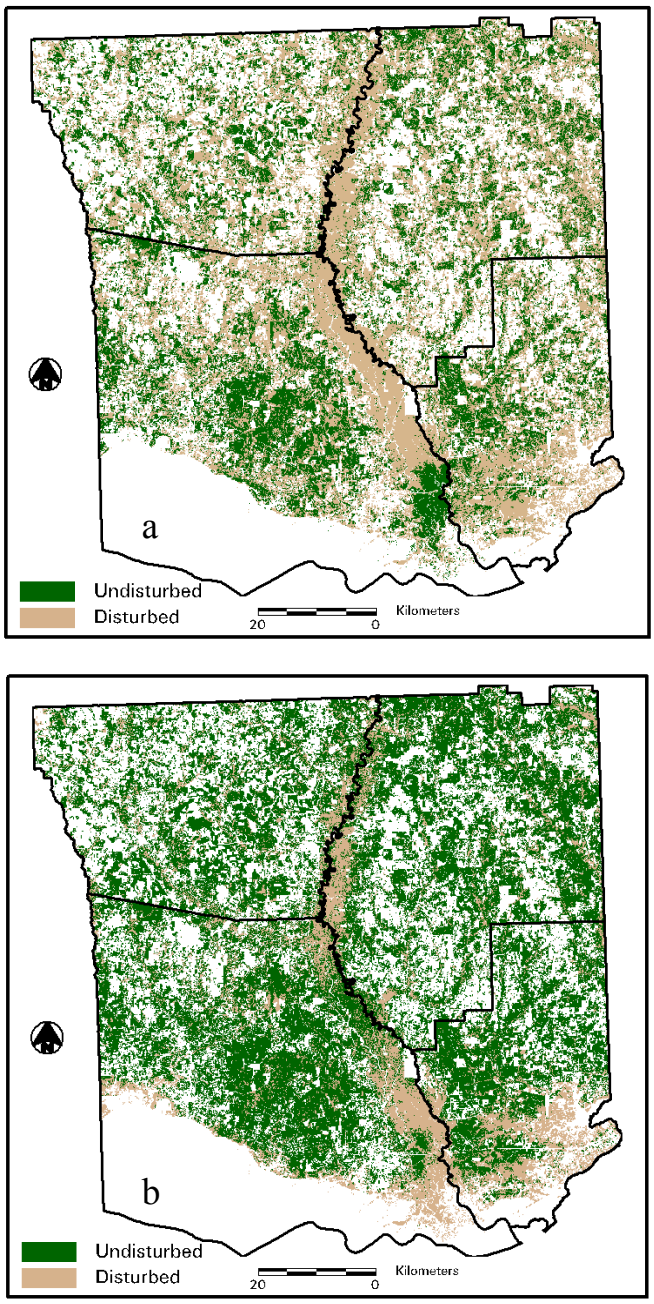

Fig. 32 Disturbed and undisturbed forested land areas identified by (a) PCC of composite of bands 4, 5 and 3, representing the techniques identified higher disturbed areas and (b) the second component of selective PCA of SAVI, representing the techniques identified lower disturbed areas.

Overall accuracies and KSs of the classification varied between 50.7% and 86.4% and between 0.02 and 0.72 (Table 7), respectively. The PCC algorithm along with a composite image of the TM bands 4, 5 and 3 appeared to be the most promising method with the highest overall accuracy and KS. The second highest overall accuracies (> 78%) and KSs (> 0.56) were achieved through CVA of TCW and TCB, and of TCG, TCB, and TCW, UID of TCW, as well as the first component of selective PCA of TCW. The UID of SAVI, the second component of selective PCA of TCW, and the first and second components of selective PCA of SAVI produced the lowest overall accuracies (50-60%) and KSs (0.02-0.16). The remaining techniques including CVA of TCW, NDVI, RVI and SAVI (ΔM_{WNRS}), of TCW, NDVI, and RVI (ΔM_{WNR}), and of NDVI and RVI (ΔM_{NR}) reached similar overall accuracies of about 68% and overall KSs of 0.32.

Comparing the overall accuracies and KSs of the three vegetation indices of NDVI, RVI, and SAVI, almost identical values were achieved between algorithm of the UID and the second component of selective PCA (Table 7). In contrast, the overall accuracies and KSs of the TCW generated by the two algorithms were clearly different. The generated overall accuracies and KSs through CVA algorithm were 81% and 0.61 for ΔM_{WB} and ΔM_{GBW}, as well as 68% and 0.32 for ΔM_{WNRS}, ΔM_{WNR} and ΔM_{NR}. These analyses indicated that the algorithms may not be crucial in achieving high accuracies of the classification, depending upon the index used.

When the supervised classification method was applied to the continuous change imagery to classify the forests into disturbed or undisturbed forests, the error matrix showed 14% to 68% of disturbed forests were classified as undisturbed (Error I) and 13% to 54% of undisturbed forests were classified as disturbed (Error II) (Table 7). The differences between Error I and Error II ranged from 0.5% to 40% and the positive values of the differences indicated an underestimation

for the damaged forestland areas, whereas a negative value would have indicated an overestimation. The PCC approach produced the lowest difference of the errors (0.5%) with a land area of 264,617 ha forests damaged, representing about 60% of the total forested land in the study area.

Discussion

Comparison of Change Detection Algorithms

The PCC algorithm along with the composite of TM band 4, 5, and 3 achieved the best result in identifying forests disturbed by Hurricane Katrina in this study. In contrast, the PCC algorithm has been frequently judged unsatisfactory (Howarth and Wickware 1981) because the approach completely depends on the accuracy of the initial classification (Coppin et al. 2004). High accuracy produced by the PCC in this study may partially be attributed to the fact that only one initial class, forests, was concerned and that the post-classification was conducted on the same forested land areas. Consequently, the initial classification accuracy was not a setback. Additionally, changes in spectral values of the TM bands 3, 4, and 5 pre- and post-Katrina may indicate why the PCC algorithm along with the composite outperformed the other techniques (Fig. 33a-c). Histograms of the TM bands 3 and 5 reflectance values show apparently declined absorption of red light (band 3) and increased near-infrared (band 5) reflectance due to tree losses and low moisture content in the disturbed forest canopies. A three-dimensional presentation of bands 4, 5, and 3 values pre-Katrina shows a random, uniform pattern in the space (Fig. 33d). After the hurricane, the pattern changes noticeably to a two-dimensional (a, b) trend, depicting separation of the damaged forests and the undisturbed forests (Fig. 33e). The two clustered groups of pixels (*a* and *b*) are suitable for application of the PCC algorithm, which has been confirmed by the spectral values of the disturbed and undisturbed forests identified by the PCC algorithm (Fig. 33f).

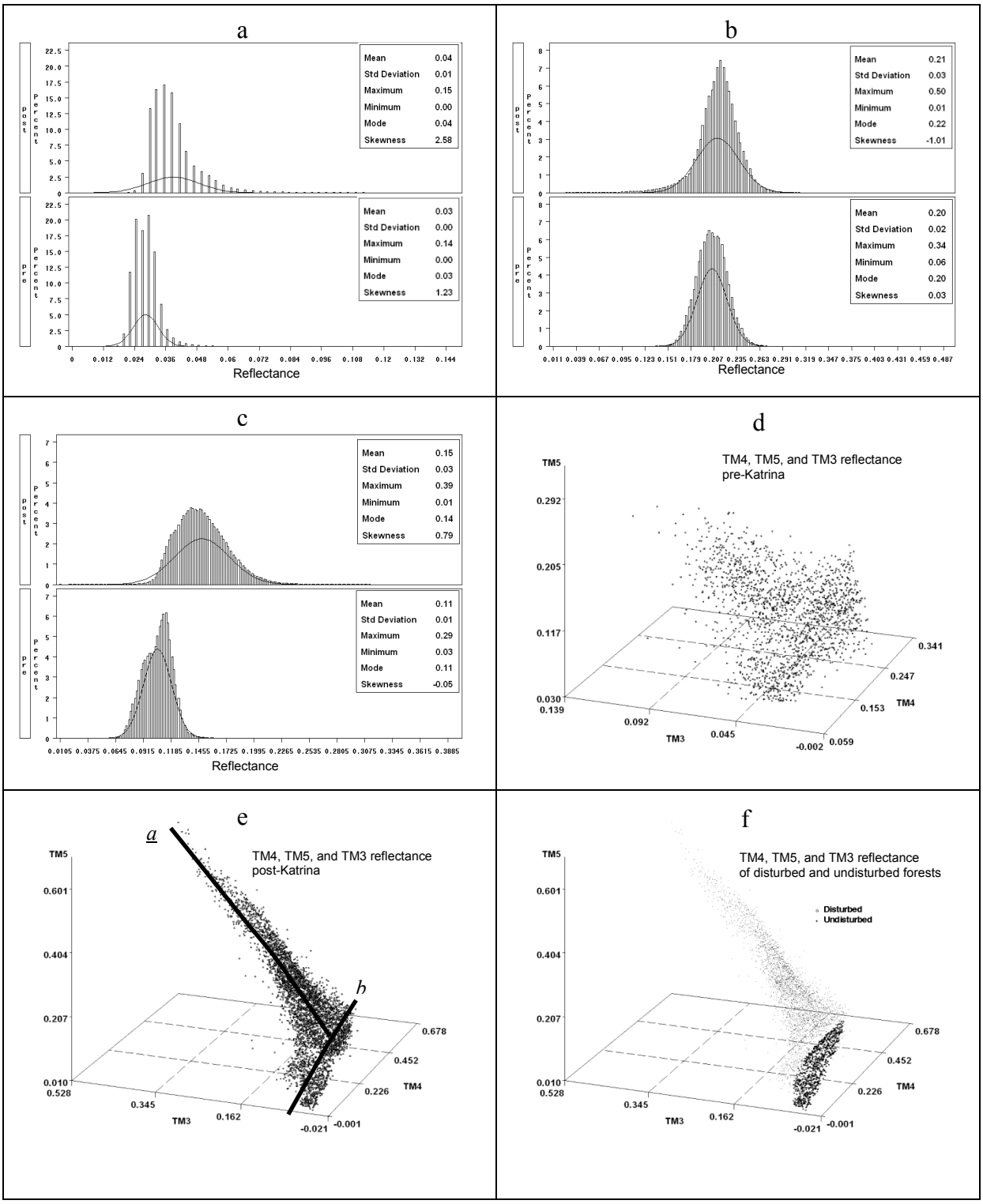

Fig. 33 Changes in distributions of (a) TM3), (b) TM4 and (c) TM5 reflectance values pre- and post-Katrina, three-dimensional views of the values (d) pre- and (e) post-Katrina, and (f) the values of disturbed and undisturbed forests identified by PCC along with composite of bands 4, 5 and 3.

Compared to the other three algorithms, the second component of selective PCA produced lower overall accuracies (Table 7) regardless of which index was used. This indicates that the algorithm is not suitable for deriving change information from the indices pre- and post-Katrina. This may be due to some second components of the PCA not pointing to the largest variance of the disturbed forests (Fig. 34), as we previously expected.

The first principal component of TCW achieved a higher accuracy than the second component (Table 7), indicating that the first component of TCW represented the maximum variance of the disturbed forests (black clouds; Fig. 34a). However, the first components of the NDVI, RVI, and SAVI generated lower accuracies than the second components, indicating that the second components of selective PCA of the three indices represented the maximum disturbance variance (Fig. 34b-d). Therefore, the first components of the TCW and the second components of the NDVI, RVI, and SAVI are appropriate for detecting the disturbance. Thus caution should be taken when using selective PCA since either the first or the second component could be continuous change imagery, relying heavily on vegetation indices.

UID and CVA algorithms did not show a clear difference in disturbance identification. Utilization of multi-indices in CVA did not increase the accuracy significantly. As compared with 78.4% of the accuracy produced by UID algorithm of TCW, the addition of TCB or TCB and TCG to TCW of CVA algorithm only resulted in a 2.2% accuracy increase (80.6%). When TCW or TCW and SAVI were used with NDVI and RVI together, the accuracies remained the same (Table 7). The capability of the UID algorithm in identifying the disturbance largely depends upon the value variations of the indices pre- and post-Katrina. Among all four indices (TCW, NDVI, RVI, and SAVI), the UID algorithm with TCW produced the highest accuracy. This is also reflected by the largest changes in mean and skewness values of the TCW distributions pre- and post-Katrina (Fig. 35a).

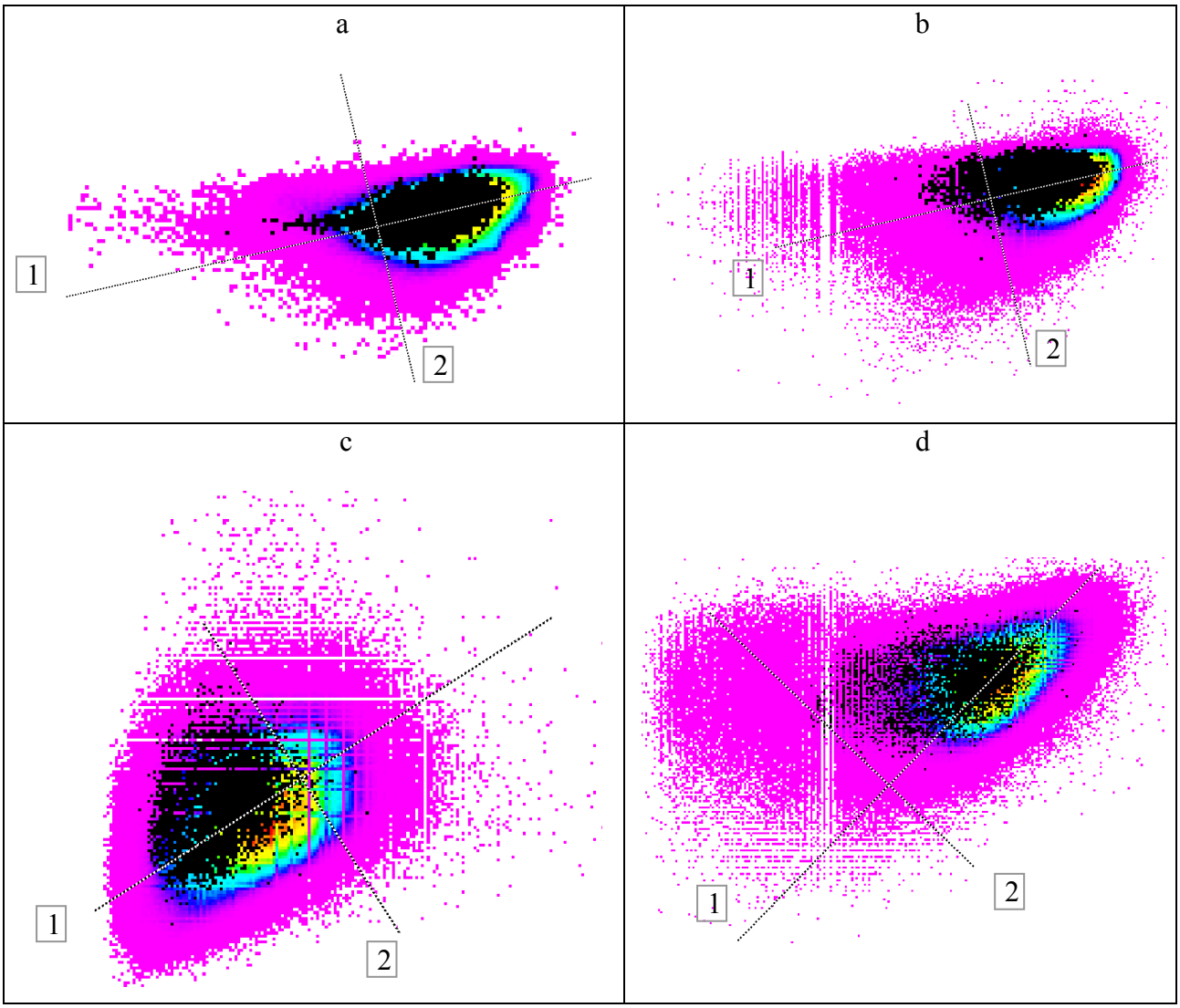

Fig. 34 Spectral images (scatter plots) of the vegetation index values of (a) TCW, (b) NDVI, (c) RVI, and (d) SAVI pre- and post-Katrina (horizontal dimension: post-Katrina index; vertical dimension: pre-Katrina index). The black clouds overlaid on the colored spectral images are spectral feature imagery of the "ground truth" of the disturbed forests. The first and second dash lines represent the first and second principal components, respectively.

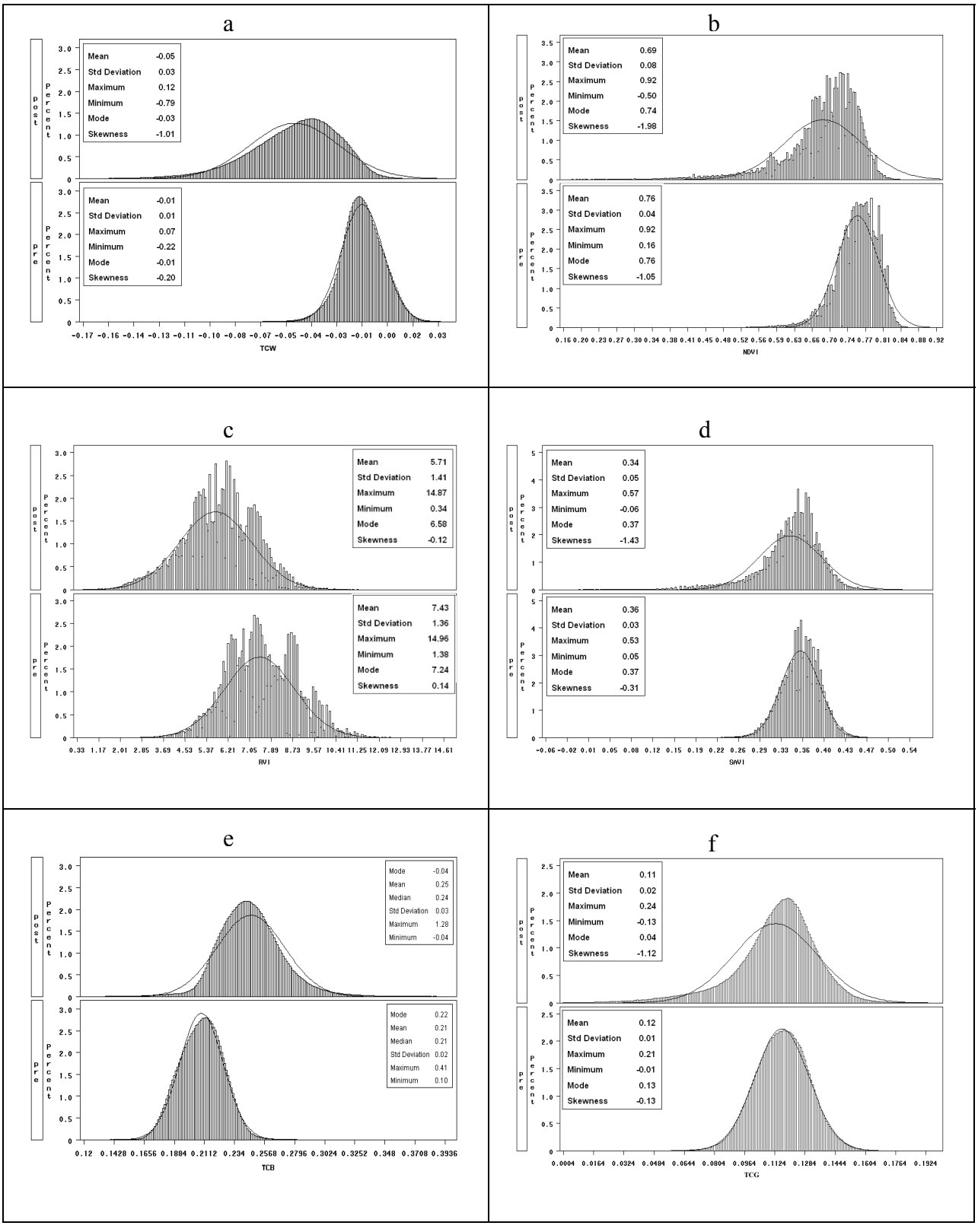

Fig. 35 Changes in the distributions of (a) TCW, (b) NDVI, (c) RVI, (d) SAVI, (e) TCB, and (f) TCG values of pre- and post-Katrina.

Comparison of Vegetation Indices

Among indices TCW, NDVI, RVI, and SAVI, change detection of TCW by applying algorithms UID, the first component of PCA, and CVA resulted in higher accuracy (78.4% - 81.2%), indicating that TCW captured forest changes caused by Hurricane Katrina at the greatest extent. Compared to distributions of TCW, NDVI, RVI, and SAVI values (Fig. 35a-d), TCW value histograms pre- and post-Katrina show the highest percentage of changes in mean (346%), STD (116%), and skewness (395%), which confirmed that TCW captured the maximum information of the forestland modifications. The decreased water content in leaves on damaged trees and more exposed branches and stems in 41 days after the hurricane may have contributed to the average increase in TM band 5 values (37.4%) and band 7 values (56.2%). The apparent changes in the TM band values resulted in lower TCW values after the hurricane and the higher accuracy in the identification of the disturbance by the UID algorithm. This result is in agreement with the findings by Collins and Woodcock (1996) and Franklin et al. (2000) that the change information in forest stands is highly correlated and concentrated in the wetness component of the TM Tasseled Cap transformation.

Accuracies achieved by NDVI, RVI and SAVI were similar with a narrow range of 59.5% to 69.5% by UID and the second component of selective PCA algorithms. When these three indices were used with CVA, a similar accuracy (67.6%) was produced. The three indices are ratio-based indices of Landsat TM red and near-infrared bands. Correlation coefficients were relatively high with 0.97 between NDVI and RVI, 0.80 between NDVI and SAVI, and 0.79 between RVI and SAVI. The high correlations may contribute to similar accuracies in identification of disturbed forest. The highest correlation coefficient between TCW and the three indices was 0.25, which explained why the accuracy of TCW differed from the accuracies of the ratio-based indices, and why combinations of the algorithms and TCW contributed to the highest

accuracies (78.4-81.2%). The correlations may also contribute to the two different classes of disturbed forestland areas and two spatial patterns of those disturbed landscapes identified in this study. Large area of disturbed forests identified by the algorithms combined with NDVI, SAVI , and RVI were bottomland forests in the lower Pearl River Valley and south part of Hancock county, where the forests were severely damaged according to our field observations. This may indicate that NDVI, SAVI, and RVI are more sensitive to severe damage as compared to TCW, which is sensitive to both light and severe damage in upland and bottomland forests.

Although a high correlation exists between NDVI and RVI, RVI was more better than NDVI in identifying hurricane damage. This is reflected by a 14% and 76% higher changes in mean and skewness of RVI than NDVI (Fig. 35b-d; and Table 7). In addition, a smaller change to the maximum NDVI value (0.3%), compared to a greater change of the maximum RVI (3.9%), further confirms the lower sensitivity of NDVI than RVI as described by Ji and Peters (2007) and Hatfield *et al.* (1985). In this study, the saturation problem of NDVI may have constrained extracting forest biophysical changes caused by Hurricane Katrina in lightly disturbed dense forests (Fig. 32b). This is in agreement with the findings by Huete *et al.* (1997a; 1997b) that changes in land cover and biophysical vegetation parameters are difficult to detect in the 'saturated' mode of NDVI.

The advantage of SAVI over NDVI as indicators of vegetation is that SAVI, derived from the NDVI by introducing a constant, L = 0.5, can minimize soil "noise" to the index. The lowest accuracy achieved in identifying the disturbed forests (Table 7) and the smallest change (4.6%) in mean values of the SAVI (Fig. 35d) indicated that soil "noise" did not change adequately pre- and post-Katrina so that the SAVI did not produce better result than NDVI. Abundant understory vegetation, high density of the forests, and woody debris on ground may limit the soil exposure even when some trees in the stands were uprooted.

No significant changes in the TCG distributions pre- and post-Hurricane Katrina (Fig. 35f) indicated that the index is not sensitive to the changes in greenness of the canopy and the forest structures caused by the hurricane. The CVA algorithm also showed that TCG did not enhance detection of the hurricane disturbance to forests. This is because when TCB or TCB and TCG were added to TCW ($\Delta M_{WB}, \Delta M_{GBW}$), an increase of the accuracy of ΔM_{WB} and ΔM_{GBW} was minimal (2.4% and 2.2%, respectively; Table 7). Even though right shift of the TCB histogram revealed a brighter surface post Katrina (Fig. 35e), it seemed that the TCB value changes were not correlated to the forest damage. Low correlation coefficient values of TCG and TCB with TCW (<0.03) also indicated that these two indices cannot be used as TCW to detect hurricane disturbance to forests.

Conclusions

This study compared four change detection algorithms with six vegetation indices and a composite imagery in order to select the most appropriate method for detecting Hurricane Katrina affected forests in the Lower Pearl River Valley and surrounding area. The unique spectral characteristics in the forested lands identified by the value distributions and space feature imagery of the vegetation indices and the Landsat TM composites resulted in a wide range of accuracies among the change detection techniques. Comparably, the vegetation indices exerted a greater influence on the detection results, suggesting that selection of vegetation indices is crucial to ensure accurate estimates of wind-induced forest damage. Among the vegetation indices, TCW showed the best results in detecting changes in forest canopy and structure prior to and following Hurricane Katrina. Forty-one days after the hurricane, changes in band 5 or 7 values could be clearly seen reflecting drastically decreased water content in leaves and branches of damaged trees. The result implies that the vegetation indices encompassing these two bands may greatly increase accuracy in detecting forest cover and structure modifications by

strong hurricane winds. Comparisons of four change detection algorithms did not determine a clear advantage of using one over another. However, detection outcomes from UID, CVA, and PCC seemed to be more reliable and consistent and caution must be taken when applying a selective principle component analysis.

Based on the results gained from this study, the following three methods can be recommended for assessment of wind-induced forest damage: (1) the PCC of composite imagery of band 4, 5 and 3, (2) the CVA of TCW and TCB, and (3) the UID of TCW. We applied the PCC algorithm along with composite imagery of the bands 4, 5, and 3 for our final assessment of Hurricane Katrina's damage to these forests, the results from which were discussed in another paper (Wang and Xu 2008).

CHAPTER 6 HURRICANE KATRINA-INDUCED FOREST DAMAGE IN RELATION TO ECOLOGICAL FACTORS AT LANDSCAPE SCALE[2]

[2] With kind permission from Spring Science + Business Media: Environmental Monitoring and Assessment, Hurricane Katrina-induced forest damage in relation to ecological factors at landscape scale, doi: 10.1007/s10661-008-0500-6, Fugui Wang and Y. Jun Xu.

Introduction

Spatial patterns of disturbed forestlands by hurricanes and severities of the damage are controlled by a series of biotic and abiotic factors including species, stem size, canopy structure, stand density, intensity of the wind, topography, and soil characteristics (Everham and Brokaw 1996). Associations between these factors and hurricane disturbances have been investigated extensively at small scales (Bellingham 1991; Brokaw and Grear 1991; Everham and Brokaw 1996; Gardner et al. 1992; Gresham et al. 1991; Imbert et al. 1996; Ostertag et al. 2005; Van Bloem et al. 2005). However, applications of remote sensing and GIS techniques to investigate relative roles of the different factors in controlling spatial patterns and severities of hurricane disturbance to forests at landscape scale is minimal and scant (Ayala-Silva and Twumasi 2004; Boose et al. 1994; Foster and Boose 1992; McMaster 2005). Based on an empirical function of wind damage with forest exposure, tree height and species composition, Foster and Boose (1992) constructed a GIS framework to analyze the forest responses to strong wind at landscape level. Boose et al. (1994) demonstrated that wind velocity gradients, variation in site exposure, local topography, and forest species composition and structure controlled hurricane damage to forests at landscape scale through assessment of actual forest damage with remotely sensed data. Furthermore, McMaster (2005) predicted forest areas damaged by a severe storm using slope, aspect, soil moisture, relative elevation and land cover as predictors and achieved an overall prediction accuracy of 60%.

Hurricane Katrina, the third deadliest hurricane in the United States since 1900 (Knabb et al. 2006), swept through the coastal region of Louisiana and Mississippi states in August 2005. Forest landscape in the Lower Pearl River Valley, a portion of coastal Louisiana and Mississippi states, was disturbed at various intensities with some forest stands disturbed severely while others undisturbed. A series of factors including hurricane gusty winds, diverse forest types and

properties, and changes in soil groups, elevation, slope and aspect may have contributed to the divergent vulnerability of forests in responses to Katrina's disturbance. Through applying remote sensing and GIS techniques, and logit regression analysis, this study was carried out to: (1) assess Hurricane Katrina damage to forests in the Lower Pearl River Valley and surrounding area; (2) analyze effects of forest characteristics and site conditions on the hurricane disturbance; and (3) model probabilities of forests disturbed by the hurricane. We hypothesize that the hurricane would create complex heterogeneous patterns across the landscape because of variations of the ecological factors within the affected area. A change detection technique, post classification comparison (PCC) algorithm along with two composites of Landsat-5 TM bands 4, 5 and 3 imagery acquired pre- and post-Katrina was applied to identify the disturbed forests and severity of the damage. The assessed factors of forests and site conditions consisted of landform characteristics of elevation, slope, and aspect, soil great groups, buffer zones along river channels, forest types, and forest attributes derived from Landsat TM vegetation indices of normalized difference vegetation index (NDVI) and Tasseled cap wetness (TCW). The factors with continuous attributes were classified into discrete categories for analysis together with the categorical factors, such as soil groups (Table 8). The relative effects of the categories in each factor on the hurricane disturbance were assessed through comparing percentages of the total disturbed forest areas, percentages of the disturbed forest areas at three severity levels (high, moderate, and light), and odds ratios (exponents of the coefficients of independent variable in a full logit model). The relative effects of each factor on the disturbance were determined through comparing the full and reduced logit models.

Study Area

In this study, we evaluated forest damage caused by Hurricane Katrina in the Lower Pearl River Valley and surrounding area in St. Tammany, Washington Parishes in Louisiana, and

Table 8 Pre-Katrina forest distribution, types and environmental conditions in the Lower Pearl River Valley

Category	1[a]			2		3		4		5		6		7	8
	Soil groups	Drainage[b]	Forest (%)	Aspect	Forest (%)	Slope	Forest (%)	Forest types (ftypes)	Forest (%)	Elevation	Forest (%)	Buffers	Forest (%)	NDVI	TCW
1	Dystrudepts	5	7.4	0-45	10.2	0	55.5	Urban	4.3	0-24	48.2	<100	22.5	<0.660	<-0.0180
2	Hapludults	5	3.4	45-90	12.8	1	16.4	Deciduous	0	24-48	21.3	100-200	17.9	0.660-0.704	-0.018- -0.011
3	Fluvaquents	2,3	17.3	90-135	14	2	11	Evergreen	39.5	48-72	18.2	200-300	14.2	0.704-0.739	-0.011- -0.003
4	Hydraquents	1	12.7	135-180	13.4	3	7.3	Mixed	1.7	72-96	10.6	300-400	11.1	0.739-1	-0.003-0.0516
5	Paleudults	2	33.8	180-225	13.4	4	4.5	Shrub/Scrub	13.2	96-122	1.8	400-500	8.4		
6	Fragiudults	4	4.4	225-270	13.8	5	2.6	Wetlands	41.3			>500	25.9		
7	Glossaqualfs	2	2.9	270-315	11.4	6	1.4								
8	Haplosaprists	1	1.9	315-360	11.2	≥7	1.3								
9	Endoaquepts	3	5.8												
10	Sulfaquents	1	0.6												
11	Paleaquults	4,3,5	9.8												

[a] Drainage 1: very poorly drained; 2: poorly drained; 3: somewhat poorly drained; 4. moderately well drained; 5: well drained
[b] The numbers from 1 to 8 above the columns a numerical representation of the factors assessed in the study.

Hancock, Pearl River Counties in Mississippi, covering a geographical region between 90°21′ W and 89°19′ W, and 31°00′ N and 30°09′ N (Fig. 36). The eye of Hurricane Katrina passed through St. Tammany Parish, Hancock County, and Pearl River County. Pearl River travels southeasterly toward the Gulf of Mexico, forming an increasingly wide floodplain in the center portion of the area. Lake Pontchartrain, a 1,619 km^2 oligohaline estuary, is located in the southwest corner of the area and the city of New Orleans is on the lake's south shore.

Forests in this region occupy an area of about 370,000 ha, which is 53% of the total area investigated in this study. The main forest cover types are wetland forests, upland forests, and urban forests. In wetland forests, over 50% of the stands were comprised of water tupelo (*Nyssa aquatica*), swamp tupelo (*Nyssa biflora*), blackgum (*Nyssa sylvatica*), sweetgum (*Liquidambar styraciflua*), oaks (*Quercus michauxii, Q. pagoda, Q. buckleyi, Q. phellos,* and *Q. lyrata*) and baldcypress (*Taxodium distichum*), and less than 25% were southern pines of loblolly pine (*Pinus taeda*), slash pine (*P. elliottii*), shortleaf pine *(P. echinata),* and longleaf pine *(P. palustris*) (Rosson Jr. 1995; USDA Forest Service 2007). Upland forests are predominantly mixed groups of loblolly-shortleaf-southern yellow pines, longleaf-slash pine forests mixed with oaks, hickories (*Carya spp*.), and gums, and oak-pine mix forests (Rosson Jr. 1995; USDA Forest Service 2007). Besides timber production, the forests in the region provide hunting, fishing and recreation opportunities, making an important contribution to the local economy and environmental well-being. The forests in the Bogue Chitto National Wildlife Refuge, the Pearl River and the Ben's Creek Wildlife Management Areas in the region are of national importance for wildlife migration in North America.

The region has a subtropical humid climate characterized by an annual average temperature of 19°C, varying from 12°C in January to 28°C in July, and by an annual average precipitation of

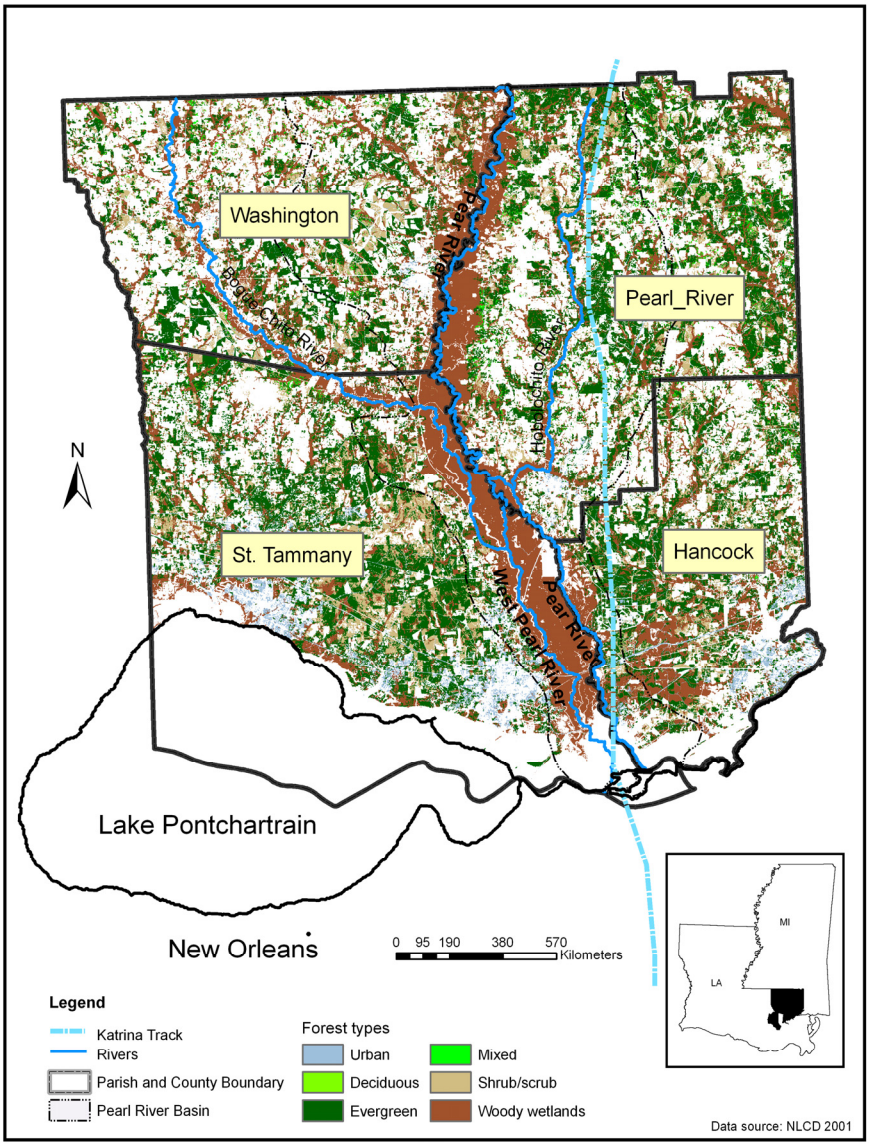

Fig. 36 Study area and spatial distribution of forest types pre-Katrina

1600 mm, ranging from 86 mm in October to 159 mm in July (Keim et al. 1995). Geologically, region has a subtropical humid climate characterized by an annual average temperature of 19°C, varying from 12°C in January to 28°C in July, and by an annual average precipitation of 1600 mm, ranging from 86 mm in October to 159 mm in July (Keim et al. 1995). Geologically, the region is dominated by Pleistocene river deposits that form terraces of decreasing elevation from approximately 122 m in the north to sea level in the south, with dominant soil great groups of

paleudults, fluvaquents and hydraquents (USGS 2002).

Assessment Approaches

Data Collection and Preparations

In addition to the disturbed forest cover map created in a previous study by Wang and Xu (2007), data collected for current study consisted of 2001 National Land Cover Data (NLCD), state soil geographic (STATSGO) data, digital elevation model (DEM) data, and national hydrography dataset (NHD).

NLCD was created on the basis of Landsat 7 ETM+ imagery acquired circa 2000. However, land covers in the region have been changed since the year of 2000. In addition, our field inventory in 2006 showed that Hurricane Katrina severely damaged urban forests, which were classified as part of developed land cover in NLCD. If NLCD had been used directly, disturbance to urban forests would have not been assessed. Moreover, the forestlands which have been deforested before the hurricane, for instance, due to timber production, would have been detected incorrectly as disturbed land by the hurricane. Therefore NLCD map was masked with a 2005 forest cover layer generated in the study by Wang and Xu (2007). The land cover type, developed land cover, was then recoded as urban forest. In the end, five land cover types, urban forests, evergreen forests, mixed forests, shrub/scrub, and wetland forests, were studied.

The STATSGO data structure was designed at three levels of organizations: map unit, component and layer. A map unit (polygon on the map) is a collection of areas defined and named in terms of their soil components, miscellaneous areas or both. Each map unit contains up to 21 components. There are up to 60 soil properties in each component and 28 properties in each layer. This study used soil taxonomy given in the component layer to map the soil great groups at map unit scale.

The DEM data (in 30 x 30 m resolution) was extracted from the U.S. Geological Survey

National Elevation Database (NED, http://ned.usgs.gov/), which is a seamless mosaic of best-available elevation data. Due to artifact removal processing, the elevation data greatly improves the quality of the slope, shaded-relief, and synthetic drainage information. Slope and aspect layers for this study were generated on the basis of the elevation layer with Topographic Tools of ERDAS Imagine 9.0 (Leica Geosystems Geospatial Imaging, LCC, California, U.S.A.).

The NHD layer of flow lines (scale: 1:100,000) was generated from the content of USGS Digital Line Graph (DLG) hydrography data integrated with reach-related information from the EPA Reach File Version 3 (RF3). A stream and river polyline GIS data layer for the study area was clipped from the NHD layer. Five buffer zones with intervals of 100 m were further created along the streamlines.

TCW and NDVI imagery pre-Katrina were derived from the Landsat 5 TM imagery taken on August 22, 2005. These two vegetation indices were used to relate to forest attributes, such as forest coverage and stand density.

After these data layers were generated, the categorical (e.g., soil groups) and the numerical attributes of the data were coded as thematic GIS data layers (column of category in Table 8) for numeric analysis.

Determination of Disturbance Severities

The damage to the forests identified by the post-classification comparison method (Wang and Xu 2007) were further classified into three categories: high, moderate, and light disturbance according to the field inventories (Wang and Xu 2007) by applying the unsupervised classification method. The layer of undisturbed forests overlaid on the disturbed forest layer generated a final map of the hurricane disturbance to forests in the region (Fig. 37).

Quantification of Landscape Metrics

Landscape metrics of the undisturbed and disturbed forests were quantified with

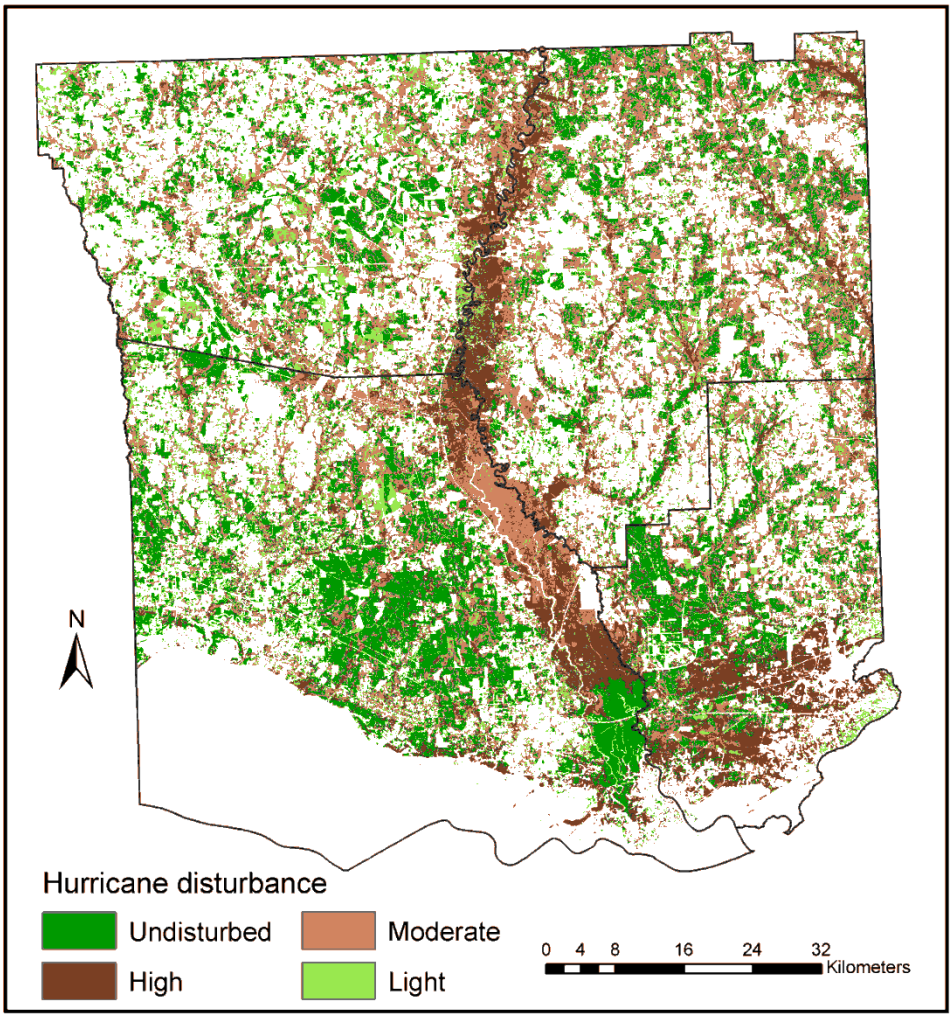

Fig. 37 Spatial distributions of the hurricane-induced forest disturbances by severity levels

FRAGSTATS 3.3, a spatial pattern analysis program developed by McGarigal and Marks (1995). Matrices of forests disturbed at the three severity levels were determined in the same fashion. The quantified metrics consisted of number of patches (NP), patch density (PD), patch area mean (AREA_MN), patch area standard deviation (AREA_SD), largest patch index (LPI), total core area (TCA), total edge (TE), edge density (ED), and landscape shape index (LSI).

Multivariate Regression Analysis

A series of full and reduced logit models were developed to analyze the effects of forest characteristics and site conditions on the hurricane disturbance and to model probabilities that

forests would be disturbed by hurricanes. First, a full model was constructed by entering forest disturbance (the disturbed forests coded as 1 and undisturbed coded as 0) as the dependent binomial variable, and the coded factors of forest type, soil, elevation, slope, aspect, buffer zone, NDVI, and TCW (Table 8) entered as independent variables. Then a series of reduced models were built by sequentially removing the independent variables. Subjects of the variables for fitting the models were from half of the total pixels (size: 28.5 by 28.5 m) in the region, and subjects from the remaining half of the pixels were used to validate the models. Criteria for evaluating the fit of models included percentages of correctly classified undisturbed and disturbed forests, percentage of the concordance of predicted probabilities and observed responses, and Akaike's information criterion (SAS 9.1, SAS Institute, Inc, 2006). Odds ratios derived from the full model were used to compare relative effects of the categories in each factor on occurrence of hurricane disturbance. The comparison is made between the categories coded as lower numbers and the one coded as the highest number (column Category in Table 9). The odds ratio that is greater than 1 indicates that the effect of the lower coded category on hurricane disturbance is less than that of the category with the highest code, suggesting that forests associated to the lower category are less likely to be disturbed by the hurricane. On the other hand, the lower coded category would have stronger effects on the occurrence of hurricane disturbance if the odds ratio is less than 1. Moreover, if the odds ratio is not significantly different from 1, then the two categories have no significant effects on the disturbance probabilities.

Results

Pre-Katrina Forest and Site Conditions

Prior to Hurricane Katrina, percentage of coverage and spatial distributions of forests in the region varied with forest types (Table 8). Wetland forests and upland evergreen forests were two

major forest types. Upland forests distributed uniformly across the entire area (Fig. 36). In contrast, wetland forests noticeably clustered in the Pearl River and Bogue Chitto River valleys. Urban forests were mainly distributed in towns or cities along the north shore of Lake Pontchartrain and Bay St. Louis. Shrub/scrub cover appeared as large patches in St. Tammy Parish.

Percentage of forest coverage also varied with soil great groups, elevation, slope, and stream buffer zones too (Table 8). Among the 11 soil groups, percentage of forest coverage decreased from 34% on paleudults to 0.6% on sulfaquents. Forest coverage declined with increasing elevation and slope. About half of the forests were on 0-24 m elevation land or on the flat plain. Less than 2% of forests were on land with elevation above 100 m or on slope equal or greater than 7 degrees. In addition, increases in distance to the river channels at interval of 100 m from 0 to 500 m were linked to gradually decreased percentage of forest coverage in each zone. Overall, approximately 75% of forests were within 500 m of the river channels. However, percentage of forested land areas did not change greatly with various aspect categories (Table 8).

Disturbed Forested Landscape

In the Lower Pearl River Valley and its surrounding areas, Hurricane Katrina damaged 60% of the forested land with 18% highly, 35% moderately, and 7% lightly disturbed (Table 9). The hurricane altered the forest landscape to a mosaic of undisturbed and disturbed forest patches across the region (Fig. 37). A large fraction of highly and a small portion of moderately disturbed forests apparently clustered in the Lower Pearl River Valley and south Hancock County (Fig. 37). Lightly disturbed forests were randomly scattered as small patches in the region, whereas undisturbed forests noticeably clustered in the Lower Pearl River Valley, the lower portion of St. Tammany Parish, and the northwestern portion of Hancock County (near the Lower Pearl River valley) (Fig. 37).

Table 9 Disturbed forestland areas and landscape metrics by the disturbance

Disturbances	Forestland	Landscape Metrics								
	Areas(ha)	NP	PD	AREA_MN	AREA_SD	LPI	TCA	TE	ED	LSI
Undisturbed	148279.1	22084.0	2.3	6.9	79.7	0.9	85568.6	27130575.0	27.7	173.7
Disturbed	228638.1	18918.0	1.9	12.1	153.6	0.9	138997.5	34672188.0	35.4	181.2
Highly disturbed	69590.2	14914.0	1.5	4.7	66.5	0.4	55504.9	14261115.0	14.6	135.2
Moderately disturbed	133444.6	27270.0	2.8	5.0	28.6	0.3	35668.2	33236073.0	33.9	225.3
Lightly disturbed	25603.3	12386.0	1.3	1.9	7.2	0.0	7371.6	7534488.0	7.7	123.5

In this table and subsequent tables and figures, the highly, moderately, and lightly disturbed categories are subsets of the disturbed category.
NP: number of patches, PD: patch density (number of patches per 100 hectares), AREA_MN: patch area mean (ha), AREA_SD: patch area standard deviation, LPI: largest patch index, TCA: total core area (ha), TE: total edge, ED: edge density (m), and LSI: landscape shape index.

Landscape metrics showed that spatial configurations of the landscapes were different between undisturbed and disturbed forests (Table 9). Compared to undisturbed forests, the lower NP, PD, and higher AREA_MN and TCA associated with disturbed forests indicate that disturbed forests were more aggregated. The higher LSI, ED, and TE of disturbed forests demonstrated that patch shape of disturbed forests was more complex and irregular. Higher TCA of disturbed forests at the three severity levels showed that patches of highly disturbed forests were more clustered than moderately and lightly disturbed forests (Table 9). Moreover, higher LSI and ED indicated that patch shape of the moderately disturbed forests was more irregular than that of lightly disturbed forests.

Spatially, there appeared to be a close association of disturbance intensity with drainage network in the watersheds (Fig. 37). Forests adjacent to streams and rivers in this area were found more severely disturbed by the hurricane (Fig. 38), indicating a high susceptibility of bottomland forests to the hurricane damage. With increasing distance away from the river channels, percentage of the highly disturbed forests declined, while percentages of the moderately and lightly disturbed forests escalated slightly.

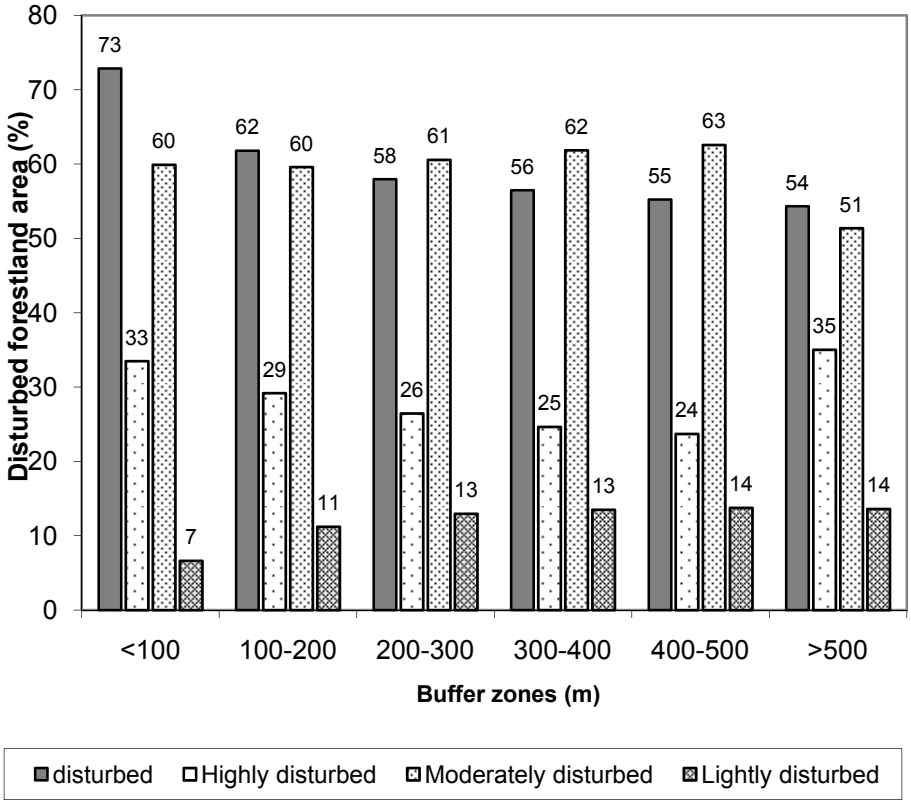

Fig. 38 Percentages of the disturbed forestland areas by the buffer zones

Stand Conditions versus Disturbance Intensities

Area of Katrina-disturbed forests and severity of the damage varied by forest types (Fig. 39). The largest portion of wetland forests was disturbed (78%), followed by urban (73%), mixed (69%), evergreen forests (47%), and shrub/scrub (43%). Among three severity levels of the disturbance, the greatest portion of wetland and urban forests were highly disturbed (39% and 30%, respectively). In contrast, percentages of the moderately disturbed areas for mixed forests and shrub/scrub were the highest (85% and 78%) even though percentages of the total disturbed areas were lowest.

As both NDVI and TCW categories (values) increased, percentage of disturbed forests declined gradually (Figs. 40-41), which indicated that hurricane disturbance was apparently

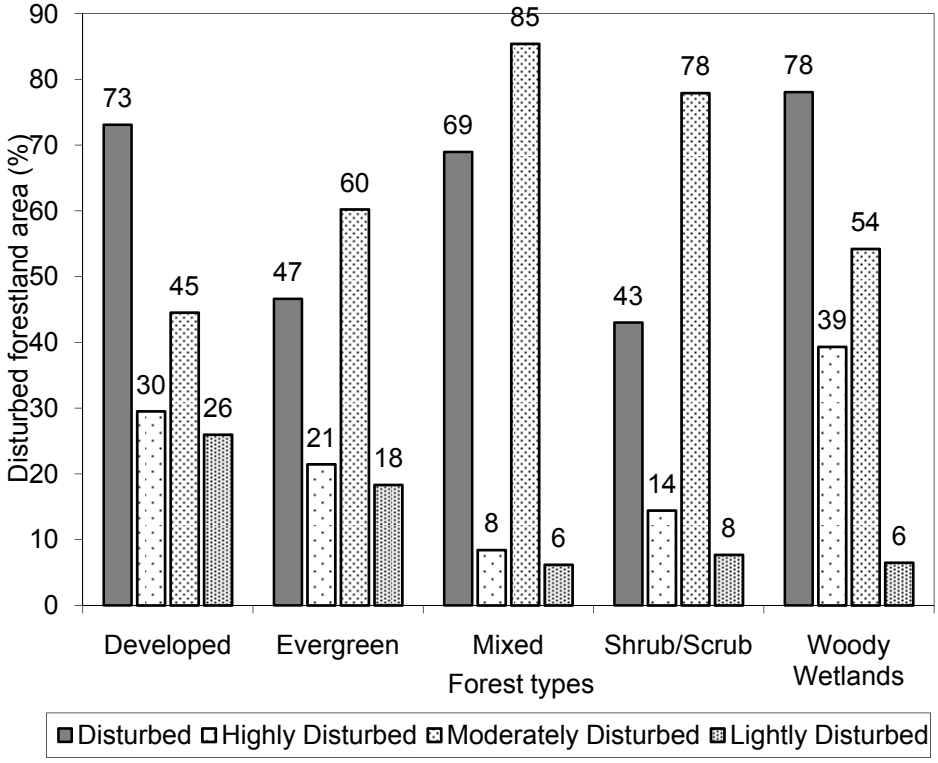

Fig. 39 Percentages of the disturbed forestland areas by the forest types

severer as NDVI and TCW values were lower. Changes in percentage at three levels of the severity under NDVI categories were more noticeable than under TCW categories. The percentage of the highly disturbed forests in category 1 of NDVI was 57 times higher than that in the fourth category. In contrast, percentages of highly disturbed forests between the first and the fourth TCW categories differed only by 2%. Therefore, NDVI could be more valuable than TCW in detecting hurricane disturbance to forests.

Site Conditions versus Disturbance Intensities

Effects of soils on disturbance magnitude depended largely on soil great groups. Forests growing on endoaquepts and sulfaquepts soils were found to be most susceptible to hurricane damage, with over 80% of the forests damaged (Table 10). In contrast, forests growing on glossaqualfs appeared to be most resistant to Katrina's winds, with less than half of the total

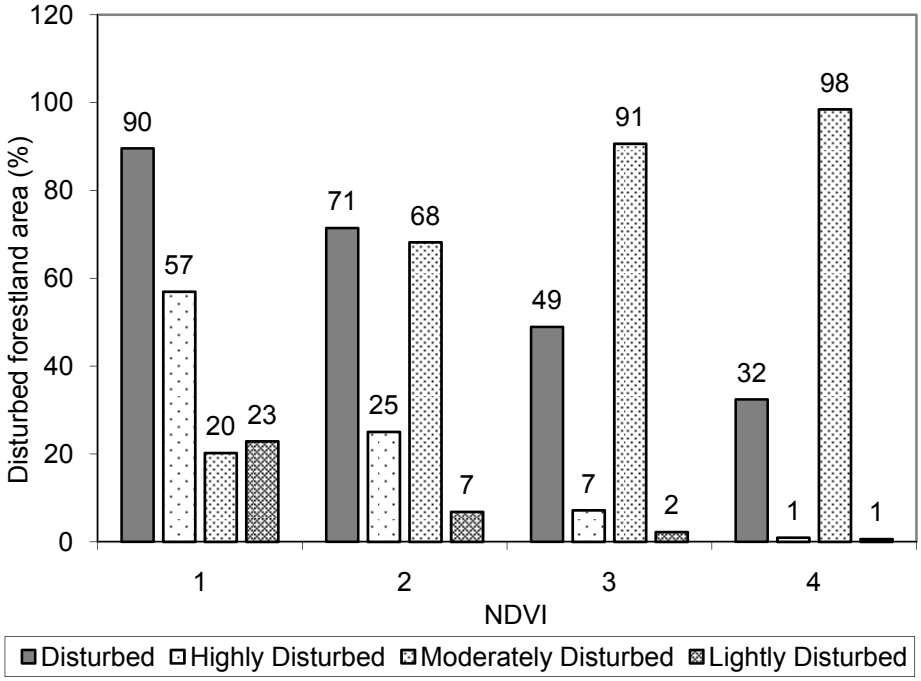

Fig. 40 Percentages of Katrina-induced forest disturbances by the four NDVI categories

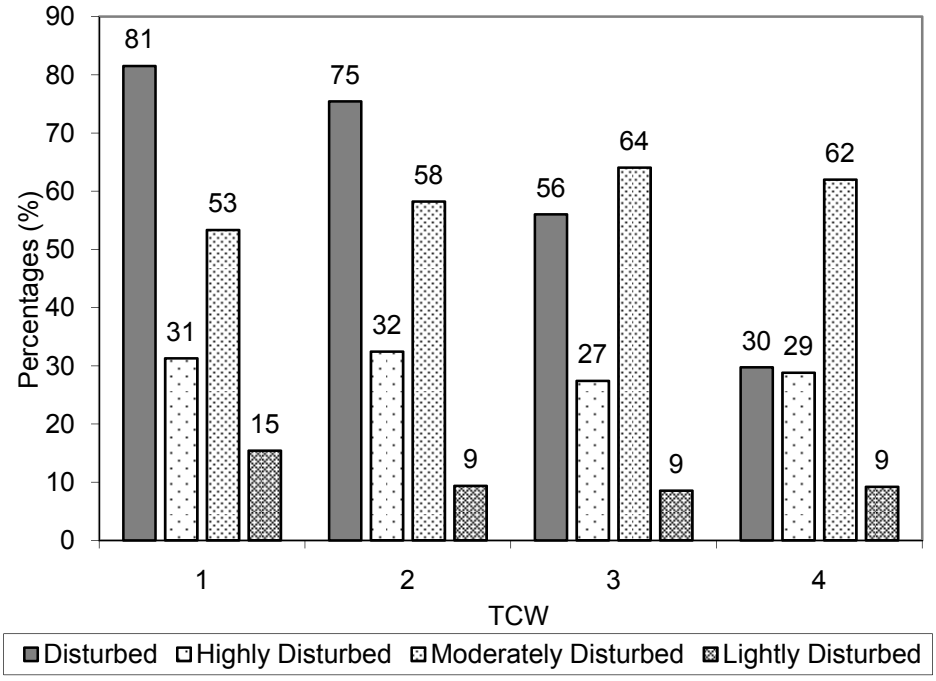

Fig. 41 Percentages of Katrina-induced forest disturbances by the four TCW categories

Table 10 Percentages of disturbed forestland areas by soil groups

Class	Undisturbed	Disturbed	Highly disturbed	Moderately disturbed	Lightly disturbed
Dystrudepts	31.53	68.47	24.28	64.54	11.18
Hapludults	47.89	52.11	4.16	78.48	17.37
Fluvaquents	39.26	60.74	19.62	72.57	7.81
Hydraquents	37.43	62.57	52.13	36.65	11.23
Paleudults	47.95	52.05	16.83	68.33	14.84
Fragiudults	32.99	67.01	23.24	63.33	13.43
Glossaqualfs	51.65	48.35	43.45	43.38	13.17
Haplosaprists	36.58	63.42	11.50	76.31	12.19
Endoaquepts	8.38	91.62	52.28	43.25	4.47
Sulfaquents	15.23	84.77	82.50	5.64	11.85
Paleaquults	34.62	65.38	52.79	38.67	8.54

forests disturbed. Forests on sulfaquents were susceptible to the hurricane winds, whereas forests on hapludults suffered only moderate and light disturbance.

Except for the coastal areas with elevation less than 24 m, percentage of disturbed forests declined gradually with increasing elevations (Fig. 42). The hurricane caused the highest percentage of disturbance at elevation 24 - 48 m, where areas of disturbed forests were twice of those of undisturbed forests. At elevation ranges 0 - 24 and 48 - 72 m, percentage of disturbed forests was about 20% higher than the undisturbed ones. At higher elevation (above 72 m), the percentage of disturbed forests was only about 5% higher than the undisturbed forests. Percentages of disturbed forests at three severity levels showed that percentage of the highly disturbed forests was higher at lower elevations while that of the moderately and lightly disturbed areas was higher at higher elevation (Fig. 42).

Percentage of the total disturbed areas gradually declined with rising aspects, except for at 0-45 and 315-360 degree (Fig. 43). The percentages at the three severity levels did not vary noticeably with aspects, except for 315-360 degree, where percentages of highly and moderately disturbed forests were much greater than those at the other aspect levels.

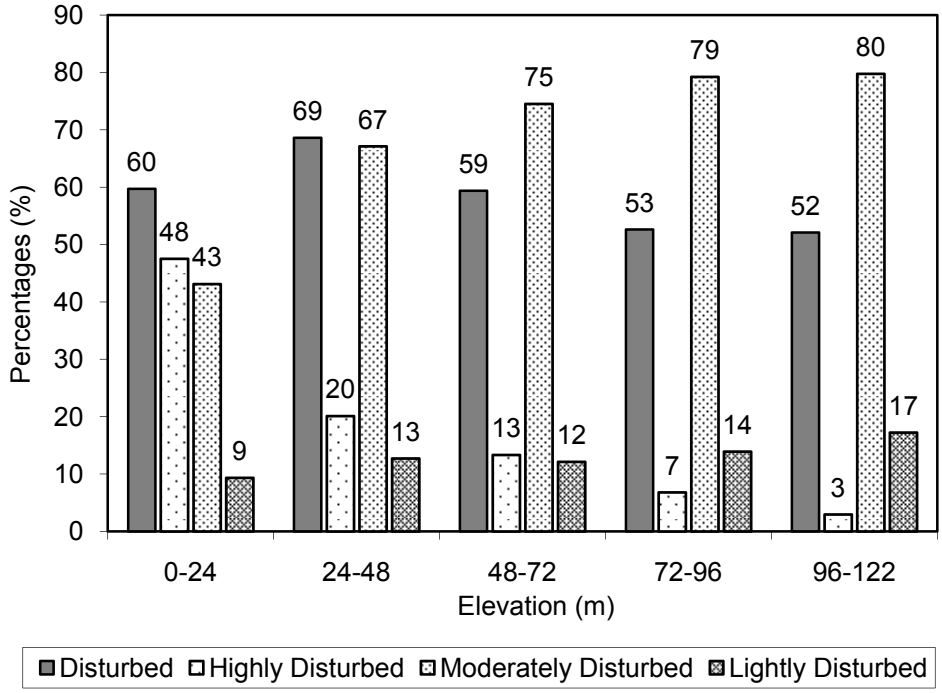

Fig. 42 Percentages of Katrina-induced forest disturbances by the elevation categories

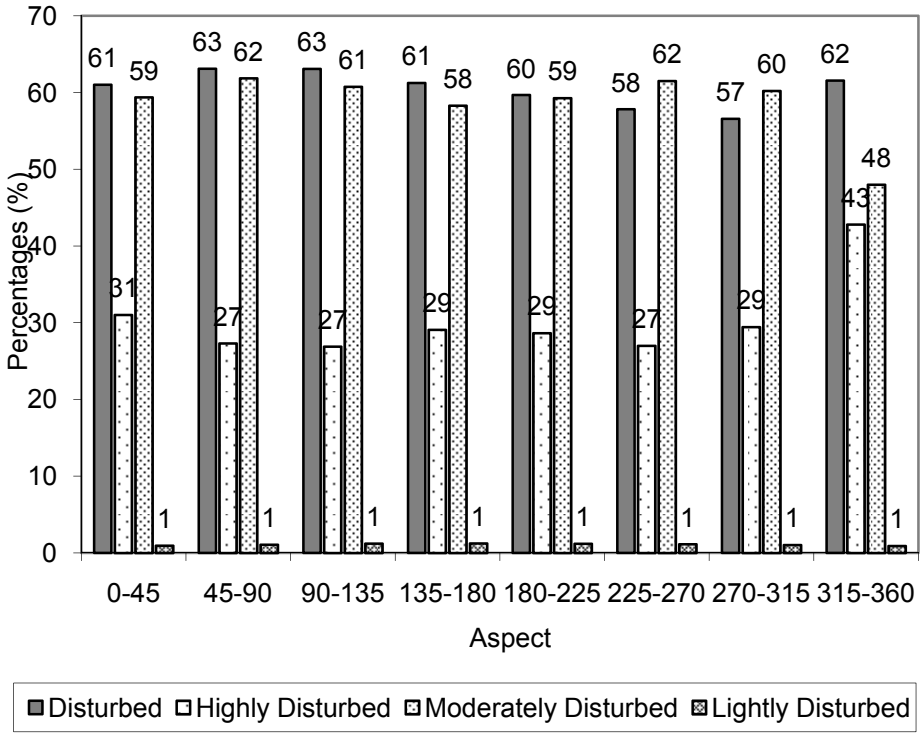

Fig. 43 Percentages of Katrina-induced forest disturbances by the aspect categories

Percentage of disturbed forests slightly increased when the slopes were greater than 2 degree (Fig. 44). Forests on 1-degree slope appeared to be most susceptible to the hurricane disturbance. Among the three levels of severity, percentage of the highly disturbed forests varied noticeably with 42% on flat land and 8.7% on 6-degree slope. Percentage of the moderately disturbed forests rose gradually from 48% on flat land to 80% on 6-degree slope. On the flat land, almost the same amount of forestland areas was highly and moderately disturbed. However, for slopes greater than 0 degree, percentage of the highly disturbed forests was considerably lower than that of the moderately disturbed ones.

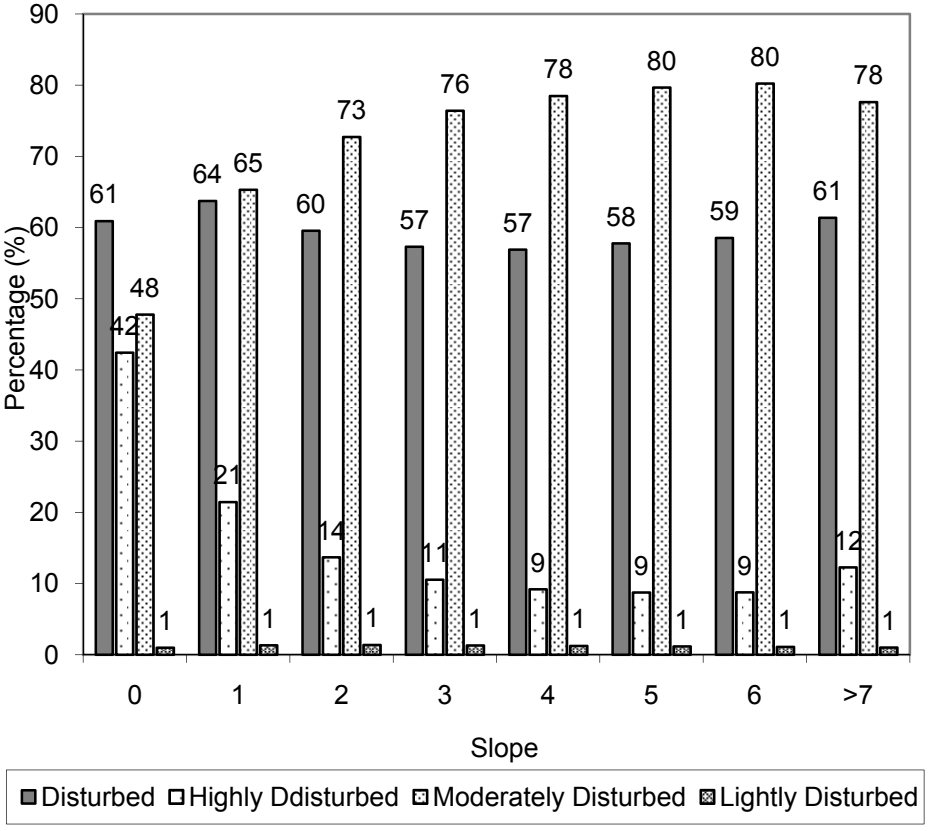

Fig. 44 Percentages of the disturbed forestland areas by the slope categories

Integrated Assessment

Results from a full logit regression model revealed that all factors were significant in explaining the variation in the probability of hurricane wind disturbance to forests in this region ($P<0.0001$, respectively). Odds ratio of the forest types with codes less than 6 to wetland forests coded as 6 were less than 1, indicating that woody wetlands had the highest probability to be disturbed by the hurricane, compared to the other four types (Table 11). The lowest odds ratio of evergreen forests and shrub/scrub to wetland forests suggested that the former two forest types were more resistant to the hurricane disturbance than the latter.

Odds ratio of both NDVI and TCW categories showed similar decreasing trends when the category codes of these two factors increased from 1 to 3 (Table 11), which implied that forests with higher values of NDVI and TCW were less likely to be disturbed.

Odds ratio among the 11 soil groups denoted that forests on endoaquepts were most likely to be disturbed by the hurricane, compared to forests on the other soil groups (Table 11). The odds of forests disturbed by the hurricane was 3.2 times higher on endoaquepts than on paleaquults. By contrast, glossaqualfs had the least effects on hurricane disturbance to forests.

The highest odds ratio among elevation pairs (Table 11) demonstrated that forests on elevation of 24-48 m were most susceptible to the hurricane damage than those in other elevation ranges. Forests in coastal area with the lowest elevation of 0-24 m had the lowest probability to be disturbed (the lowest odds ratio = 0.4).

Forests on lands with an aspect of 0-225 degree showed a higher probability to be disturbed by the hurricane (odds ratio > 1) than those in the areas with an aspect of 225-315 degree (odds ratio < 1) (Table 11), indicating greater exposure to the hurricane winds resulted in higher chances of forest damage.

Forests growing in areas with 0-, 2-, 3-, and 4-degree slopes had a lower disturbance

Table 11 Estimates of the odds ratios and the confidence limits

Pairs of the factors	Odds ratios	95% Wald Confidence Limits	
ftype 1 vs 6	0.642[a]	0.630	0.654
ftype 3 vs 6	0.340[a]	0.337	0.343
ftype 4 vs 6	0.870[a]	0.847	0.892
ftype 5 vs 6	0.387[a]	0.383	0.391
NDVI 1 vs 4	24.975[a]	24.666	25.287
NDVI 2 vs 4	6.028[a]	5.970	6.087
NDVI 3 vs 4	2.010[a]	1.992	2.028
TCW 1 vs 4	8.501[a]	8.408	8.596
TCW 2 vs 4	6.452[a]	6.386	6.518
TCW 3 vs 4	2.921[a]	2.894	2.948
soil 1 vs 11	0.779[a]	0.766	0.793
soil 2 vs 11	0.618[a]	0.604	0.632
soil 3 vs 11	1.039[a]	1.024	1.054
soil 4 vs 11	0.489[a]	0.481	0.496
soil 5 vs 11	0.641[a]	0.633	0.650
soil 6 vs 11	0.806	0.790	0.823
soil 7 vs 11	0.248[a]	0.242	0.254
soil 8 vs 11	0.741[a]	0.721	0.761
soil 9 vs 11	3.294[a]	3.212	3.378
soil 10 vs 11	1.219[a]	1.157	1.285
elevation 1 vs 5	0.411[a]	0.400	0.422
elevation 2 vs 5	1.146[a]	1.117	1.176
elevation 3 vs 5	0.987[a]	0.962	1.012
elevation 4 vs 5	0.856[a]	0.834	0.878
aspect 1 vs 8	1.052[a]	1.037	1.068
aspect 2 vs 8	1.193[a]	1.177	1.210
aspect 3 vs 8	1.232[a]	1.215	1.249
aspect 4 vs 8	1.161[a]	1.145	1.177
aspect 5 vs 8	1.089[a]	1.074	1.104
aspect 6 vs 8	0.991[a]	0.977	1.004
aspect 7 vs 8	0.890[a]	0.877	0.903
slope 1 vs 8	0.783[a]	0.760	0.807
slope 2 vs 8	1.010[a]	0.980	1.040
slope 3 vs 8	0.976[a]	0.947	1.006
slope 4 vs 8	0.959	0.929	0.989
slope 5 vs 8	0.970	0.939	1.001
slope 6 vs 8	1.005[a]	0.970	1.040
slope 7 vs 8	1.031[a]	0.991	1.073
buffer 1 vs 6	1.040[a]	1.027	1.054
buffer 2 vs 6	0.951[a]	0.938	0.964
buffer 3 vs 6	0.976[a]	0.962	0.990
buffer 4 vs 6	0.996	0.982	1.011
buffer 5 vs 6	0.999	0.984	1.014

[a] Odds ratio is significantly different from 1 (P.<0.05)

probability compared to those on slopes greater than 7 degrees (odds ratio < 1) (Table 11). Forests in areas with 1-, 5-, and 6-degree slopes showed a higher probability to be damaged by the hurricane than those on slopes greater than 7-degree (odds ratio >1). Forests on 1-degree slope appeared to be most susceptible to the hurricane disturbance (the greatest odds ratio).

Probabilities of the hurricane disturbance in stream buffer zones 1, 2 and 3 were significantly different from zone 6 (Table 11), whereas those in zones 4 and 5 were comparable to zone 6. This suggested that probabilities of the hurricane disturbance within 300 m of a river channel were significantly different from those at distances greater than 300 m. The highest odds ratio of buffer zone 1 versus zone 6 revealed that forests within 100 m of the river channel had a highest chance to be disturbed by the hurricane.

The reduced models showed that, when independent variables of buffer zone, aspect, slope and elevation were removed from the full model, the percentages of the correctly classified undisturbed and disturbed forests, the percentage of the concordance, and AIC value changed 0.27, 1.14, 1.1, and 3.2%, respectively. Then, when the soil variable was excluded along with buffer, aspect, slope and elevation, the percentages increased by 3.9, 0.23, 2.8, and 7.2%, respectively. Additionally, when forest type, NDVI and TCW variables were sequentially removed from the model, the percentage of the concordance decreased 6.4, 23.8 and 20.6%, and AIC value increased 11.9, 25.6, and 30.5%. Therefore, a model including only soil, forest types, TCW, and NDVI, which had only 3.2% increase of AIC value compared to the full model, was used to predict the probabilities of hurricane disturbance to the forests (Fig. 45). These four variables contributed to 85% concordance in prediction of the disturbance probabilities.

Discussion

Forest Characteristics and Stand Stability

Our study showed that wetland forests in this region were more susceptible to the hurricane

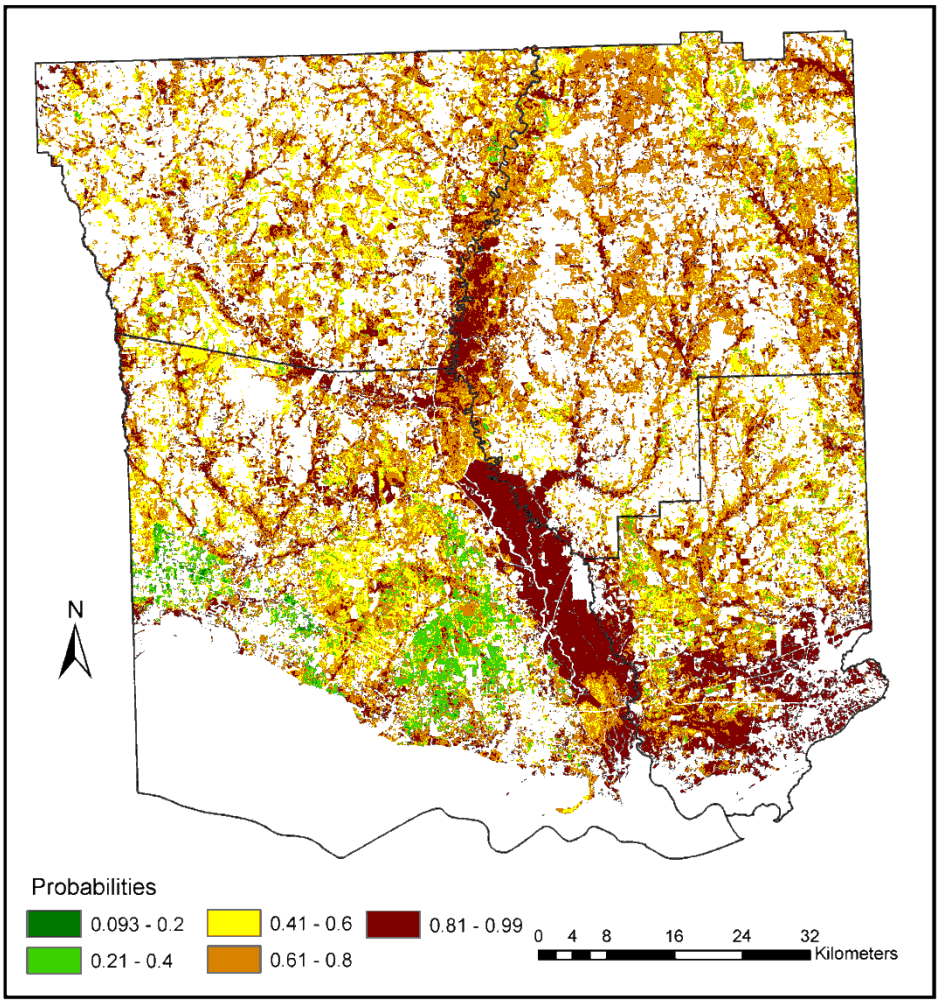

Fig. 45 Predicted probabilities of the forests disturbed by hurricanes

disturbance, followed by urban forests, mixed forests, evergreen forests, and shrub/scrub. In wetland forests, cypress (Putz and Sharitz 1991; Touliatos and Roth 1971) and tupelo (Gresham et al. 1991) were reported to be highly resistant to strong winds and their resistance may be related to presence of buttressed boles (Mattheck and Bethge 1990; Peterson 2000; Putz et al. 1983; Touliatos and Roth 1971) and deciduous habit of cypress, which greatly reduces the surface area exposed to high winds (Gresham et al. 1991). Southern red oak (*Q. falcate*), water oak (*Q. nigra*), and sweetgum were found to be more susceptible to strong tornado winds, compared to loblolly and longleaf pines (Glitzenstein and Harcombe 1988). This susceptibility

may be attributed to their shallow rooting (Chambers 2006). In addition, Hurricane Katrina pushed Gulf waters up towards inner Lower Pearl River Valley, causing extensive flooding and saltwater intrusion in the area for several weeks, which may affected the wetland forests too.

In upland forests, we found that evergreen pines were more resistant to wind damage than the other types of forests. Gresham et al. (1991) also reported that in upland, oaks were more heavily damaged than pines. The resistance of longleaf pine to wind damage may be related to the firm anchorage of its large taproot and widespread lateral root system (Gresham et al. 1991).

Urban forests in the region were identified as the second most susceptible forest type to the hurricane disturbance. Urbanization, and changed environments, site quality, and management practices may result in changes in structure and resistance of forests to hurricane winds. Johnson and Johnson (1999) reported that roots cut during construction, root development hindered by restricted spaces, degraded old tissues, and incorrect irrigation could leave trees unstable and more prone to windthrow.

Shorter and smaller diameter trees are usually less severely damaged than taller and larger diameter trees (Francis 2000; Lugo et al. 1983; Ostertag et al. 2005; Reilly et al. 2002). We achieved similar results that shrub/scrub appeared to be the most resistant cover type to hurricane disturbance. The shrub/scrub in the valley was in general less than 5 m tall and consisted of true shrubs, young trees in an early successional stage, or trees stunted from environmental conditions. The high resistance of shrub/scrub to Hurricane Katrina was apparently associated with its shorter height, smaller diameter, and smaller canopy.

This study demonstrated that NDVI and TCW values were closely related to percentage variations of the disturbed forests, and greatly contributed to the high accuracy in modeling probabilities of the hurricane disturbance to forests. NDVI is not an intrinsic physical measurement of vegetation characteristics, but is indeed correlated with certain vegetation

properties such as percent vegetation cover, leaf area index (LAI), annual productivity, and stand density. NDVI values had a positive linear relationship with vegetation coverage (correlation values > 0.89) (Ormsby et al. 1987b; Purevdorj et al. 1998). NDVI values less than 0.3 signify vegetation cover of 5% or less, whereas a value of 0.7 or higher represents coverage greater than 80% (Ormsby et al. 1987a). The relationship between NDVI and LAI is not linear across vegetation types. When LAI is greater than 5, NDVI tends to be asymptotic. In addition, in old conifer stands, NDVI values decline despite high LAIs (Turner et al. 1999). Forest growth is highly correlated to average NDVI values, with a correlation coefficient over 0.70 (Brown et al. 1989; Wang et al. 2004).

TCW is a linear combination of the Landsat TM six Bands (Crist and Cicone 1984). Cohen and Spies (1992) found that TCW was highly correlated to all 16 closed canopy forest stand structural attributes and appeared to respond to the degree of maturity in forest stands. Todd and Hoffer (1998) reported that TCW values increased as green vegetation cover increased for all soil backgrounds. Overall, these studies show that the TCW values are only positively correlated to the forest density and vegetation cover.

All of these previous studies on the relationships of attributes of forest structures and growths with values of NDVI and TCW indicate that NDVI or TCW values are correlated with numerous forest attributes, and percentage of coverage and stand density are the only ones that are positively correlated to both NDVI and TCW values. Therefore, we conclude that the relationships of NDVI/TCW values with the percentage and probability of hurricane disturbance to forests are negative. In other words, higher percentage of the forest cover and stand density are linked to lower forest susceptibilities to hurricane disturbance.

Soils and Stand Stability

Many studies have found a direct association between windthrow and tree rooting depth

(Coutts 1986; Mattheck and Bethge 1990; Nicoll and Ray 1996). Soil chemical, physical and hydraulic properties have profound impacts on tree root development (Coutts 1986; Nicoll et al. 2006; Xu et al. 1997). In general, soil properties that contribute to shallow root development, such as poor drainage and seasonal water logging (Mayer 1989; Ray and Nicoll 1998), can lead to lower stand stability against wind damage. Gardner et al. (1992) documented that the most severe damage occurred in mixed bottomland hardwood sites on poorly drained Rutledge soils.

In our study, forests on endoaquept and sulfaquent soil groups were most susceptible to hurricane damage, whereas those on glossaqualfs were most resistant (Table 11). However, drainage properties of these three soil groups were similar (Table 8). Furthermore, forests on sulfaquents, a very poorly drained soil, were most susceptible to high disturbance. In contrast, forests on hapludults, a well drained soil, typically exhibited moderate and light disturbances. Our study was conducted at a landscape level with many tree species and various drainage conditions. Some forests such as cypress grow on poorly drained soils but are resistant to hurricane disturbance because the species has developed a unique root system resistant to wind damage. Therefore, we concluded that the soil drainage property alone cannot explain the relationships between soil groups and hurricane disturbance over a large area, which was supported by Lindemann and Baker (2002) and Lin et al. (2004). The frequencies of trees that die of uprooting do not differ significantly among soil drainage classes (Lin et al. 2004), and soil permeability and water-holding capacity are not correlated significantly with the blowdown pattern (Lindemann and Baker 2002).

Topographic Features and Stand Stability

Topographic characteristics of forested land, such as aspect, slope, and elevation often help explain the spatial variations in wind damage and severity (Martin and Ogden 2006). Wind speeds usually peak above ridge crests and therefore the leeward side of hills experience

increased turbulence (Finnigan and Brunet 1995). Forests growing on windward slopes are more vulnerable to windthrow than those on leeward slopes (Bellingham 1991; Foster and Boose 1992; Lugo et al. 1983; Reilly 1991), and forests in lower elevation receive more damage than those in higher elevation (Reilly et al. 2002). Lugo et al. (1983) and Putz and Sharitz (1991) found that hurricane winds caused greater damage to forests in coastal flat lowland areas. However, those topographic characteristics may not be able to solely explain the intensities of hurricane disturbance. For instance, Bellingham (1991) reported that mortality and uprooting did not seem to conform to a pattern that could be linked to topography. Walker (1991) found that most forest damage by Hurricane Hugo occurred on north-facing sites in Puerto Rico, whereas the hurricane struck the island from the southeast. Brokaw and Grear (1991) observed that a cloud forest plot sustained equal damage on windward and leeward slopes. Our results of descriptive statistics and logit regression analysis confirmed the sheltering effects of landform characteristics on hurricane disturbance, particularly in terms of disturbance severities (Figs. 40-42, and Table 11). Windward slope (225-315 degree aspect) protected forests when Katrina made landfall in a south to north direction (Fig. 36). The hurricane tended to cause more severe damage (high disturbance) at lower slope and elevation areas (Figs. 41 and 42).

Disturbance versus Landscape Patterns

Spatial patterns of forested landscape disturbed by hurricanes are controlled by interactions of a series of biota and abiota factors, such as wind properties, topographic exposure, and differential stand susceptibility to strong hurricane wind (Foster et al. 1998). The patterns are highly variable at all scales with a patchy damage pattern characterized by a highly irregular border at a landscape scale (Foster and Boose 1992). Our study also showed Hurricane Katrina produced a heterogeneous disturbance pattern with the big patchy of damage within the study area as we hypothesized. The patchy damage pattern with more complex and irregular patch

shapes clustered in the Lower Pearl River Valley and the southern portion of Hancock County (Fig. 37). The spatial continuity of the forest types, such as bottomland forests in the Lower Pearl River Valley and the same soil groups covering a large area, and high density of streams may have contributed to the aggregated and clustered patterns of the disturbed forests in the valley. The clustered patches of highly disturbed forests in the Lower Pearl River Valley may also contribute to lower patch density (1.5) and lower edge density (14.6) of highly disturbed forests compared to the undisturbed forests and moderately disturbed forests.

Conclusions

This study provides comprehensive assessment of the forest damage caused by Hurricane Katrina in the Lower Pearl River Valley and surrounding areas, USA. The hurricane disturbed 60% of forested lands across the region. The disturbance resulted in a highly fragmented landscape, with a large portion of the disturbed forests clustered on the Pear River floodplain and the southern portion of Hancock County. The factors of forest type, soil great group, elevation, slope, aspect, buffer zone along the river channels, forest coverage, stand density had various effects on overall percentage of the disturbed forests and percentages of the disturbed forests at three severity levels. These factors collectively played important roles in vulnerability of the coastal forests in response to Hurricane Katrina. Forest types, forest coverage and stand density, and soils groups contributed to 85% of accuracy in modeling the probability of hurricane disturbance to forests in this region.

Integration of a series of biotic and abiotic factors with GIS, remote sensing, and statistics modeling techniques showed a great advantage in revealing relationships between hurricane disturbance and the factors at landscape scale. With this approach, disturbance patterns at various severity levels were mapped with high accuracy over a large area based on changes in spectral properties of the forests before and after the hurricane event. Interpreting configurations of the

disturbed landscape indicated how the hurricane disturbance spread across the wind swath and patterned the landscape. Without GIS algorithms and spatial data layers, effects of such factors as buffer zones along river channels could not be evaluated. Furthermore, forest attributes, including percentages of coverage and stand density, could not be derived for a large area if remotely sensed data are not available.

CHAPTER 7 SUMMARY AND CONCLUSIONS

This dissertation research quantified current forest biomass carbon stored in Louisiana forests at grid and watershed scales, predicted effects of future climate change on forest NPP, and assessed Hurricane Katrina damage to forests in the Lower Pearl River Valley. Occupying 5.2 million hectares land, forests in Louisiana stored 219.2 Tg of carbon, with an average density of 43.2 Mg/ha. Wetland and evergreen forests accounted for 89% of the forested land, and stored over 90% of the carbon. Spatial distribution of forest carbon density in Louisiana presented apparent variability at grid and watershed scales. Spatial distribution of forests is the main factor affecting spatial patterns and the quantity of standing biomass stock of carbon. No correlations were identified between the total carbon storage in the watersheds with average watershed slope (R^2=0.09) and drainage density (R^2=0.004).

Prediction of forest NPP with an ecosystem model, PnET-II, revealed that forest productivity may increase in future climate change scenarios A1B and A2, but would decline under scenario B1. The predicted average forest NPP under B1 scenario over the years from 2000 to 2050 was significantly different from those under A1B and A2 scenarios. Sensitivity analysis of the four forest parameters (a) foliar N concentration (FolNCon), (b) slope of the relationship between maximum net photosynthesis and foliar N concentration (AmaxB), (c) daily max net photosynthesis as fraction of early morning instantaneous rate (AmaxFrac), and (d) specific leaf weigh (SLWMax) showed that PnET-II was more sensitive to FolNCon and AmaxB than AmaxFrac and SLWMax, in terms of changes in standard deviations (*s*) of the predicted NPP of the parameters. Sensitivity analysis of four climate inputs of mean maximum and minimum temperature, precipitation, and radiation showed that the model was more sensitive to temperature than the other two inputs. Forest NPP appeared to be primarily a function of minimum temperature and precipitation rather than maximum temperature, indicating that future temperature change in later winter and fall could be especially critical because of its

determination of the length of a growing season. Uncertainties of the NPP prediction were noticeable, owing to spatial resolution of the climate variables.

The change detection techniques exerted apparent influence on detection results with an overall accuracy varying between 51% and 86% and a Kappa Statistics ranging from 0.02 to 0.72. Detected areas of disturbed forestlands in lower Pearl River Valley were noticeable in two groups: 180,832 - 264,617 ha and 85,861 - 124,205 ha. The landscape of disturbed forests also displayed two unique patterns, depending upon the area group. The PCC algorithm along with the composite image contributed the highest accuracy and lowest error (0.5%) in estimating areas of disturbed forestlands. Both UID and CVA performed similarly, but caution should be taken when using selective PCA in detecting hurricane disturbance to forests. Among the six indices, TCW outperformed the other indices owing to its maximum sensitivity to forest modification. Overall, the following three methods are recommended for assessment of wind-induced forest damage: (1) the PCC of composite imagery of band 4, 5 and 3, (2) the CVA of TCW and TCB, and (3) the UID of TCW.

The distribution and intensity of Katrina disturbance to forests in lower Pearl River Valley varied across the landscape, with the bottomland hardwood forests on river floodplains most severely affected. All these factors including forest type, forest coverage, stand density, soil great group, elevation, slope, aspect, and stream buffer zone had a variety of effects on the vulnerability of the forests to the hurricane disturbance and thereby spatial patterns of the disturbance. But soil groups and stand factors including forest types, forest coverage, and stand density were the most important, and contributed to 85% of accuracy in the modeling probability of Hurricane Katrian disturbance to forests in this region.

In conclusion, this research suggests that quantification of forest biomass carbon, using geo-referenced datasets and GIS techniques, provides a credible approach to increase accuracy and

constrain the uncertainty of large-scale carbon assessment. Particularly, the quantified biomass carbon storage on the watersheds in Louisiana could be applied in ecosystem models to investigate carbon cycles between terrestrial ecosystem and aquatic environments, as well as to manage natural resources at the watershed scale. A combination of ecosystem modeling and GIS techniques can usefully gain insights into future climate change effects on forest carbon change at the landscape scale. The NPP prediction with the climate data derived from the general circulation model outputs provides a more realistic prediction of NPP in response to climate change in early 20th century. Increase of the intensity of severe weather in the future would likely increase the turn-over rate of coastal forest carbon stock. On the bases of these findings, decision makers could make long-term plans to raise forest productivity, increases carbon stocks by afforestation and reforestation, reduce carbon loss from disturbances, and consequently utilize the forests as a carbon sink to mitigate carbon dioxide greenhouse effects. Application of remote sensing and GIS in the study reveals that remote sensing and GIS techniques are valuable tools in developing applicable approaches in natural resources monitoring and assessment.

For future research, integrating current carbon storage and predicted NPP from this research with potential carbon changes caused by other factors is needed to provide a comprehensive understanding of carbon cycle in Louisiana forest (even terrestrial) ecosystem. Factors that can be included in such a complex modeling system are, among others, forest management scenarios (e.g., timber harvest), land use change, and severe natural disturbance (wildfires, hurricane disturbance, forest insect and disease defoliation). Other factors that contribute to increase of carbon storage in forests, such CO_2, nitrogen and phosphorus fertilization, reforestation, and afforestation, should also be incorporated in modeling prediction. Furthermore, in order to address the spatial variations of all these factors and forest carbon cycle, the model parameters need to be parameterized at the gird level instead of utilizing a constant value. This step can be

especially useful in enhancing accuracy and constraining uncertainties of large-scale carbon assessment.

Given the importance of parameters in spatial forecasting with an ecosystem model, the uncertainty caused by model parameterization should be minimized through generating spatial layers of the parameters at finer spatial scales. In some cases, using hyperspectral remotely-sensed data to generate spatial parameter layers, such as foliar N concentration is possible. However, such an approach is impracticable because of limited availability of the hyperspectral data. Therefore, spatial layers of the parameters should be generated by incorporating multispectral remotely-sensed data, inventory data (e.g., forest inventory and analysis data, and SSURGO soil data), field investigations and long-term records with geospatial techniques, such as k-nearest neighbors, segmented regression, and geospatial statistics. The generated spatial data layers will represent variations of vegetation parameters at a local scale. Particularly, it would be a better choice for heterogeneous landscape that has various vegetation types. Through this approach, uncertainties caused by parameters, particularly those to which models are most sensitive, could be minimized. Consequently, model prediction could result in a more realistic pattern over space.

REFERENCES

Aber, J. D., & Federer, C. A. (1992). A generalized, lumped-parameter model of photosynthesis, evapotranspiration and net primary production in temperate and boreal forest ecosystems. *Oecologia,* 92**,** 463-474.

Aber, J. D., Neilson, R. P., McNulty, S., Lenihan, J. M., Bachelet, D., & Drapek, R. J. (2001). Forest processes and global environmental change: Predicting the effects of individual and multiple stressors. *Bioscience,* 51**,** 735-751.

Aber, J. D., Ollinger, S. V., Federer, C. A., Reich, P. B., Goulden, M. L., Kicklighter, D. W., Melillo, J. M., & Lathrop, R. G. (1995). Predicting the effects of climate change on water yield and forest production in the northeastern United States. *Climate Research,* 5**,** 207-222.

Aber, J. D., Reich, P. B., & Goulden, M. L. (1996). Extrapolating leaf CO2 exchange to the canopy: A generalized model of forest photosynthesis compared with measurements by eddy correlation. *Oecologia,* 106**,** 257-265.

Abrahams, A. D., & Ponczynski, J. J. (1984). Drainage Density in Relation to Precipitation Intensity in the USA. *Journal of Hydrology,* 75**,** 383-388.

Alerich, C. L., Klevgard, L., Liff, C., Knight, B., & Conkling, B. L., (2006). The forest inventory and analysis database: Database description and users guide, version 2.1. Forest Inventory and Analysis Program, U.S. Department of Agriculture, Forest Service.

Allen, T. R., & Kupfer, J. A. (2001). Spectral response and spatial pattern of Fraser fir mortality and regeneration, Great Smoky Mountains, USA. *Plant Ecology,* 156**,** 59-74.

Arrhenius, S. (1896). On the influence of carbonic acid in the air upon the temperature of the ground. *Philosophical magazine and Journal of Science,* 41**,** 237-276.

Asshoff, R., Zotz, G., & Korner, C. (2006). Growth and phenology of mature temperate forest trees in elevated CO2. *Global Change Biology,* 12**,** 848-861.

Ayala-Silva, T., & Twumasi, Y. A. (2004). Hurricane Georges and vegetation change in Puerto Rico using AVHRR satellite data. *International Journal of Remote Sensing,* 25**,** 1629-1640.

Bale, C. L., Williams, J. B., & Charley, J. L. (1998). The impact of aspect on forest structure and floristics in some Eastern Australian sites. *Forest Ecology and Management,* 110**,** 363-377.

Band, L. E., Patterson, P., Nemani, R., & Running, S. W. (1993). Forest Ecosystem Processes at the Watershed Scale - Incorporating Hillslope Hydrology. *Agricultural and Forest Meteorology,* 63**,** 93-126.

Bazzaz, F. A., Coleman, J. S., & Morse, S. R. (1990). Growth responses of seven major co-occurring tree species of the northeastern United States to elevated CO_2. *Canadian Journal of Forest Research* 20**,** 1479-1484.

Bellingham, P. J. (1991). Landforms influence patterns of hurricane damage - evidence from Jamaican montane forests. *Biotropica,* 23**,** 427-433.

Birdsey, R., Pregitzer, K., & Lucier, L. (2005). Forest carbon management in the United States: 1600-2100. *Third USDA Symposium on Greenhouse Gases & Carbon Sequestration in Agriculture and Forestry,* Baltimore, Maryland.

Birdsey, R. A., (1992). Carbon storage and accumulation in United States forest ecosystems. USDA Forest Service. Report number WO-59.

Birdsey, R. A., (1996). Carbon storage for major forest types and regions in the conterminous United States. In R. N. Sampson & D. Hair, (Ed.), Forest and global change, volume 2: Forest management opportunities for mitigating carbon emissions (pp. 1-25). Washington, DC: American Forests.

Birdsey, R. A., & Lewis, G. M., (2002). Carbon in United States forests and wood products, 1987-1997: State-by-state estimates. WWW document, http://www.fs.fed.us/ne/global/pubs/books/epa/index.html. Accessed August 2006.

Birdsey, R. A., Plantinga, A. J., & Heath, L. S. (1993). Past and prospective carbon storage in United-States forests. *Forest Ecology and Management,* 58**,** 33-40.

Boisvenue, C., & Running, S. W. (2006). Impacts of climate change on natural forest productivity - evidence since the middle of the 20th century. *Global Change Biology,* 12**,** 862-882.

Boose, E. R., Foster, D. R., & Fluet, M. (1994). Hurricane impacts to tropical and temperate forest landscapes. *Ecological Monographs,* 64**,** 369-400.

Bove, M. C., Zierden, D. F., & O'Brien, J. J. (1998). Are Gulf landfalling hurricanes getting stronger? *Bulletin of the American Meteorological Society,* 79**,** 1327-1328.

Brokaw, N. V. L., & Grear, J. S. (1991). Forest structure before and after Hurricane Hugo at 3 elevations in the Luquillo Mountains, Puerto-Rico. *Biotropica,* 23**,** 386-392.

Brown, S. (2002). Measuring carbon in forests: Current status and future challenges. *Environmental Pollution,* 116**,** 363-372.

Brown, S., Gillespie, A. J. R., & Lugo, A. E. (1989). Biomass estimation methods for tropical forests with applications to forest inventory data. *Forest Science,* 35**,** 881-902.

Brown, S. L., Schroeder, P., & Kern, J. S. (1999). Spatial distribution of biomass in forests of the eastern USA. *Forest Ecology and Management,* 123**,** 81-90.

Bruzzone, L., & Prieto, D. F. (2000). Automatic analysis of the difference image for unsupervised change detection. *IEEE Transactions on Geoscience and Remote Sensing,* 38**,** 1171-1182.

Campbell, J. L., Rustad, L. E., Boyer, E. W., Christopher, S. F., Driscoll, C. T., Fernandez, I. J., Groffman, P. M., Houle, D., Kiekbusch, J., Magill, A. H., Mitchell, M. J., & Ollinger, S. V. (2009). Consequences of climate change for biogeochemical cycling in forests of northeastern North America. *Canadian Journal of Forest Research-Revue Canadienne De Recherche Forestiere,* 39**,** 264-284.

Caspersen, J. P., Pacala, S. W., Jenkins, J. C., Hurtt, G. C., Moorcroft, P. R., & Birdsey, R. A. (2000). Contributions of land-use history to carbon accumulation in US forests. *Science,* 290**,** 1148-1151.

Chambers, J. L. (2006). Protecting coastal wetland forests: what can you do to help? *Louisiana Agriculture,* 49**,** 4-9.

Chavez, P. S. (1996). Image-based atmospheric corrections revisited and improved. *Photogrammetric Engineering and Remote Sensing,* 62**,** 1025-1036.

Chavez, P. S., & Kwarteng, A. Y. (1989). Extracting spectral contrast in Landsat Thematic Mapper image data using selective principal component analysis. *Photogrammetric Engineering and Remote Sensing,* 55**,** 339-348.

Chen, J., Gong, P., He, C. Y., Pu, R. L., & Shi, P. J. (2003). Land-use/land-cover change detection using improved change-vector analysis. *Photogrammetric Engineering and Remote Sensing,* 69**,** 369-379.

Ciais, P., Tans, P. P., Trolier, M., White, J. W. C., & Francey, R. J. (1995). A large northern-hemisphere terrestrial CO_2 sink indicated by the C-13/C-12 ratio of atmospheric CO_2. *Science,* 269**,** 1098-1102.

Clark, D. A., Brown, S., Kicklighter, D. W., Chambers, J. Q., Thomlinson, J. R., & Ni, J. (2001). Measuring net primary production in forests: Concepts and field methods. *Ecological Applications,* 11**,** 356-370.

Cohen, W. B., & Spies, T. A. (1992). Estimating structural attributes of douglas-fir Western Hemlock forest stands from Landsat and Spot imagery. *Remote Sensing of Environment,* 41**,** 1-17.

Collins, J. B., & Woodcock, C. E. (1996). An assessment of several linear change detection techniques for mapping forest mortality using multitemporal Landsat TM data. *Remote Sensing of Environment,* 56**,** 66-77.

Conner, W. H., Mixon, W. D., & Wood, G. W. (2005). Maritime forest habitat dynamics on Bulls Island, Cape Romain National Wildlife Refuge, SC, following Hurricane Hugo. *Forest Ecology and Management,* 212**,** 127-134.

Coppin, P., Jonckheere, I., Nackaerts, K., Muys, B., & Lambin, E. (2004). Digital change detection methods in ecosystem monitoring: A review. *International Journal of Remote Sensing,* 25**,** 1565-1596.

Coppin, P. R., & Bauer, M. E. (1994). Processing of multitemporal Landsat TM imagery to optimize extraction of forest cover change features. *IEEE Transactions on Geoscience and Remote Sensing,* 32**,** 918-927.

Coutts, M. P. (1986). Components of tree stability in Sitka spruce on peaty gley soil. *Forestry,* 59**,** 173-197.

Crist, E. P., & Cicone, R. C. (1984). A physically-based transformation of Thematic Mapper data - the TM Tasseled Cap. *IEEE Transactions on Geoscience and Remote Sensing,* 22**,** 256-263.

Crist, E. P., Laurin, R., & Cicone, R. C. (1986). Vegetation and soils information contained in transformed Thematic Mapper data. *Proceedings of International Geosciences and Remote Sensing Symposium (IGARSS)' 86 Symposium,* European Space Agency, Paris**,** 1465-70.

Cuffey, K. M., & Vimeux, F. (2001). Covariation of carbon dioxide and temperature from the Vostok ice core after deuterium-excess correction. *Nature,* 412**,** 523-527.

DeLucia, E. H., Hamilton, J. G., Naidu, S. L., Thomas, R. B., Andrews, J. A., Finzi, A., Lavine, M., Matamala, R., Mohan, J. E., Hendrey, G. R., & Schlesinger, W. H. (1999). Net primary production of a forest ecosystem with experimental CO2 enrichment. *Science,* 284**,** 1177-1179.

Dixon, R. K., Brown, S., Houghton, R. A., Solomon, A. M., Trexler, M. C., & Wisniewski, J. (1994). Carbon Pools and Flux of Global Forest Ecosystems. *Science,* 263**,** 185-190.

Drake, B. G., GonzalezMeler, M. A., & Long, S. P. (1997). More efficient plants: A consequence of rising atmospheric CO2? *Annual Review of Plant Physiology and Plant Molecular Biology,* 48**,** 609-639.

Ellsworth, D. S., & Reich, P. B. (1992). Leaf mass per area, nitrogen-content and photosynthetic carbon gain in acer-saccharum seedlings in contrasting forest light environments. *Functional Ecology,* 6**,** 423-435.

Emanuel, K. (2005). Increasing destructiveness of tropical cyclones over the past 30 years. *Nature,* 436**,** 686-688.

Everham, E. M., & Brokaw, N. V. L. (1996). Forest damage and recovery from catastrophic wind. *Botanical Review,* 62**,** 113-185.

Fan, S. M., Blaine, T. L., & Sarmiento, J. L. (1999). Terrestrial carbon sink in the Northern

Hemisphere estimated from the atmospheric CO_2 difference between Manna Loa and the South Pole since 1959. *Tellus Series B-Chemical and Physical Meteorology,* 51**,** 863-870.

FAO, (2006). Global forest resources assessment 2005 - progress towards sustainable forests management FAO, Viale delle Terme di Caracalla, 00100 Rome, Italy.

Field, C. B., & Fung, I. Y. (1999). Biogeochemical cycles - The not-so-big US carbon sink. *Science,* 285**,** 544-545.

Finnigan, J. J., & Brunet, Y., (1995). Turbulent airflow in forests on flat and hilly terrain. In M. P. Coutts & J. Grace, (Ed.), Wind and Trees (pp. 3-40). Cambridge, U. K. : Cambridge University Press.

Forster, P., Ramaswamy, V., Artaxo, P., Berntsen, T., Betts, R., Fahey, D. W., Haywood, J., Lean, J., Lowe, D. C., Myhre, G., Nganga, J., Prinn, R., Raga, G., Schulz, M., & Dorland, R. V., (2007). Changes in atmospheric constituents and in radiative forcing. In S. Solomon, D. Qin, M. Manning, Z. Chen, M. Marquis, K. B. Averyt, M. Tignor & H. L. Miller, (Ed.), Climate change 2007 - the physical science basis. contribution of working group I to the fourth assessment report of the Intergovernmental Panel on Climate Change (pp. 130-234). Cambridge, United Kingdom and New York, NY, USA: Cambridge University Press.

Foster, D. R., & Boose, E. R. (1992). Patterns of forest damage resulting from catastrophic wind in Central New-England, USA. *Journal of Ecology,* 80**,** 79-98.

Fournier, R. A., Luther, J. E., Guindon, L., Lambert, M. C., Piercey, D., Hall, R. J., & Wulder, M. A. (2003). Mapping aboveground tree biomass at the stand level from inventory information: Test cases in Newfoundland and Quebec. *Canadian Journal of Forest Research-Revue Canadienne De Recherche Forestiere,* 33**,** 1846-1863.

Francis, J. K. (2000). Comparison of hurricane damage to several species of urban trees in San Juan, Puerto Rico. *Journal of Arboriculture,* 26**,** 189-197.

Franklin, S. E., Moskal, L. M., Lavigne, M. B., & Pugh, K. (2000). Interpretation and classification of partially harvested forest stands in the Fundy model forest using multitemporal Landsat TM digital data. *Canadian Journal of Remote Sensing,* 26**,** 318-333.

Frey, P. D., (2005). 2005 Louisiana Forestry Facts. WWW document, http://www.ldaf.state.la.us/multimedia/forestry/publications/2005-Louisiana-Forestry-Facts.pdf. Accessed December 2005.

Fung, T. (1990). An assessment of TM imagery for land-cover change detection. *IEEE Transactions on Geoscience and Remote Sensing,* 28**,** 681-684.

Gardner, L. R., Michener, W. K., Williams, T. M., Blood, E. R., Kjerve, B., Smock, L. A., Lipscomb, D. J., & Gresham, C. (1992). Disturbance effects of hurricane hugo on a

pristine coastal landscape - North Inlet, South-Carolina, USA. *Netherlands Journal of Sea Research,* 30**,** 249-263.

Glitzenstein, J. S., & Harcombe, P. A. (1988). Effects of the December 1983 tornado on forest vegetation of the Big Thicket, Southeast Texas, USA. *Forest Ecology and Management,* 25**,** 269-290.

Goodale, C. L., Apps, M. J., Birdsey, R. A., Field, C. B., Heath, L. S., Houghton, R. A., Jenkins, J. C., Kohlmaier, G. H., Kurz, W., Liu, S. R., Nabuurs, G. J., Nilsson, S., & Shvidenko, A. Z. (2002). Forest carbon sinks in the Northern Hemisphere. *Ecological Applications,* 12**,** 891-899.

Gresham, C. A., Williams, T. M., & Lipscomb, D. J. (1991). Hurricane Hugo wind damage to southeastern United-States coastal forest tree species. *Biotropica,* 23**,** 420-426.

Guldin, R. W., & Kaiser, H. F., (2004). National report on sustainable forests - 2003. United States Deparment of Agriculture, Forest Service. Report number FS-766.

Hansen, M. J., Franklin, S. E., Woudsma, C., & Peterson, M. (2001). Forest structure classification in the North Columbia Mountains using the Landsat TM Tasseled Cap wetness component. *Canadian Journal of Remote Sensing,* 27**,** 20-32.

Harmon, M. E., Ferrell, W. K., & Franklin, J. F. (1990). Effects on carbon storage of conversion of old-growth forests to young forests. *Science,* 247**,** 699-702.

Hatfield, J. L., Kanemasu, E. T., Asrar, G., Jackson, R. D., Pinter, P. J., Reginato, R. J., & Idso, S. B. (1985). Leaf-area estimates from spectral measurements over various planting dates of wheat. *International Journal of Remote Sensing,* 6**,** 167-175.

Hegarat-Mascle, S. L., Seltz, R., Hubert-Moy, L., Corgne, S., & Stach, N. (2006). Performance of change detection using remotely sensed data and evidential fusion: comparison of three cases of application. *International Journal of Remote Sensing,* 27**,** 3515-3532.

Hendrey, G. R., Ellsworth, D. S., Lewin, K. F., & Nagy, J. (1999). A free-air enrichment system for exposing tall forest vegetation to elevated atmospheric CO2. *Global Change Biology,* 5**,** 293-309.

Holden, G. R., Nelson, M. D., & McRoberts, R. E. (2003). Accuracy assessment of FIA's nationwide biomass mapping products: Results from the north central FIA region. *Proceedings of the fifth annual forest inventory and analysis symposium,* New Orleans, LA**,** pp. 222.

Horler, D. N. H., & Ahern, F. J. (1986). Forestry information-content of Thematic Mapper data. *International Journal of Remote Sensing,* 7**,** 405-428.

Houghton, R. A., & Hackler, J. L. (2000). Changes in terrestrial carbon storage in the United States. 1: The roles of agriculture and forestry. *Global Ecology and Biogeography,* 9**,**

125-144.

Houghton, R. A., Hackler, J. L., & Lawrence, K. T. (1999). The US carbon budget: Contributions from land-use change. *Science,* 285**,** 574-578.

Howarth, P. J., & Wickware, G. M. (1981). Procedures for change detection using Landsat digital data. *International Journal of Remote Sensing,* 2**,** 277-291.

Huete, A., Justice, C., & Liu, H. (1994). Development of vegetation and soil indexes for MODIS-EOS. *Remote Sensing of Environment,* 49**,** 224-234.

Huete, A. R. (1988). A soil-adjusted vegetation index (SAVI). *Remote Sensing of Environment,* 25**,** 295-309.

Huete, A. R., Liu, H., & van Leeuwen, W. J. D. (1997a). The use of vegetation indices in forested regions: Issues of linearity and saturation. *Geoscience and Remote Sensing, 1997. IGARSS '97. 'Remote Sensing - A Scientific Vision for Sustainable Development'., 1997 IEEE International,* 1966-1968.

Huete, A. R., Liu, H. Q., Batchily, K., & vanLeeuwen, W. (1997b). A comparison of vegetation indices global set of TM images for EOS-MODIS. *Remote Sensing of Environment,* 59**,** 440-451.

Imbert, D., Labbe, P., & Rousteau, A. (1996). Hurricane damage and forest structure in Guadeloupe, French West Indies. *Journal of Tropical Ecology,* 12**,** 663-680.

IPCC, (2007a). Climate change 2007: impacts, adaptation and vulnerability. contribution of working group II to the fourth assessment report of the Intergovernmental Panel on Climate Change (M. Parry, O. Canziani, J. Palutikof, P. v. d. Linden & C. Hanson (Eds.)). Cambridge, UK: Cambridge University Press.

IPCC, (2007b). Climate change 2007: mitigation. contribution of working group III to the fourth assessment report of the Intergovernmental Panel on Climate Change (B. Metz, O. Davidson, P. Bosch, R. Dave & L. Meyer (Eds.)). Cambridge, United Kingdom and New York, NY, USA.: Cambridge University Press.

IPCC, (2007c). Climate change 2007: synthesis report. contribution of working group I, II and III to the fourth assessment report of the Intergovernmental Panel on Climate Change (Core Writing Team, R. K. Pachauri & A. Reisinger (Eds.)). Geneva, Switzerland: IPCC.

IPCC, (2007d). Climate change 2007: the physical science basis. working group I contribution to the fourth assessment report of the Intergovernmental Panel on Climate Change (S. Solomon, D. Qin, M. Manning, Z. Chen, M. Marquis, K. B. Averyt, M. Tignor & H. L. Miller (Eds.)). Cambridge, United Kingdom and New York, NY, USA: Cambridge University Press.

Jarrell, J. D., Mayfield, M., & Rappaport, E. N., (2001). The deadliest, costliest, and most intense

United States hurricanes from 1900 to 2000. Technical Memorandum NWS TPC-1.

Jenkins, J. C., Chojnacky, D. C., Heath, L. S., & Birdsey, R. A. (2003). National-scale biomass estimators for United States tree species. *Forest Science,* 49**,** 12-35.

Ji, L., & Peters, A. J. (2007). Performance evaluation of spectral vegetation indices using a statistical sensitivity function. *Remote Sensing of Environment,* 106**,** 59-65.

Johnson, G. R., & Johnson, B., (1999). Storm damage to landscape trees: Prediction, prevention, treatment. WWW document, http://www.extension.umn.edu/distribution/naturalresources/DD7415.html. Accessed Sept. 6, 2006.

Johnson, R. D., & Kasischke, E. S. (1998). Change vector analysis: A technique for the multispectral monitoring of land cover and condition. *International Journal of Remote Sensing,* 19**,** 411-426.

Johnston, M. H., Homann, P. S., Engstrom, J. K., & Grigal, D. F. (1996). Changes in ecosystem carbon storage over 40 years on an old-field forest landscape in east-central Minnesota. *Forest Ecology and Management,* 83**,** 17-26.

Jordan, C. F. (1969). Derivation of leaf area index from quality of light on the forest floor. *Ecology,* 50**,** 663-666.

Jozsa, L. A., & Powell, J. M. (1987). Some Climatic Aspects of Biomass Productivity of White Spruce Stem Wood. *Canadian Journal of Forest Research-Revue Canadienne De Recherche Forestiere,* 17**,** 1075-1079.

Kauppi, P. E., Mielikainen, K., & Kuusela, K. (1992). Biomass and Carbon Budget of European Forests, 1971 to 1990. *Science,* 256**,** 70-74.

Keeling, R. F., Piper, S. C., Bollenbacher, A. F., & Walker, J. S., (2009). Atmospheric carbon dioxide record from Mauna Loa. WWW document, http://cdiac.ornl.gov/trends/co2/sio-mlo.html. Accessed March, 2009.

Keim, B. D., Faiers, G. E., Muller, R. A., Grymes, J. M., & Rohli, R. V. (1995). Long-term trends of precipitation and runoff in Louisiana, USA. *International Journal of Climatology,* 15**,** 531-541.

Kienast, F., & Luxmoore, R. J. (1988). Tree-Ring Analysis and Conifer Growth-Responses to Increased Atmospheric Co2 Levels. *Oecologia,* 76**,** 487-495.

Kirschbaum, M. U. F. (2004). Direct and indirect climate change effects on photosynthesis and transpiration. *Plant Biology,* 6**,** 242-253.

Kittel, T. G. F., Rosenbloom, N. A., Painter, T. H., & Schimel, D. S. (1995). The VEMAP Integrated Database for Modelling United States Ecosystem/Vegetation Sensitivity to

Climate Change. *Journal of Biogeography,* 22**,** 857-862.

Knabb, R. D., Rhome, J. R., & Brown, D. P., (2006). Tropical cyclone report, Hurricane Katrina 23-30 August 2005. WWW document, http://www.nhc.noaa.gov/pdf/TCR-AL122005_Katrina.pdf. Accessed May 5, 2007.

Korner, C., Asshoff, R., Bignucolo, O., Hattenschwiler, S., Keel, S. G., Pelaez-Riedl, S., Pepin, S., Siegwolf, R. T. W., & Zotz, G. (2005). Carbon flux and growth in mature deciduous forest trees exposed to elevated CO2. *Science,* 309**,** 1360-1362.

Kwarteng, A. Y., & Chavez, P. S. (1998). Change detection study of Kuwait City and environs using multi-temporal Landsat Thematic Mapper data. *International Journal of Remote Sensing,* 19**,** 1651-1662.

Labrecque, S., Fournier, R. A., Luther, J. E., & Piercey, D. (2006). A comparison of four methods to map biomass from Landsat-TM and inventory data in western Newfoundland. *Forest Ecology and Management,* 226**,** 129-144.

Landsberg, J. J., & Waring, R. H. (1997). A generalised model of forest productivity using simplified concepts of radiation-use efficiency, carbon balance and partitioning. *Forest Ecology and Management,* 95**,** 209-228.

Law, B. E., Thornton, P. E., Irvine, J., Anthoni, P. M., & Van Tuyl, S. (2001). Carbon storage and fluxes in ponderosa pine forests at different developmental stages. *Global Change Biology,* 7**,** 755-777.

Leininger, T. D., Wilson, A. D., & Lester, D. G. (1997). Hurricane Andrew damage in relation to wood decay fungi and insects in bottomland hardwoods of the Atchafalaya Basin, Louisiana. *Journal of Coastal Research,* 13**,** 1290-1293.

Lin, Y., Hulting, M. L., & Augspurger, C. K. (2004). Causes of spatial patterns of dead trees in forest fragments in Illinois. *Plant Ecology,* 170**,** 15-27.

Lindemann, J. D., & Baker, W. L. (2002). Using GIS to analyse a severe forest blowdown in the Southern Rocky Mountains. *International Journal of Geographical Information Science,* 16**,** 377-399.

Louisiana Department of Agriculture & Forestry, Wildfire information. WWW document, http://www.ldaf.state.la.us/portal/Offices/Forestry/ForestProtection/tabid/135/Default.aspx. Accessed December 2005.

Louisiana Geographic Information Center, (2004). Basin Subsegments from LDEQ source data, Geographic NAD83, LOSCO (2004) [basin_subsegments_LDEQ_2004]. WWW document, http://lagic.lsu.edu/data/losco/basin_subsegments_ldeq_2004.html. Accessed December 2008.

Lu, D., Mausel, P., Brondizio, E., & Moran, E. (2004). Change detection techniques.

International Journal of Remote Sensing, 25**,** 2365-2407.

Lugo, A. E., Applefield, M., Pool, D. J., & Mcdonald, R. B. (1983). The impact of Hurricane David on the forests of Dominica. *Canadian Journal of Forest Research-Revue Canadienne De Recherche Forestiere,* 13**,** 201-211.

Lyon, J. G., Yuan, D., Lunetta, R. S., & Elvidge, C. D. (1998). A change detection experiment using vegetation indices. *Photogrammetric Engineering and Remote Sensing,* 64**,** 143-150.

Maier, C. A., Palmroth, S., & Ward, E. (2008). Short-term effects of fertilization on photosynthesis and leaf morphology of field-grown loblolly pine following long-term exposure to elevated CO2 concentration. *Tree Physiology,* 28**,** 597-606.

Martin, T. J., & Ogden, J. (2006). Wind damage and response in New Zealand forests: A review. *New Zealand Journal of Ecology,* 30**,** 295-310.

Maselli, F., & Chiesi, M. (2006). Evaluation of statistical methods to estimate forest volume in a Mediterranean region. *IEEE Transactions on Geoscience and Remote Sensing,* 44**,** 2239-2250.

Mattheck, C., & Bethge, K. (1990). Wind breakage of trees initiated by root delamination. *Trees-Structure and Function,* 4**,** 225-227.

Mayer, H. (1989). Windthrow. *Philosophical Transactions of the Royal Society of London Series B-Biological Sciences,* 324**,** 267-281.

Mcgarigal, K., & Marks, B. J., (1995). FRAGSTATS: Spatial pattern analysis program for quantifying landscape structure. General technical report PNW-GTR-351.

McMaster, K. J. (2005). Forest blowdown prediction: A correlation of remotely sensed contributing factors. *Northern Journal of Applied Forestry,* 22**,** 48-53.

McNulty, S. G., Iverson, L., Abt, R., Smith, B., Murray, B., Mickler, R. A., & Aber, J. D. (2000). Application of linked regional scale growth, biogeography, and economic models for southeastern United States pine forets. *World Resource Review,* 12**,** 298-320.

McNulty, S. G., Vose, J. M., & Swank, W. T. (1996a). Loblolly pine hydrology and productivity across the southern United States. *Forest Ecology and Management,* 86**,** 241-251.

McNulty, S. G., Vose, J. M., & Swank, W. T. (1996b). Potential climate change effects on loblolly pine forest productivity and drainage across the southern United States. *Ambio,* 25**,** 449-453.

McNulty, S. G., Vose, J. M., Swank, W. T., Aber, J. D., & Federer, C. A. (1994). Regional-scale forest ecosystem modeling: database development, model predictions and validation using a Geographic Information System. *Climate research,* 4**,** 223-231.

Meehl, G. A., Stocker, T. F., Collins, W. D., Friedlingstein, P., Gaye, A. T., Gregory, J. M., Kitoh, A., Knutti, R., Murphy, J. M., Noda, A., Raper, S. C. B., Watterson, I. G., Weaver, A. J., & Zhao, Z.-C., (2007). Global climate projections. In S. Solomon, D. Qin, M. Manning, Z. Chen, M. Marquis, K. B. Averyt, M. Tignor & H. L. Miller, (Ed.), Climate change 2007: the physical science basis: contribution of working group I to the fourth assessment report of the Intergovernmental Panel on Climate Change (pp. 748-845). Cambridge, United Kingdom and New York, NY, USA: Cambridge University Press.

Meynendonckx, J., Heuvelmans, G., Muys, B., & Feyen, J. (2006). Effects of watershed and riparian zone characteristics on nutrient concentrations in the River Scheldt Basin. *Hydrology and Earth System Sciences,* 10**,** 913-922.

Mickler, R. A., Earnhardt, T. S., & Moore, J. A. (2002a). Modeling and spatially distributing forest net primary production at the regional scale. *Journal of the Air & Waste Management Association,* 52**,** 407-415.

Mickler, R. A., Earnhardt, T. S., & Moore, J. A. (2002b). Regional estimation of current and future forest biomass. *Environmental Pollution,* 116**,** S7-S16.

Mickler, R. A., Smith, J. E., & Heath, L. S., (2004). Forest carbon trends in the southern United States. In H. M. Rauscher, (Ed.), Southern forest science: past, present, and future (pp. 383-393). Asheville, NC: Southern Research Station.

Multi-Resolution Land Characteristics Consortium, (1992). 1992 national land cover data (NLCD). WWW document, http://www.epa.gov/mrlc/nlcd.html. Accessed March 2008.

Multi-Resolution Land Characteristics Consortium, (2001). 2001 national land cover data (NLCD 2001). WWW document, http://www.epa.gov/mrlc/nlcd-2001.html. Accessed March 2008.

Nackaerts, K., Vaesen, K., Muys, B., & Coppin, P. (2005). Comparative performance of a modified change vector analysis in forest change detection. *International Journal of Remote Sensing,* 26**,** 839-852.

Nakicenovic, N., Alcamo, J., Davis, G., Vries, B. d., Fenhann, J., Gaffin, S., Gregory, K., Grübler, A., Jung, T. Y., Kram, T., Rovere, E. L. L., Michaelis, L., Mori, S., Morita, T., Pepper, W., Pitcher, H., Price, L., Riahi, K., Roehrl, A., Rogner, H., Sankovski, A., Schlesinger, M., Shukla, P., Smith, S., Swart, R., Rooijen, S. v., Victor, N., & Zhou, D., (2000). Special report on emissions scenarios: a special report of working group III of the Intergovernmental Panel on Climate Change (N. Nakicenovic & R. Swart (Eds.)). Cambridge, United Kingdom and New York, NY, USA: Cambridge University Press.

National Climatic Data Center, (2009). Climate of Louisiana. WWW document, http://cdo.ncdc.noaa.gov/climatenormals/clim60/states/Clim_LA_01.pdf. Accessed May 19, 2009.

Nicoll, B. C., Gardiner, B. A., Rayner, B., & Peace, A. J. (2006). Anchorage of coniferous trees in relation to species, soil type, and rooting depth. *Canadian Journal of Forest Research-Revue Canadienne De Recherche Forestiere,* 36**,** 1871-1883.

Nicoll, B. C., & Ray, D. (1996). Adaptive growth of tree root systems in response to wind action and site conditions. *Tree Physiology,* 16**,** 891-898.

Nilsson, L. O., & Wiklund, K. (1992). Influence of Nutrient and Water-Stress on Norway Spruce Production in South Sweden - the Role of Air-Pollutants. *Plant and Soil,* 147**,** 251-265.

Nishizono, T., Iehara, T., Kuboyama, H., & Fukuda, M. (2005). A forest biomass yield table based on an empirical model. *Journal of Forest Research,* 10**,** 211-220.

Norby, R. J., DeLucia, E. H., Gielen, B., Calfapietra, C., Giardina, C. P., King, J. S., Ledford, J., McCarthy, H. R., Moore, D. J. P., Ceulemans, R., De Angelis, P., Finzi, A. C., Karnosky, D. F., Kubiske, M. E., Lukac, M., Pregitzer, K. S., Scarascia-Mugnozza, G. E., Schlesinger, W. H., & Oren, R. (2005). Forest response to elevated CO2 is conserved across a broad range of productivity. *Proceedings of the National Academy of Sciences of the United States of America,* 102**,** 18052-18056.

Olivero, A. M., & Hix, D. M. (1998). Influence of aspect and stand age on ground flora of southeastern Ohio forest ecosystems. *Plant Ecology,* 139**,** 177-187.

Ollinger, S. V., Aber, J. D., & Federer, C. A. (1998). Estimating regional forest productivity and water yield using an ecosystem model linked to a GIS. *Landscape Ecology,* 13**,** 323-334.

Ollinger, S. V., & Smith, M. L. (2005). Net primary production and canopy nitrogen in a temperate forest landscape: An analysis using imaging spectroscopy, modeling and field data. *Ecosystems,* 8**,** 760-778.

Ormsby, J. P., Choudhury, B. J., & Owe, M. (1987a). Vegetation spatial variability and its effect on vegetation indices *International Journal of Remote Sensing,* 8**,** 1301-1306.

Ormsby, J. P., Choudhury, B. J., & Owe, M. (1987b). Vegetation spatial variability and its effect on vegetation indices. *International Journal of Remote Sensing,* 8**,** 1301-1306.

Ostertag, R., Silver, W. L., & Lugo, A. E. (2005). Factors affecting mortality and resistance to damage following hurricanes in a rehabilitated subtropical moist forest. *Biotropica,* 37**,** 16-24.

Peierls, B. L., Christian, R. R., & Paerl, H. W. (2003). Water quality and phytoplankton as indicators of hurricane impacts on a large estuarine ecosystem. *Estuaries,* 26**,** 1329-1343.

Peng, C. H., Liu, J. X., Dang, Q. L., Apps, M. J., & Jiang, H. (2002). TRIPLEX: A generic hybrid model for predicting forest growth and carbon and nitrogen dynamics. *Ecological Modelling,* 153**,** 109-130.

Peterson, A. G., Ball, J. T., Luo, Y. Q., Field, C. B., Reich, P. B., Curtis, P. S., Griffin, K. L., Gunderson, C. A., Norby, R. J., Tissue, D. T., Forstreuter, M., Rey, A., Vogel, C. S., & Participants, C. (1999). The photosynthesis leaf nitrogen relationship at ambient and elevated atmospheric carbon dioxide: a meta-analysis. *Global Change Biology,* 5**,** 331-346.

Peterson, C. J. (2000). Catastrophic wind damage to North American forests and the potential impact of climate change. *Science of the Total Environment,* 262**,** 287-311.

Petit, J. R., Jouzel, J., Raynaud, D., Barkov, N. I., Barnola, J. M., Basile, I., Bender, M., Chappellaz, J., Davis, M., Delaygue, G., Delmotte, M., Kotlyakov, V. M., Legrand, M., Lipenkov, V. Y., Lorius, C., Pepin, L., Ritz, C., Saltzman, E., & Stievenard, M. (1999). Climate and atmospheric history of the past 420,000 years from the Vostok ice core, Antarctica. *Nature,* 399**,** 429-436.

Piedallu, C., & Gegout, J. C. (2007). Multiscale computation of solar radiation for predictive vegetation modelling. *Annals of Forest Science,* 64**,** 899-909.

Prasad, V. K., Ortiz, A., Stinner, B., McCartney, D., Parker, J., Hudgins, D., Hoy, C., & Moore, R. (2005). Exploring the relationship between hydrologic parameters and nutrient loads using digital elevation model and GIS - A case study from Sugarcreek Headwaters, Ohio, USA. *Environmental Monitoring and Assessment,* 110**,** 141-169.

Purevdorj, T., Tateishi, R., Ishiyama, T., & Honda, Y. (1998). Relationships between percent vegetation cover and vegetation indices. *International Journal of Remote Sensing,* 19**,** 3519-3535.

Putz, F. E., Coley, P. D., Lu, K., Montalvo, A., & Aiello, A. (1983). Uprooting and snapping of trees - structural determinants and ecological consequences. *Canadian Journal of Forest Research-Revue Canadienne De Recherche Forestiere,* 13**,** 1011-1020.

Putz, F. E., & Sharitz, R. R. (1991). Hurricane damage to old-growth forest in Congaree Swamp National Monument, South-Carolina, USA. *Canadian Journal of Forest Research-Revue Canadienne De Recherche Forestiere,* 21**,** 1765-1770.

Ramsey, E. W., Chappell, D. K., & Baldwin, D. G. (1997). AVHRR imagery used to identify hurricane damage in a forested wetland of Louisiana. *Photogrammetric Engineering and Remote Sensing,* 63**,** 293-297.

Ramsey, E. W., Hodgson, M. E., Sapkota, S. K., & Nelson, G. A. (2001). Forest impact estimated with NOAA AVHRR and Landsat TM data related to an empirical hurricane wind-field distribution. *Remote Sensing of Environment,* 77**,** 279-292.

Ray, D., & Nicoll, B. C. (1998). The effect of soil water-table depth on root-plate development and stability of Sitka spruce. *Forestry,* 71**,** 169-182.

Reich, P. B., Kloeppel, B. D., Ellsworth, D. S., & Walters, M. B. (1995). Different

Photosynthesis-Nitrogen Relations in Deciduous Hardwood and Evergreen Coniferous Tree Species. *Oecologia,* 104**,** 24-30.

Reilly, A. E. (1991). The effects of Hurricane Hugo in 3 tropical forests in the United-States Virgin-Islands. *Biotropica,* 23**,** 414-419.

Reilly, J., Mayer, M., & Harnisch, J. (2002). The Kyoto Protocol and non-CO2 greenhouse gases and carbon sinks. *Environmental Modeling & Assessment,* 7**,** 217-229.

Ridd, M. K., & Liu, J. J. (1998). A comparison of four algorithms for change detection in an urban environment. *Remote Sensing of Environment,* 63**,** 95-100.

Rodrigueziturbe, I., & Escobar, L. A. (1982). The Dependence of Drainage Density on Climate and Geomorphology. *Hydrological Sciences Journal-Journal Des Sciences Hydrologiques,* 27**,** 129-137.

Rosson Jr., J. F., (1995). Forest resources of Louisiana, 1991. United States Department of Agriculture, Forest Service, Southern Forest Experiment Station. Resource Bulletin SO-1 92.

Rouse, J. W., Hass, R. H., Schell, J. A., & Deering, D. W. (1973). Monitoring vegetation systems in the Great Plains with ERTS. *Proceedings of the Third ERTS Symposium,* NASA, Washington, DC**,** 309-317.

Running, S. W., & Coughlan, J. C. (1988). A meneral-model of forest ecosystem processes for regional applications .1. Hdrologic balance, canopy gas-exchange and primary production processes. *Ecological Modelling,* 42**,** 125-154.

Running, S. W., & Gower, S. T. (1991). Forest-BGC, a general-model of forest ecosystem processes for regional applications .2. Dynamic carbon allocation and nitrogen budgets. *Tree Physiology,* 9**,** 147-160.

Saxe, H., Cannell, M. G. R., Johnsen, B., Ryan, M. G., & Vourlitis, G. (2001). Tree and forest functioning in response to global warming. *New Phytologist,* 149**,** 369-399.

Saxe, H., Ellsworth, D. S., & Heath, J. (1998). Tree and forest functioning in an enriched CO2 atmosphere. *New Phytologist,* 139**,** 395-436.

Schimel, D. S., Emanuel, W., Rizzo, B., Smith, T., Woodward, F. I., Fisher, H., Kittel, T. G. F., McKeown, R., Painter, T., Rosenbloom, N., Ojima, D. S., Parton, W. J., Kicklighter, D. W., McGuire, A. D., Melillo, J. M., Pan, Y., Haxeltine, A., Prentice, C., Sitch, S., Hibbard, K., Nemani, R., Pierce, L., Running, S., Borchers, J., Chaney, J., Neilson, R., & Braswell, B. H. (1997). Continental scale variability in ecosystem processes: Models, data, and the role of disturbance. *Ecological Monographs,* 67**,** 251-271.

Schimel, D. S., House, J. I., Hibbard, K. A., Bousquet, P., Ciais, P., Peylin, P., Braswell, B. H., Apps, M. J., Baker, D., Bondeau, A., Canadell, J., Churkina, G., Cramer, W., Denning, A.

S., Field, C. B., Friedlingstein, P., Goodale, C., Heimann, M., Houghton, R. A., Melillo, J. M., Moore, B., Murdiyarso, D., Noble, I., Pacala, S. W., Prentice, I. C., Raupach, M. R., Rayner, P. J., Scholes, R. J., Steffen, W. L., & Wirth, C. (2001). Recent patterns and mechanisms of carbon exchange by terrestrial ecosystems. *Nature,* 414**,** 169-172.

Schroeder, P., Brown, S., Mo, J. M., Birdsey, R., & Cieszewski, C. (1997). Biomass estimation for temperate broadleaf forests of the United States using inventory data. *Forest Science,* 42**,** 424-434.

Simard, Y., Legendre, P., Lavoie, G., & Marcotte, D. (1992). Mapping, Estimating Biomass, and Optimizing Sampling Programs for Spatially Autocorrelated Data - Case-Study of the Northern Shrimp (Pandalus-Borealis). *Canadian Journal of Fisheries and Aquatic Sciences,* 49**,** 32-45.

Smith, J. E., & Heath, L. S. (2001). Identifying influences on model uncertainty: An application using a forest carbon budget model. *Environmental Management,* 27**,** 253-267.

Smith, J. E., & Heath, L. S., (2002). A model of forest floor carbon mass for united states forest types. USDA Forest Service, Northeastern Research Station.

Smith, J. E., & Heath, L. S. (2004). Carbon stocks and projections on public forestlands in the United States, 1952-2040. *Environmental Management,* 33**,** 433-442.

Smith, J. E., Heath, L. S., & Jenkins, J. C., (2003). Forest volume-to-biomass models and estimates of mass for live and standing dead trees of U.S. Forests. USDA Forest Service, Northeastern Research Station.

Soil Survey Staff, (2004). Soil Survey Geographic (SSURGO) Database. United States Department of Agriculture, Natural Resources Conservation Service. .

Song, C., Woodcock, C. E., Seto, K. C., Lenney, M. P., & Macomber, S. A. (2001). Classification and change detection using Landsat TM data: When and how to correct atmospheric effects? *Remote Sensing of Environment,* 75**,** 230-244.

Song, C. H., & Woodcock, C. E. (2003). A regional forest ecosystem carbon budget model: Impacts of forest age structure and landuse history. *Ecological Modelling,* 164**,** 33-47.

Sonzogni, W. C. (1980). Pollution from Land Runoff. *Environmental Science & Technology,* 14**,** 148-153.

Springer, C. J., DeLucia, E. H., & Thomas, R. B. (2005). Relationships between net photosynthesis and foliar nitrogen concentrations in a loblolly pine forest ecosystem grown in elevated atmospheric carbon dioxide. *Tree Physiology,* 25**,** 385-394.

Stone, G. W., Grymes, J. M., Dingler, J. R., & Pepper, D. A. (1997). Overview and significance of hurricanes on the Louisiana coast, USA. *Journal of Coastal Research,* 13**,** 656-669.

Talling, P. J., & Sowter, M. J. (1999). Drainage density on progressively tilted surfaces with different gradients, Wheeler Ridge, California. *Earth Surface Processes and Landforms,* 24**,** 809-824.

Tang, Z. M., Sayer, M. A., Chambers, J. L., & Barnett, J. P. (2004). Interactive effects of fertilization and throughfall exclusion on the physiological responses and whole-tree carbon uptake of mature loblolly pine. *Canadian Journal of Botany-Revue Canadienne De Botanique,* 82**,** 850-861.

Tissue, D. T., Thomas, R. B., & Strain, B. R. (1993). Long-Term Effects of Elevated Co2 and Nutrients on Photosynthesis and Rubisco in Loblolly-Pine Seedlings. *Plant Cell and Environment,* 16**,** 859-865.

Tissue, D. T., Thomas, R. B., & Strain, B. R. (1996). Growth and photosynthesis of loblolly pine (Pinus taeda) after exposure to elevated CO2 for 19 months in the field. *Tree Physiology,* 16**,** 49-59.

Tissue, D. T., Thomas, R. B., & Strain, B. R. (1997). Atmospheric CO2 enrichment increases growth and photosynthesis of Pinus taeda: a 4 year experiment in the field. *Plant Cell and Environment,* 20**,** 1123-1134.

Todd, S. W., & Hoffer, R. M. (1998). Responses of spectral indices to variations in vegetation cover and soil background. *Photogrammetric Engineering and Remote Sensing,* 64**,** 915-921.

Touliatos, P., & Roth, E. (1971). Hurricanes and Trees: Ten Lessons from Camille. *Journal of Forestry,* 69**,** 285-289.

Turner, D. P., Cohen, W. B., Kennedy, R. E., Fassnacht, K. S., & Briggs, J. M. (1999). Relationships between leaf area index and Landsat TM spectral vegetation indices across three temperate zone sites. *Remote Sensing of Environment,* 70**,** 52-68.

Turner, D. P., Koerper, G. J., Harmon, M. E., & Lee, J. J. (1995a). A carbon budget for forests of the conterminous United-States. *Ecological Applications,* 5**,** 421-436.

Turner, D. P., Koerper, G. J., Harmon, M. E., & Lee, J. J. (1995b). Carbon sequestration by forests of the United-States - current status and projections to the year 2040. *Tellus Series B-Chemical and Physical Meteorology,* 47**,** 232-239.

Ucuncuoglu, E., Arli, O., & Eronat, A. H. (2006). Evaluating the impact of coastal land uses on water-clarity conditions from Landsat TM/ETM+ imagery: Candarli Bay, Aegean Sea. *International Journal of Remote Sensing,* 27**,** 3627-3643.

USDA Forest Service, (2007). The forest inventory and analysis database: Database description and users guide version 2.1. U.S. Department of Agriculture, Forest Service, National Forest Inventory and Analysis Program.

USGS, (2002). Environmental atlas of the Lake Pontchartrain basin. WWW document, http://pubs.usgs.gov/of/2002/of02-206/env-overview/water-quality.html. Accessed 6 September 2006.

Van Bloem, S. J., Murphy, P. G., Lugo, A. E., Ostertag, R., Costa, M. R., Bernard, I. R., Colon, S. M., & Mora, M. C. (2005). The influence of hurricane winds on Caribbean dry forest structure and nutrient pools. *Biotropica,* 37**,** 571-583.

Van Tuyl, S., Law, B. E., Turner, D. P., & Gitelman, A. I. (2005). Variability in net primary production and carbon storage in biomass across Oregon forests - an assessment integrating data from forest inventories, intensive sites, and remote sensing. *Forest Ecology and Management,* 209**,** 273-291.

Vandermeer, J., & Granzow De La Cerda, I. (2004). Height dynamics of the thinning canopy of a tropical rain forest: 14 years of succession in a post-hurricane forest in Nicaragua. *Forest Ecology and Management,* 199**,** 125-135.

Varotsos, C., Assimakopoulos, M. N., & Efstathiou, M. (2007). Technical Note: Long-term memory effect in the atmospheric CO2 concentration at Mauna Loa. *Atmospheric Chemistry and Physics,* 7**,** 629-634.

Vivin, P., Gross, P., Aussenac, G., & Guehl, J. M. (1995). Whole-Plant Co2 Exchange, Carbon Partitioning and Growth in Quercus-Robur Seedlings Exposed to Elevated Co2. *Plant Physiology and Biochemistry,* 33**,** 201-211.

Walker, L. R. (1991). Tree damage and recovery from Hurricane Hugo in Luquillo Experimental Forest, Puerto-Rico. *Biotropica,* 23**,** 379-385.

Wang, F., & Xu, Y. J. (2007). Comparison of remote sensing change detection techniques for assessing hurricane damage to forests. *Environmental Monitoring and Assessment,* doi: 10.1007/s10661-009-0798-8.

Wang, F., & Xu, Y. J. (2008). Hurricane Katrina-induced forest damage in relation to ecological factors at landscape scale. *Environmental Monitoring and Assessment,* doi: 10.1007/s10661-008-0500-6.

Wang, H., & Hall, C. A. S. (2004). Modeling the effects of Hurricane Hugo on spatial and temporal variation in primary productivity and soil carbon and nitrogen in the Luquillo Experimental Forest, Puerto Rico. *Plant and Soil,* 263**,** 69-84.

Wang, J., Rich, P. M., Price, K. P., & Kettle, W. D. (2004). Relations between NDVI and tree productivity in the central Great Plains. *International Journal of Remote Sensing,* 25**,** 3127-3138.

Wear, D. N., & Greis, J. G., (2002). Southern forest resource assessment - summary report. United States Department Agriculture, Forest Service, Southern Research Station. General technical report SRS-54.

Webster, P. J., Holland, G. J., Curry, J. A., & Chang, H. R. (2005). Changes in tropical cyclone number, duration, and intensity in a warming environment. *Science,* 309**,** 1844-1846.

Winnett, S. M. (1998). Potential effects of climate change on US forests: A review. *Climate Research,* 11**,** 39-49.

Winter, K., Garcia, M., Gottsberger, R., & Popp, M. (2001). Marked growth response of communities of two tropical tree species to elevated CO2 when soil nutrient limitation is removed. *Flora,* 196**,** 47-58.

Wolff, E. W. (2005). Understanding the past - climate history from Antarctica. *Antarctic Science,* 17**,** 487-495.

Xu, Y. J., Rohrig, E., & Folster, H. (1997). Reaction of root systems of grand fir (Abies grandis Lindl) and Norway spruce (Picea abies Karst) to seasonal waterlogging. *Forest Ecology and Management,* 93**,** 9-19.

Xu, Y. J., & Wang, F. (2006). The role of Louisiana's forest ecosystems in carbon sequestration. *Louisiana Agriculture,* 49**,** 22-23.

Zheng, D. L., Heath, L. S., & Ducey, M. J. (2007). Forest biomass estimated from MODIS and FIA data in the Lake States: MN, WI and MI, USA. *Forestry,* 80**,** 265-278.

Zushi, K. (2006). Spatial distribution of soil carbon and nitrogen storage and forest productivity in a watershed planted to Japanese cedar (Cryptomeria japonica D. Don). *Journal of Forest Research,* 11**,** 351-358.

APPENDIX: PERMISSION

SPRINGER LICENSE
TERMS AND CONDITIONS

Jun 03, 2009

This is a License Agreement between Fugui Wang ("You") and Springer ("Springer") provided by Copyright Clearance Center ("CCC"). The license consists of your order details, the terms and conditions provided by Springer, and the payment terms and conditions.

All payments must be made in full to CCC. For payment instructions, please see information listed at the bottom of this form.

License Number	2201480199384
License date	Jun 03, 2009
Licensed content publisher	Springer
Licensed content publication	Environmental Monitoring and Assessment
Licensed content title	Comparison of remote sensing change detection techniques for assessing hurricane damage to forests
Licensed content author	Fugui Wang
Licensed content date	Feb 25, 2009
Type of Use	Thesis/Dissertation
Portion	Full text
Number of copies	1
Author of this Springer article	Yes and you are the sole author of the new work
Order reference number	
Title of your thesis / dissertation	SPATIAL-TEMPORAL RESPONSES OF LOUISIANA FORESTS TO CLIMATE CHANGE AND HURRICANE DISTURBANCE
Estimated size(pages)	170
Total	0.00 USD
Terms and Conditions	

Introduction
The publisher for this copyrighted material is Springer Science + Business Media. By clicking "accept" in connection with completing this licensing transaction, you agree that the following terms and conditions apply to this transaction (along with the Billing and Payment terms and conditions established by Copyright Clearance Center, Inc. ("CCC"), at the time that you opened your Rightslink account and that are available at any time at http://myaccount.copyright.com).

Limited License
With reference to your request to reprint in your thesis material on which Springer Science and Business Media control the copyright, permission is granted, free of charge, for the use indicated in your enquiry. Licenses are for one-time use only with

a maximum distribution equal to the number that you identified in the licensing process.

This License includes use in an electronic form, provided it is password protected or on the university's intranet, destined to microfilming by UMI and University repository. For any other electronic use, please contact Springer at (permissions.dordrecht@springer.com or permissions.heidelberg@springer.com)

The material can only be used for the purpose of defending your thesis, and with a maximum of 100 extra copies in paper.

Although Springer holds copyright to the material and is entitled to negotiate on rights, this license is only valid, provided permission is also obtained from the (co) author (address is given with the article/chapter) and provided it concerns original material which does not carry references to other sources (if material in question appears with credit to another source, authorization from that source is required as well). Permission free of charge on this occasion does not prejudice any rights we might have to charge for reproduction of our copyrighted material in the future.

Altering/Modifying Material: Not Permitted
However figures and illustrations may be altered minimally to serve your work. Any other abbreviations, additions, deletions and/or any other alterations shall be made only with prior written authorization of the author(s) and/or Springer Science + Business Media. (Please contact Springer at permissions.dordrecht@springer.com or permissions.heidelberg@springer.com)

Reservation of Rights
Springer Science + Business Media reserves all rights not specifically granted in the combination of (i) the license details provided by you and accepted in the course of this licensing transaction, (ii) these terms and conditions and (iii) CCC's Billing and Payment terms and conditions.

Copyright Notice:
Please include the following copyright citation referencing the publication in which the material was originally published. Where wording is within brackets, please include verbatim.
"With kind permission from Springer Science+Business Media: <book/journal title, chapter/article title, volume, year of publication, page, name(s) of author(s), figure number(s), and any original (first) copyright notice displayed with material>."

Warranties: Springer Science + Business Media makes no representations or warranties with respect to the licensed material.

Indemnity
You hereby indemnify and agree to hold harmless Springer Science + Business Media and CCC, and their respective officers, directors, employees and agents, from and against any and all claims arising out of your use of the licensed material other than as specifically authorized pursuant to this license.

SPRINGER LICENSE
TERMS AND CONDITIONS

Jun 03, 2009

This is a License Agreement between Fugui Wang ("You") and Springer ("Springer") provided by Copyright Clearance Center ("CCC"). The license consists of your order details, the terms and conditions provided by Springer, and the payment terms and conditions.

All payments must be made in full to CCC. For payment instructions, please see information listed at the bottom of this form.

License Number	2201480473195
License date	Jun 03, 2009
Licensed content publisher	Springer
Licensed content publication	Environmental Monitoring and Assessment
Licensed content title	Hurricane Katrina-induced forest damage in relation to ecological factors at landscape scale
Licensed content author	Fugui Wang
Licensed content date	Aug 20, 2008
Type of Use	Thesis/Dissertation
Portion	Full text
Number of copies	1
Author of this Springer article	Yes and you are the sole author of the new work
Order reference number	
Title of your thesis / dissertation	SPATIAL-TEMPORAL RESPONSES OF LOUISIANA FORESTS TO CLIMATE CHANGE AND HURRICANE DISTURBANCE
Estimated size(pages)	170
Total	0.00 USD
Terms and Conditions	

Introduction
The publisher for this copyrighted material is Springer Science + Business Media. By clicking "accept" in connection with completing this licensing transaction, you agree that the following terms and conditions apply to this transaction (along with the Billing and Payment terms and conditions established by Copyright Clearance Center, Inc. ("CCC"), at the time that you opened your Rightslink account and that are available at any time at http://myaccount.copyright.com).

Limited License
With reference to your request to reprint in your thesis material on which Springer Science and Business Media control the copyright, permission is granted, free of charge, for the use indicated in your enquiry. Licenses are for one-time use only with

VITA

Fugui Wang was born in Ganxu Province, China. He received a Bachelor of Science degree from Northwest A&F University in Yangling, Shaanxi Province in 1992, and a Master of Science degree in 1995 with a major in forest resource protection. During that time period, his studies and research focused mainly on forest entomology, particularly, interactions between forests and insects. After his graduation in summer 1995, He moved to Beijing and started working as a research associate at the Chinese Academy of Forestry. His main research activities were to monitor and assess forest damage by pest insects and diseases with airborne video remote sensing, GIS, and real-time DGPS techniques. In early 2001, He moved to Tennessee, U.S., and became a graduate student in the Department of Earth Sciences at the University of Memphis. His research focused on risk assessment of natural hazards, development of hazard mitigation plan, and monitoring water quality in Reelfoot Lake with multispectral and hyperspectral remote sensing techniques. In addition, as an undergraduate lab instructor, he took sole responsibility for lab "Weather and Climate" in the course Physical Geography. In spring 2005, he joined the Forestry Program for a Doctor of Philosophy degree in the School of Renewable Natural Resources at Louisiana State University. He conducted studies in four topics, including quantification of spatial distribution of Louisiana forest biomass carbon storage, prediction of the forest productivity in response to climate change during 2000 to 2050, identification and assessment of hurricane disturbance to Louisiana coastal forests, and remote sensing estuarine water quality. After his graduation, he will continue to pursue an academic career related to application of remote sensing and GIS techniques in natural resources and environmental management issues. You may contact him on this dissertation research by his email address: wang_fugui@yahoo.com.